

2

AD-A247 094



DTIC  
ELECTE  
MAR 5 1992  
S C D

Appendix A: An Integrated Geophysical and Geological Investigation of the Transition Zone Between the Colorado Plateau, Rio Grande Rift and Basin and Range Provinces: Arizona and New Mexico.

DISTRIBUTION STATEMENT A  
Approved for public release;  
Distribution Unlimited

92-05588



92 3 03 061

AN INTEGRATED GEOPHYSICAL AND GEOLOGICAL INVESTIGATION OF  
 THE TRANSITION ZONE BETWEEN THE COLORADO PLATEAU,  
 RIO GRANDE RIFT AND BASIN AND RANGE  
 PROVINCES: ARIZONA AND NEW MEXICO  
 by  
 ROBERT VINCENT SCHNEIDER, B.S., M.S.

Accession For	
NTIS GRA&I	<input checked="" type="checkbox"/>
DTIC TAB	<input type="checkbox"/>
Unannounced	<input type="checkbox"/>
Justification	
By	
Distribution/	
Availability Codes	
Dist	Avail and/or Special
A-1	



DISSERTATION  
 Presented to the Faculty of the Graduate School of  
 The University of Texas at El Paso  
 in Partial Fulfillment  
 of the Requirements  
 for the Degree of  
 DOCTOR OF GEOLOGICAL SCIENCES

Department of Geological Sciences  
 THE UNIVERSITY OF TEXAS AT EL PASO  
 December, 1990

AIR FORCE OF SCIENTIFIC RESEARCH (AFSC)  
 NOTICE OF RESEARCH REVIEWED AND IS  
 APPROVED FOR DISTRIBUTION  
 GEORGE MILLER  
 STINFO Program Manager  
 15M 190-12

## ACKNOWLEDGEMENTS

This project would not have been accomplished without the help of many people. The author wishes to express deep appreciation to Dr. G. R. Keller, without whose ideas, patience and guidance, this project would have been impossible to complete. Thanks is also expressed to the other members of the thesis committee: E. A. Dean, D. I. Doser, J. H. Hinojosa, and R. F. Roy.

Much appreciation is reserved for S. Harder and M. Baker, who taught the author how to use the field equipment and also helped maintain it during the project. M. Martin, D. Yarwood, A. Githui, S. Schneider, R. Barrow, C. Montana, J. Chang, A. Suleiman and G. Kaip assisted in the field work. M. and S. Hernandez brought the equipment out of the field when the department vehicle broke down. C. Montana, J. Gridley and D. Roberts provided technical assistance on the computer. Many fruitful discussions were held with professors, scientists and students not mentioned above.

The support and cooperation of the Phelps-Dodge copper mine in Tyrone, New Mexico made this project possible. In particular, R. Rhoads provided a site for a seismic base station to be occupied on mine property, and F. Gonzalez and T. Jones provided important information for each blast used

in this study.

Many landowners allowed placement of seismic recording equipment on their property. Many thanks are given to: T. and P. Burris, Innovative Engineering, Inc., D. R. Woodward, R. Muncy, J. and J. Hand, J. R. McKinley, E. and S. Farrington, C. Roberson, J. Hertiage and B. W. Cox.

Finally, deep graditude is expressed to the author's parents, J. R. Schneider and A. T. Schneider, for their emotional and financial assistance, and to Dr. and Mrs. Rolf Jore for their support. Special thanks also goes to Susan E. Schneider for typing this manuscript.

This study has been funded, in part, by an Air Force grant #F449620-89-C-0076.

## ABSTRACT

The area comprising southwestern New Mexico and southeastern Arizona has experienced a complex tectonic history. In particular, the period of time from the late Cretaceous to the present has brought varying degrees of compression, magmatic activity, uplift and extension. Three major provinces that developed as a result of this tectonism are the Colorado Plateau, Basin and Range and Rio Grande Rift.

The Colorado Plateau is a region which is uplifted and relatively undeformed with respect to surrounding provinces. It is characterized by gently dipping strata that have undergone minor folding and warping, volcanism, and epeirogenic uplift during Cenozoic time. To the west, south and southeast, the Colorado Plateau is bounded by the Basin and Range and Rio Grande Rift extensional provinces. They have undergone extensive deformation and volcanic activity during the past 40 Ma, with signs of active tectonism continuing to the present.

The transition zones between the Colorado Plateau, Rio Grande Rift and Basin and Range provinces meet in southeastern Arizona and southwestern New Mexico. There is no physiographic boundary nor is there a distinctive change

in structural style observed in this region. Instead, the surface is covered by the mid-Tertiary Mogollon-Datil volcanic field, which hides underlying structures that might aid in determining the nature of the transition. Therefore, the use of geophysical techniques in conjunction with known geology must be employed to determine the present-day state of the lithosphere, as well as its tectonic history.

A combined analysis of seismic refraction and gravity data has identified a major upper crustal low-velocity, low-density body in this region. This body is associated with a thickening of the crust where it is present. It underlies the Mogollon-Datil volcanic field, but extends to the north through the Plains of St. Augustine and under the Datil Mountains. Because of its proximity to the volcanic field, this body is interpreted as a massive plutonic complex nearly 170 km long by 130 km wide in the study area. It presumably is the source for the volcanics, implying that this complex is mid-Tertiary in age. When correlated with long wavelength gravity trends, the complex extends northwest into Arizona, and is approximately 230 km by 155 km in extent.

Beneath this plutonic complex, seismic and gravity data indicate that the Moho deepens markedly from 32 to 37 km about 60 km north of Silver City. This is identified as the

present-day structural boundary between the Colorado Plateau and the Basin and Range and Rio Grande Rift provinces. Compressional wave arrivals and gravity analysis demonstrate anomalously slow velocities and low density in the upper mantle along both profiles examined in this study. This supports heat flow studies which conclude that the upper mantle and lower crust contain a thermal anomaly. Although high heat flow values are observed in both the Basin and Range and Rio Grande Rift, the highest heat flow values are spatially associated with the transition zone. Because of the extensive volcanism and evidence for geothermal activity throughout the Cenozoic, the thermal anomaly is interpreted to be present over the same time interval. A two-dimensional finite difference model has therefore been derived and a computer code generated which maps the progression of a temperature pulse over time. Surface heat flow and isostatic uplift are also calculated by this program. These values are compared to observed values of heat flow and elevation in Arizona and New Mexico to constrain both the magnitude and width of the thermal pulse.

Results of the analysis are consistent with thermal anomalies present at both the base of the crust and the base of the lithosphere. The deep anomaly produces a steady-state solution after nearly 28 Ma, producing the bulk of

isostatic uplift but making little contribution to surface heat flow. The shallow anomaly becomes steady-state after 5.4 Ma, and is responsible for present-day surface heat flow readings. It contributes a minor component of uplift to the region. The time span over which these thermal perturbations operate implies that the deeper anomaly is the cause for much of the volcanic activity since Laramide time, and that the shallow anomaly is associated with recent extension and basaltic volcanism.

TABLE OF CONTENTS

	Page
Acknowledgements . . . . .	iv
Abstract . . . . .	vi
Table of Contents . . . . .	x
List of Figures . . . . .	xii
Introduction . . . . .	1
Geologic History . . . . .	9
Precambrian . . . . .	9
Paleozoic . . . . .	11
Mesozoic . . . . .	12
Laramide . . . . .	16
Mid-Tertiary . . . . .	22
Late Cenozoic . . . . .	25
Present-Day Structure and Tectonics . . . . .	30
Colorado Plateau . . . . .	30
Southern Arizona Basin and Range Province . . . . .	32
Rio Grande Rift . . . . .	37
Mogollon-Datil Volcanic Field . . . . .	44
Introduction . . . . .	44
General Geology . . . . .	48
Timing of Volcanism . . . . .	50
Mogollon Plateau . . . . .	52
Data Collection and Compilation . . . . .	55

Seismic Refraction . . . . .	55
Gravity . . . . .	62
Heat Flow . . . . .	63
Data Analysis, Modeling, and Discussion . . . . .	69
Seismic Refraction and Gravity Profiling . . . . .	69
Technique . . . . .	69
Refraction Observations . . . . .	73
Gravity Observations . . . . .	77
Model Generation and Evolution . . . . .	79
Thermal Modeling of the Lithosphere . . . . .	110
Derivation of the Algorithm . . . . .	119
Consequences of Lithosphere Heating . . . . .	128
Surface Heat Flow . . . . .	128
Isostatic Uplift . . . . .	129
Consequences of the Model . . . . .	129
Discussion . . . . .	130
Conclusions . . . . .	153
References . . . . .	166
Abbreviations . . . . .	182
Appendix I . . . . .	183
Appendix II . . . . .	185
Appendix III . . . . .	188
Appendix IV . . . . .	191
Appendix V . . . . .	193
Curriculum Vitae . . . . .	204

## LIST OF FIGURES

Figure		Page
1.	Location map of the major tectonic provinces of the western United States .....	2
2.	Location of study area.....	5
3.	Precambrian provinces of North America.....	10
4.	Paleozoic tectonic features of the southwestern United States and northern Chihuahua, Mexico.....	13
5.	Tectonic model for typical Laramide structures in southern New Mexico.....	18
6.	Late Laramide tectonic configuration, including Eocene uplifts and basins, eastern Arizona and western New Mexico.....	19
7.	Distribution of sediments off the Laramide Mogollon highland and paleocurrent directions of the Mogollon Rim gravels, Eager fm and Baca fm.....	23
8.	Map showing the Colorado Plateau and its relationship to surrounding provinces, including late Cenozoic volcanism.....	29
9.	Sketch map of mid-Tertiary Mogollon-Datil volcanic field in southwestern New Mexico and far eastern Arizona.....	45
10.	Map showing Mogollon-Datil volcanic field as part of a mid-Tertiary volcanic event that involved much of the western United States and Mexico.....	46
11.	Intermediate to silicic ash-flow tuff cauldrons associated with the Mogollon-Datil volcanic field, southwestern New Mexico.....	47
12.	Timing and volume of post-Laramide volcanic activity in southwestern New Mexico and its relationship to tectonic events in the western United States.....	49

13.	Location of seismic refraction lines used in the present study.....	56
14.	Seismic record section of the Tyrone-Acoma refraction line.....	59
15.	Filtered (2-8 Hz) record section, Tyrone-Acoma refraction line.....	60
16.	Seismic refraction line of Jaksha (1982) ...	61
17.	Residual Bouguer gravity map of eastern Arizona and western New Mexico.....	65
18.	Regional Bouguer gravity anomaly map of eastern Arizona and western New Mexico constructed with a 125 km low-pass filter ..	66
19.	Regional Bouguer gravity anomaly map of eastern Arizona and western New Mexico constructed with a 15-125 km band-pass filter.....	67
20.	Heat flow readings in Arizona and New Mexico.....	68
21.	Location map for seismic analyses of the tectonic provinces and their boundaries in Arizona and New Mexico.....	70
22.	a) Repicked arrivals for Jaksha (1982) Morenci-Dice Throw refraction line b) Arrival picks for reversed Pn branch.....	74
23.	Arrival picks for Tyrone-Acoma refraction line.....	75
24.	a) Gravity field for profile along Jaksha (1982) refraction line b) Gravity field for profile along Tyrone- Acoma refraction line.....	78
25.	Ray trace model using Jaksha's (1982) interpretation of crustal structure from the Morenci-Dice Throw refraction line.....	81
26.	Gravity profile based on Jaksha's (1982) earth model.....	82

27.	Gravity model for thickened crust along the Jaksha (1982) refraction line.....	83
28.	Thickened crust seismic ray-tracing model for the Jaksha (1982) refraction line.....	84
29.	Gravity model along Morenci-Dice Throw line, with 3.1 km thick pluton.....	87
30.	Gravity model along Morenci-Dice Throw line, with 12.5 km thick pluton.....	88
31.	Gravity profile along the Tyrone-Acoma refraction line with a 3.1 km thick buried pluton.....	90
32.	Gravity profile along the Tyrone-Acoma refraction line with a 12.5 km thick buried pluton.....	91
33.	Gravity profile along the Tyrone-Acoma refraction line involving crustal thickening alone.....	93
34.	Seismic ray-tracing model along the Tyrone-Acoma line for thickened crust.....	94
35.	Ray-trace model of the Tyrone-Acoma line, attempting to model step change in PmP by crustal thinning.....	95
36.	Gravity profile along the Tyrone-Acoma refraction line showing crustal thinning to 23 km.....	96
37.	Ray-tracing model for Tyrone-Acoma line attempting to match Pn branch by upper mantle velocity anomalies alone.....	101
38.	Gravity profile for Tyrone-Acoma refraction line, final model.....	102
39.	Ray-tracing model for Tyrone-Acoma line, final configuration.....	104
40.	Gravity profile for Jaksha (1982) cross-line, including the final model.....	105

41.	Ray-tracing model for the Jaksha (1982) cross-line, final configuration.....	106
42.	Ray-tracing model for the Jaksha (1982) cross-line, reversed Pn branch, final configuration.....	107
43.	Heat flow for the Colorado Plateau and adjacent areas.....	113
44.	Heat flow for the Rio Grande Rift and adjacent areas.....	116
45.	Initial temperature distribution for program HF2D.....	133
46.	Initial density distribution for program HF2D.....	134
47.	Gaussian curve with amplitude = 100, exponential coefficient term = 0.0002.....	136
48.	Gaussian curve with amplitude = 100, exponential coefficient term = 0.0005.....	137
49.	Thermal model of Reiter and others (1978) showing heat flow rise over the Rio Grande Rift.....	138
50.	Calculated heat flow for a 1500°C thermal pulse at 100 km depth.....	139
51.	Calculated isostatic uplift for a 1500°C thermal pulse at 100 km depth.....	141
52.	Calculated heat flow for a 400°C thermal pulse at 100 km depth.....	143
53.	Calculated isostatic uplift for a 400°C thermal pulse at 100 km depth.....	144
54.	Calculated heat flow for a 350°C thermal pulse at 30 km depth.....	146

55.	Calculated isostatic uplift for a 350°C thermal pulse at 30 km depth.....	147
56.	Calculated isostatic uplift for a 230°C thermal pulse at 30 km depth.....	150
57.	Extent of the proposed upper crustal pluton and its relationship to the 125 km low-pass gravity field.....	158

## INTRODUCTION

The Colorado Plateau is one of the major tectonic and physiographic provinces of western North America. It is approximately  $3.5 \times 10^5$  km<sup>2</sup> in area, and is centered near the common boundaries of New Mexico, Colorado, Utah and Arizona (Figure 1). It is bounded on three sides by the extensional tectonic provinces of the Basin and Range and Rio Grande Rift, and to the north and northeast by the Middle and Southern Rockies, respectively. The origin of the plateau, its late Mesozoic and Cenozoic evolution, its deep structure and its relationship to adjacent provinces pose questions of broad interest to the earth science community.

The interior of the Colorado Plateau appears to be relatively unaffected by the extension and associated volcanism that border it on three sides. Deformation within the plateau during and since Laramide tectonism has been restricted to gentle warping and minor faulting. Cenozoic volcanic activity has been less extensive on the plateau than in most other areas of the western United States (Christiansen and Lipman, 1972; Lipman and others, 1972), but its margins have been loci of igneous activity (Morgan and Swanberg, 1985).

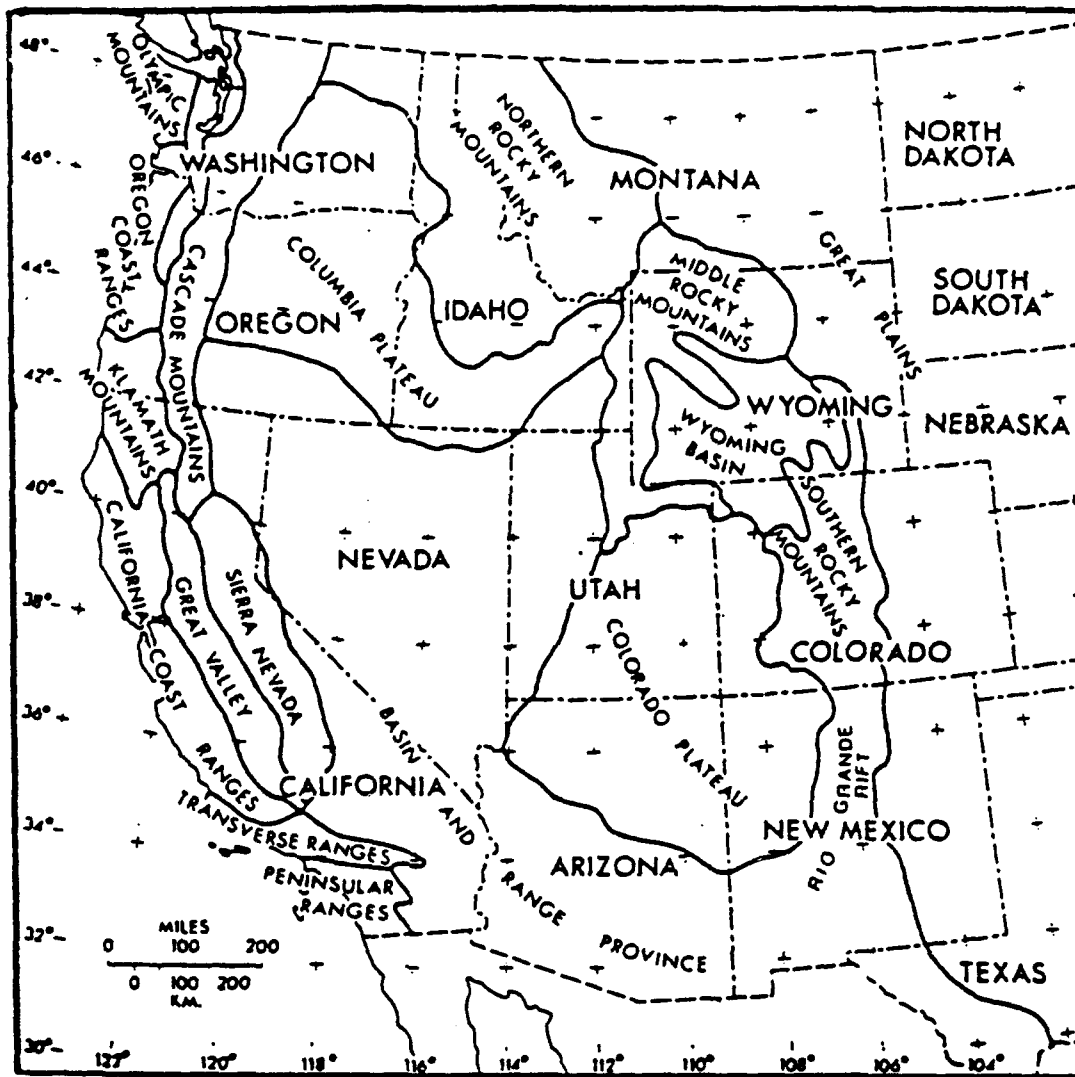


Figure 1. Map of the western United States showing locations and boundaries of major tectonic provinces. Modified after Thompson and Zoback (1979).

Despite its relative tectonic stability and lack of magmatism, the Colorado Plateau has been epeirogenically uplifted approximately 2 km since the latest Mesozoic, based on the present elevation of the Cretaceous (marine) Mancos shale (Morgan and Swanberg, 1985). Although the timing of uplift is still debated, the basic geologic history of the plateau is reasonably well documented (Hunt, 1956).

The margins where the Colorado Plateau is bounded by the Basin and Range and Rio Grande Rift provinces have been tectonically active and are of much current interest (e.g. Keller and others, 1975; Aldrich and Laughlin, 1984; Brumbaugh, 1987). These margins are divided into three distinct sectors: western (Utah and northwestern Arizona), southern (central Arizona) and southeastern (southeast Arizona and southwest New Mexico). These boundaries have been classically drawn on a physiographic basis, although no physiographic expression exists along the southeastern margin.

The basis for defining province boundaries by physiographic means has left room for much debate. There exists a considerable body of geophysical information indicating that the margins are transitional (Keller and others, 1975; Thompson and Zoback, 1979, Brumbaugh, 1987). Furthermore, in those areas where the physiographic

boundaries are not well defined, the placement of the transition zone is still in question (Brumbaugh, 1987). Of particular interest to this study is the transition between the Colorado Plateau, Basin and Range, and Rio Grande Rift provinces in southeastern Arizona and southwestern New Mexico (Figure 2).

The Mogollon-Datil volcanic field (MDVF) lies within the Colorado Plateau-Basin and Range-Rio Grande Rift transition zone in southwest New Mexico. It hides underlying structures that may aid in determining the extent and nature of this transition (Elston and others, 1976a; Gish and others, 1981). A careful integrated geophysical and geological analysis is required to determine the validity of previous models and determine the deep structure of this region.

A gravity study by Daggett and others (1986) delineated two regional gravity anomalies in southwestern New Mexico. A positive anomaly occurs along the Rio Grande Rift axis near El Paso, and a negative anomaly corresponds to the MDVF. Their crustal model indicates crustal thickening under the MDVF. Sinno and others (1986) also interpret an increase in crustal thickness from the Rio Grande Rift into the MDVF based on seismic data. Gish and others (1981) concluded that crustal thickening occurs in the MDVF with

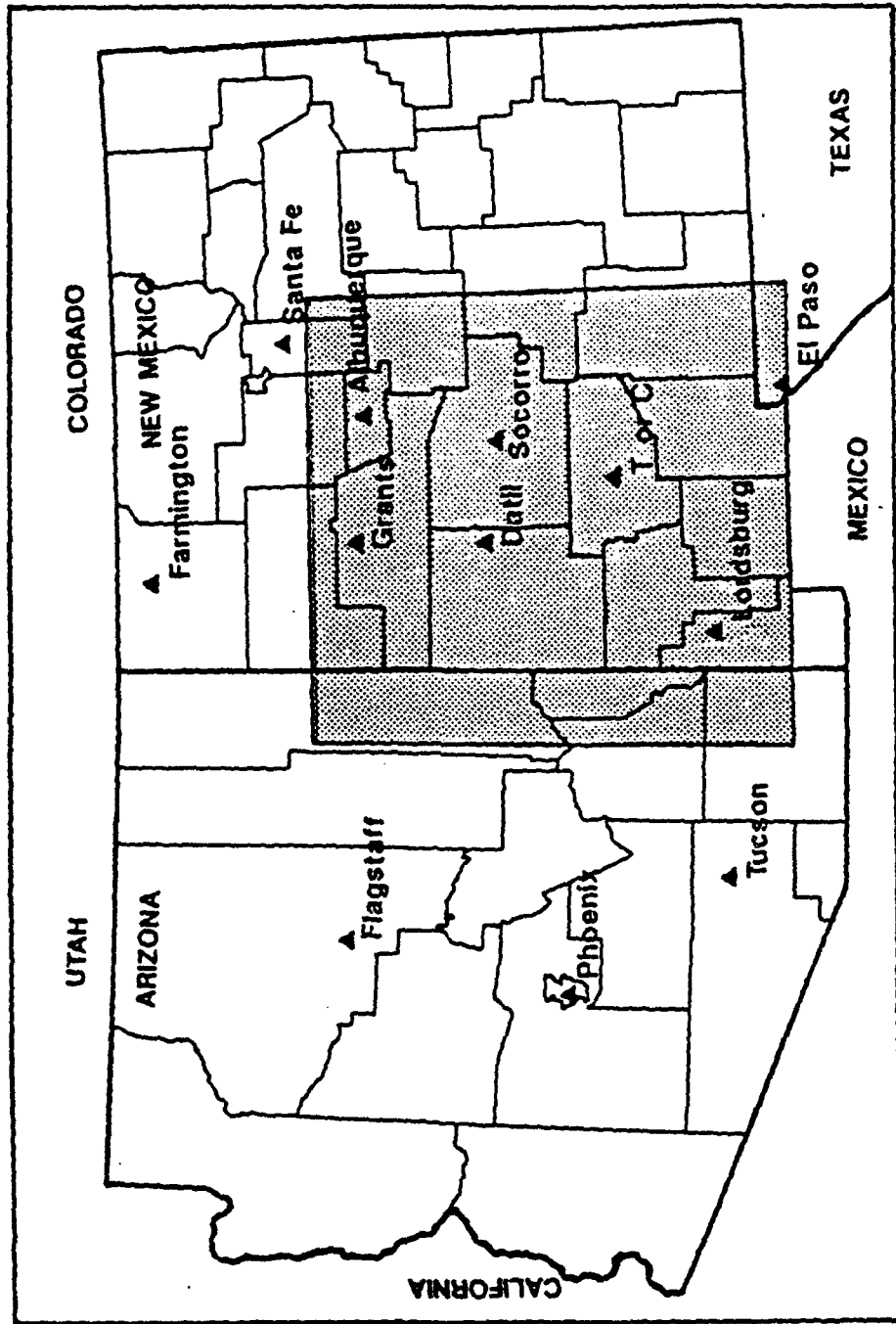


Figure 2. Location of study area.

respect to southern Arizona, primarily caused by a five km thick low-density surface layer composed of intermediate to felsic volcanic rocks. Further north, however, Jaksha (1982) suggests that little crustal thickening occurs across the field between the Rio Grande and Morenci, Arizona.

Elston (1976), Rhodes (1976), Elston and others (1976a), Krohn (1976) and Coney (1976a) agree that a shallow plutonic complex underlies the high-silica rhyolite extrusives of the Mogollon plateau. Gravity anomalies were used to infer that this complex is presumably less dense than the material it displaced (Coney, 1976a; Krohn, 1976), but the boundaries and thickness of the body were not determined.

The extrusives of the MDVF have completely buried the material which previously formed the surface. To the south of the volcanics, Basin and Range structures predominate. The Rio Grande Rift lies immediately to the east, and Colorado Plateau structural features predominate to the northwest. However, no physiographic boundary between the provinces is discernible within the MDVF. Thus, a major objective of this study is to use a combination of geophysical techniques and regional geologic data to study the nature and history of the transition zone between the

southeastern Colorado Plateau and the Rio Grande Rift and Basin and Range province.

The present day state of the lithosphere is a culmination of preceding tectonic events. Understanding the thermal history of the region is therefore a second goal of this study. Post mid-Tertiary history in southwest New Mexico and southeast Arizona is dominated by block faulting and basaltic volcanism associated with Rio Grande Rift and Basin and Range extension. The volcanism within the rift, however, has been of relatively minor volume when compared to the similarly-dimensioned East African Rift in Kenya (Baldrige and others, 1984). The presence of hot springs and late Cenozoic volcanism along with observed geophysical data indicate that elevated temperatures are present in the lower crust and upper mantle (Decker and Smithson, 1975; Seager and Morgan, 1979; Gish and others, 1981; Morgan and others, 1986; Sinno and others, 1986). Heat flow data are elevated near the late Cenozoic volcanic centers and near deep basin-bounding faults in the region, but are of more intermediate values elsewhere. However, the heat flow data are complicated in the area by extensive groundwater circulation, and therefore must be interpreted with caution (Morgan and others, 1986).

Within this context, a broad zone of elevated heat flow values is observed near the boundary of the Colorado Plateau in southeastern Arizona and south and central New Mexico (Swanberg, 1979). Combined with the crustal uplift in the region (Morgan and Swanberg, 1985), which is at least partially due to thermal expansion, a long-standing thermal anomaly is inferred at the base of the lithosphere. A major goal of this study, therefore, is the development of a two-dimensional finite difference model in which the evolution of temperature, heat flow and isostatic uplift is calculated over time. The results of this program are compared with observed heat flow and elevation for the purpose of defining the thermal history of the region.

## GEOLOGIC HISTORY

### Precambrian

Precambrian basement is exposed in scattered locations throughout the region (Dane and Bachman, 1965; Wilson and others, 1969). It is composed primarily of crystalline schists, gneisses, and granites to the west; and slightly younger Precambrian sediments in the eastern part of the region (Ross and Ross, 1986; Seager and Mack, 1986). The basement is usually unconformably overlain by Paleozoic rocks.

The Precambrian basement in southern Arizona and New Mexico consists of a complex assemblage of rocks ranging in age from 1.68 to 1.8 Ga using U-Pb zircon dates (Figure 3; Condie, 1986). These ages are supported by Nd isotope studies (Bennett and DePaolo, 1987). The rocks show evidence of tectonic activity prior to and during emplacement (Grambling and others, 1988; Karlstrom and Bowring, 1988). The structural grain in the Arizona transition zone strikes northeast, becoming more easterly in central New Mexico. Anorogenic granites (1.4 to 1.5 Ga) intrude all rocks in the southwestern United States, and are especially prevalent in southeast Arizona and southern New Mexico (Condie, 1982). The region experienced an anorogenic

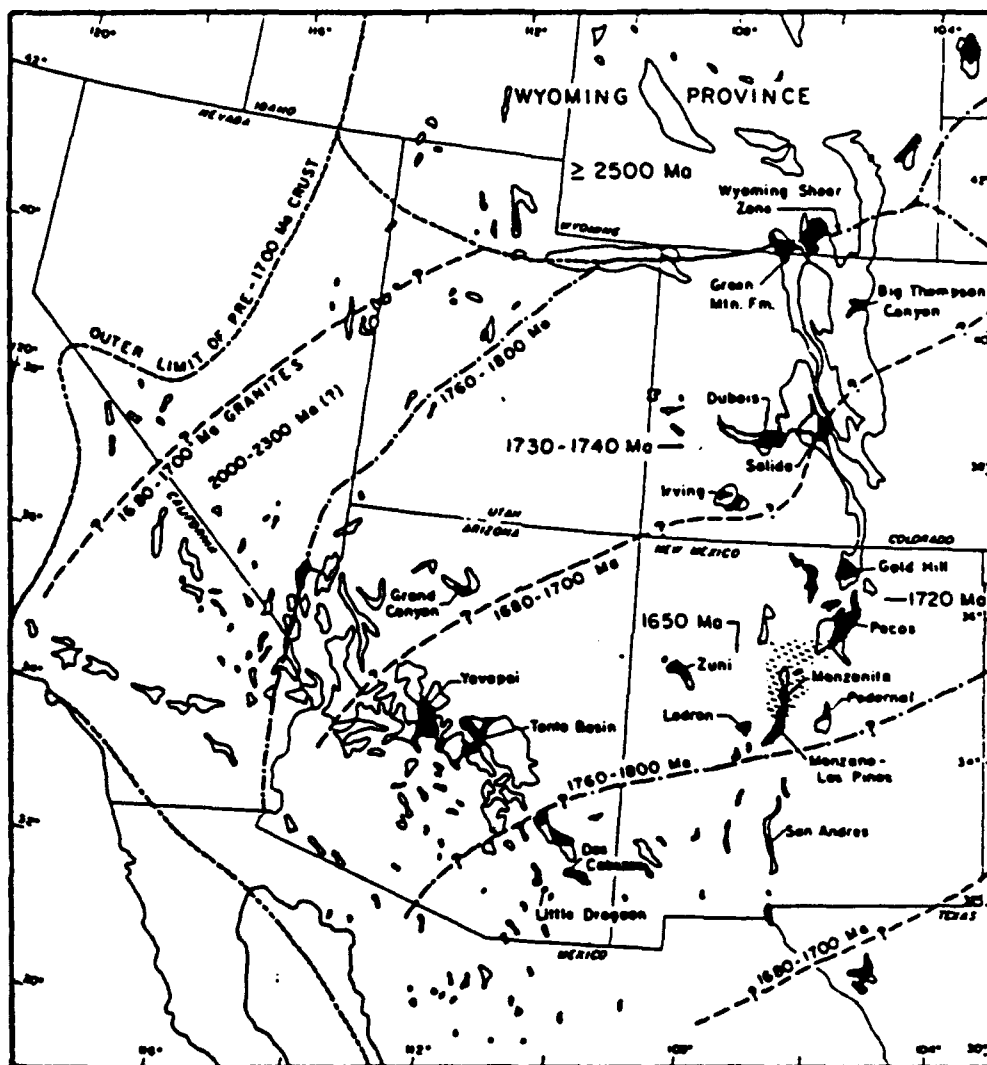


Figure 3. Precambrian provinces of North America. After Condie (1986).

volcano-plutonic event of middle Proterozoic age (1.1 Ga), as recorded in the Franklin mountains in El Paso (Shannon, 1989).

Karlstrom and Bowring (1988) have mapped at least eight tectonostratigraphic terranes along the transition zone in Arizona. The easternmost is the Pinal block adjacent to Cenozoic volcanic cover near the New Mexico border. To the east of Cenozoic volcanic cover, six tectonostratigraphic terranes are reported in New Mexico (Grambling and others, 1988). The structural grain resulting from emplacement of these blocks may have exerted considerable control on post-Precambrian regional tectonic style.

### Paleozoic

The Paleozoic section in southeastern Arizona reflects deposition in a stable, cratonal shelf environment with no highlands nearby (Coney, 1978a). Despite this indication of regional stability, there were two Paleozoic orogenic events in southern and western North America: 1) within 800 km to the west, the Cordilleran miogeocline experienced the effects of the Antler and Sonora orogenic events; and 2) the Appalachian-Ouachita-Marathon orogenies, resulting from interactions between North America and Africa-South America,

came within 500 km to the east. It is possible that these two belts may have intersected somewhere to the south of Arizona, possibly within 1000 km. Southeastern Arizona can therefore be thought of as part of a southwest-trending peninsular extension of the Paleozoic North American craton.

The closure of the Iapetus ocean and ancestral Gulf of Mexico initiated two important events in the present study area: 1) the Pennsylvanian Ouachita-Marathon orogeny, which created the Ancestral Rocky Mountains and produced faulting and zones of weakened crust in the region (Coney, 1978a, 1978b; Kluth, 1986; Ross and Ross, 1986). 2) although southeastern Arizona was relatively stable throughout this time, southwestern New Mexico lay at the southwest boundary of a large basin-uplift regime that extended onto the present Colorado Plateau (Figure 4). By the late Early Permian, the entire region was uplifted, and sedimentation was mostly nonmarine to the end of the period (Ross and Ross, 1986).

### Mesozoic

South of the Colorado Plateau, little information exists from the early Mesozoic (Coney, 1978a; Jahns and others, 1978; Seager and Mack, 1986). However, a Jurassic

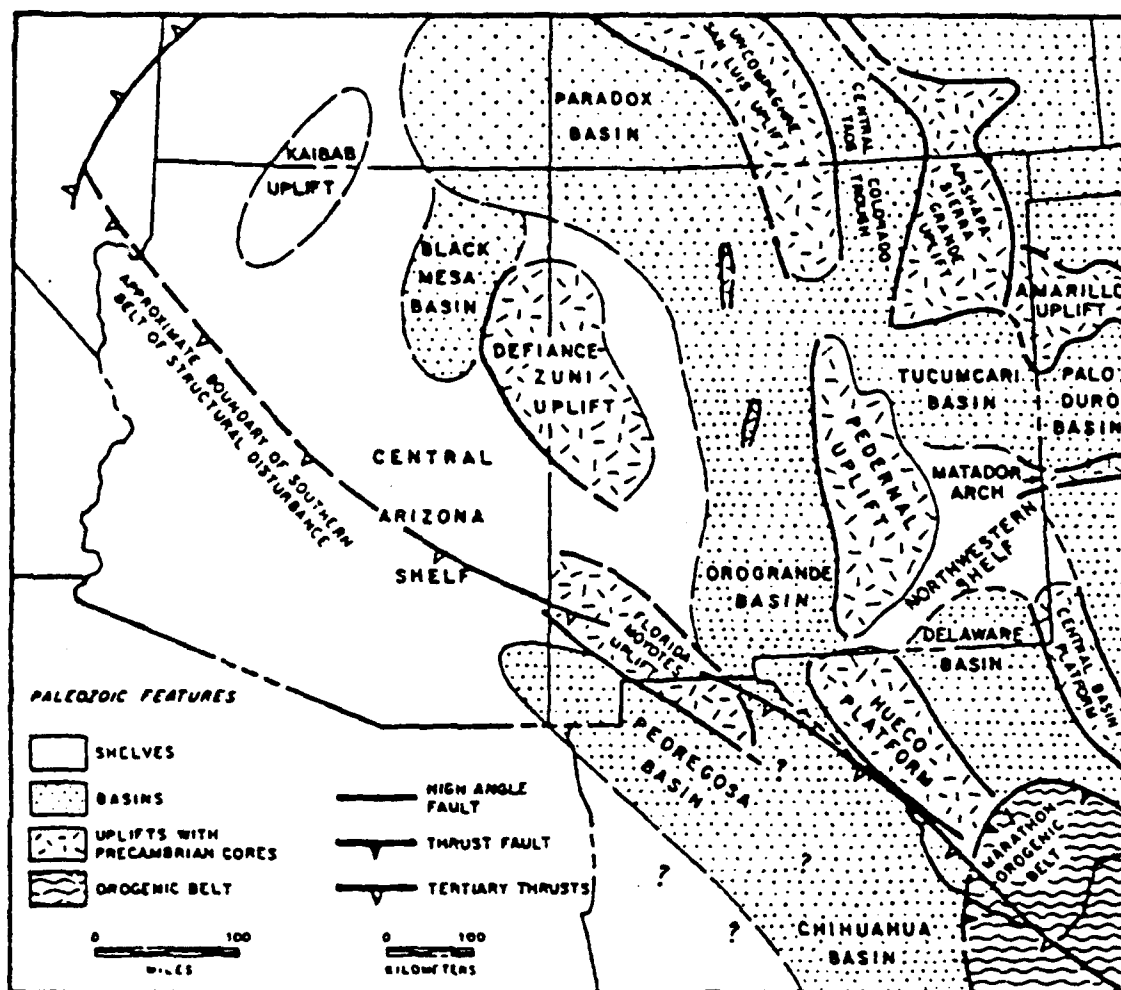


Figure 4. Map showing Paleozoic tectonic features of the southwestern United States and northern Chihuahua, Mexico. After Ross and Ross (1986).

magmatic zone existed in Arizona (Coney, 1978a). It had a northwest-southeast trend, parallel to and just south of the present day transition zone between the Colorado Plateau and Basin and Range provinces. It continued into Mexico, passing just to the southwest of New Mexico.

This zone was summarized by Hamilton (1969), Burchfiel and Davis (1972), and Coney (1978a) as being representative of an Andean-type arc setting, implying a compressional regime in late Triassic to early Jurassic time. However, citing modern analogs in Central America and Kamchatka, Busby-Spera (1988) suggests an extensional, graben-related volcanic episode. Sediments from volcanic complexes were not shed to the north and northeast, due to the presence of a low-lying Precambrian-cored ancestral Mogollon Highland, near the present transition zone (Coney, 1978a).

The Gulf of Mexico began to open during Jurassic time (Coney, 1978a). This produced two events of note in southern Arizona and New Mexico, one structural and one stratigraphic: 1) as the gulf opened, a major transform fault or "megashear" (Silver and Anderson, 1974) may have developed on the southwest edge of the magmatic arc, transporting much of northern Mexico to its present location, and 2) the opening of the gulf initiated a marine transgression that grew out of the gulf into western North

America (Coney, 1978a, 1978b). The earliest known Mesozoic sediments in southern New Mexico are marine Jurassic rocks found in a single oil test well near Las Cruces (Thompson and Bieberman, 1975).

Tectonism and volcanism diminished in southern Arizona and New Mexico during the latter part of the Jurassic (Coney, 1978a, 1978b). During the Cretaceous, the Sevier orogeny commenced in western North America (Armstrong, 1968; Coney, 1978b). In the southwestern United States, the volcanic arc was reinstated to the southwest of the Jurassic arc (Figure 3, Coney, 1978a). A remnant of the Mogollon Highland persisted as the Burro-Deming Axis from the West Potrillo Mountains to the northwest into Arizona (Seager and Mack, 1986), but the rest of the region was covered by a shallow sea. Near the arc, significant deformation occurred in southwest Arizona and northwest Sonora. This created a highland that shed sediments towards southwest New Mexico (Coney, 1978a). It is unclear whether this deformation was a precursor to the Laramide compressional event, yet it apparently predates Laramide plutonism in the region.

## Laramide

The Laramide orogeny began in late Cretaceous time, and involved the entire crust in the southwestern United States (Coney, 1978a, 1978b). In western North America, the volcanic arc broke up into scattered volcano-plutonic complexes. Basement cored Laramide uplifts developed where gaps in volcanism occurred.

In southern Arizona and New Mexico, Epis and Chapin (1975) report that the Laramide event began with widespread erosion to a surface of little relief. This was followed by uplift, volcanism, compression, then further volcanism and plutonism. Coney (1978a) states that volcanism progressed from west to east (into Trans-Pecos Texas), then swept westward again. This "retrograde motion" of volcanism swept through heated crustal material.

Compressive deformation in southern Arizona and New Mexico is typical of that found throughout the western United States during Laramide time, but individual structures are smaller (Seager and Mack, 1986). In southern New Mexico, Laramide compressive features are displayed as west-northwest trending asymmetric block uplifts with complementary basins. The asymmetry is found in the style of uplift, where the northeast boundary generally consists

of reverse and thrust fault zones that dip to the southwest under the uplift (Figure 5). Laramide basin sediments lap onto the unfaulted southwest edge of the uplifts. These structures are spatially and temporally related to structures in the Rocky Mountains (Berg, 1962; Tweto, 1975; Cather and Johnson, 1986), thin-skinned deformation in the Sierra Madre Oriental (Coney, 1976b), and to the Laramide monoclines of the Colorado Plateau (Kelley, 1955; Coney, 1976b; Davis, 1978).

The thrust faults often contain enough strike-slip motion to be termed oblique faults (Seager and Mack, 1986). Problems occur in defining the Laramide stress field in southern New Mexico and Arizona, as right-hand slip in New Mexico occurs on the same fault systems as left-hand slip in Arizona. Apparently there existed some complex interaction between ENE-WSW maximum principal horizontal stress (mphs) to the southwest of the Colorado Plateau (Rehrig and Heidrick, 1976) and N-S mphs in the Rocky Mountains (Gries, 1983). Furthermore, Drewes (1981) and Bilodeau (1984) report that strike-slip motion may involve pre-existing faults, possibly faults associated with the Antler orogeny (Coney, 1978b). This may also serve as an explanation for right-lateral reverse faults near Datil (Figure 6). The Hickman and Red Lake fault zones strike at a high angle to

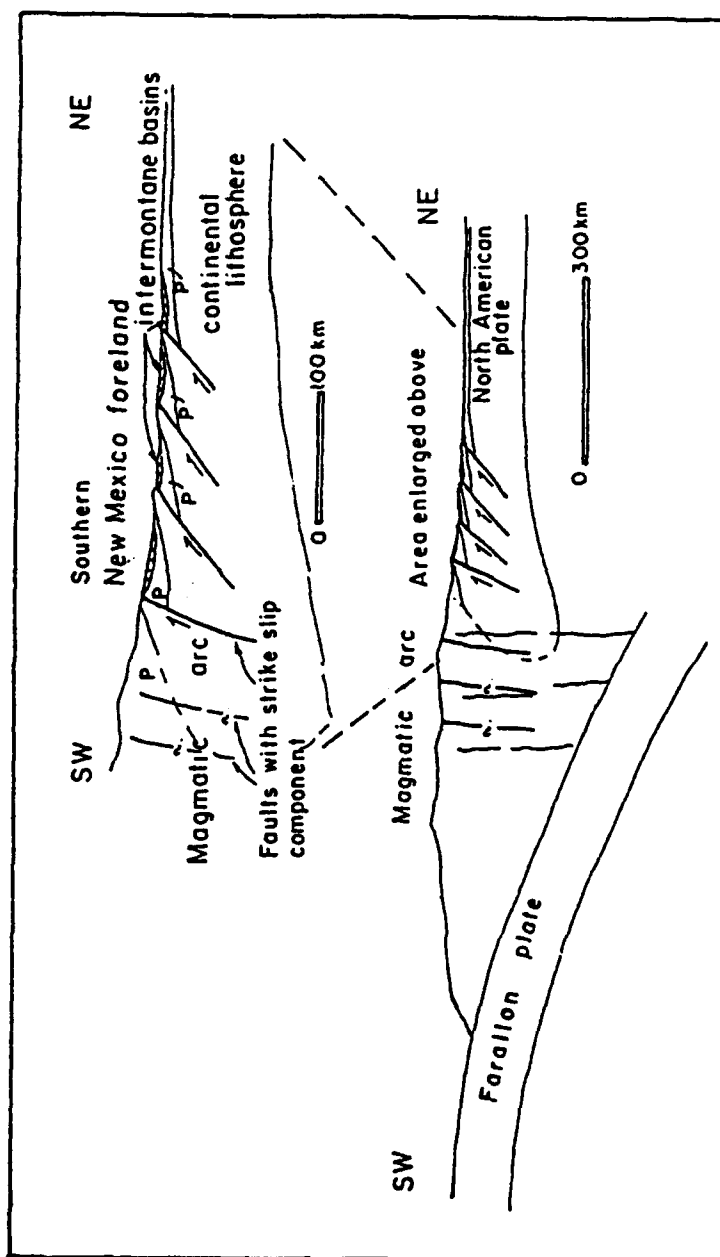


Figure 5. Map showing tectonic model for typical Laramide structures in southern New Mexico. The North American craton was driving southwestward, underthrusting continental blocks to form asymmetric uplifts. After Seager and Mack (1986).

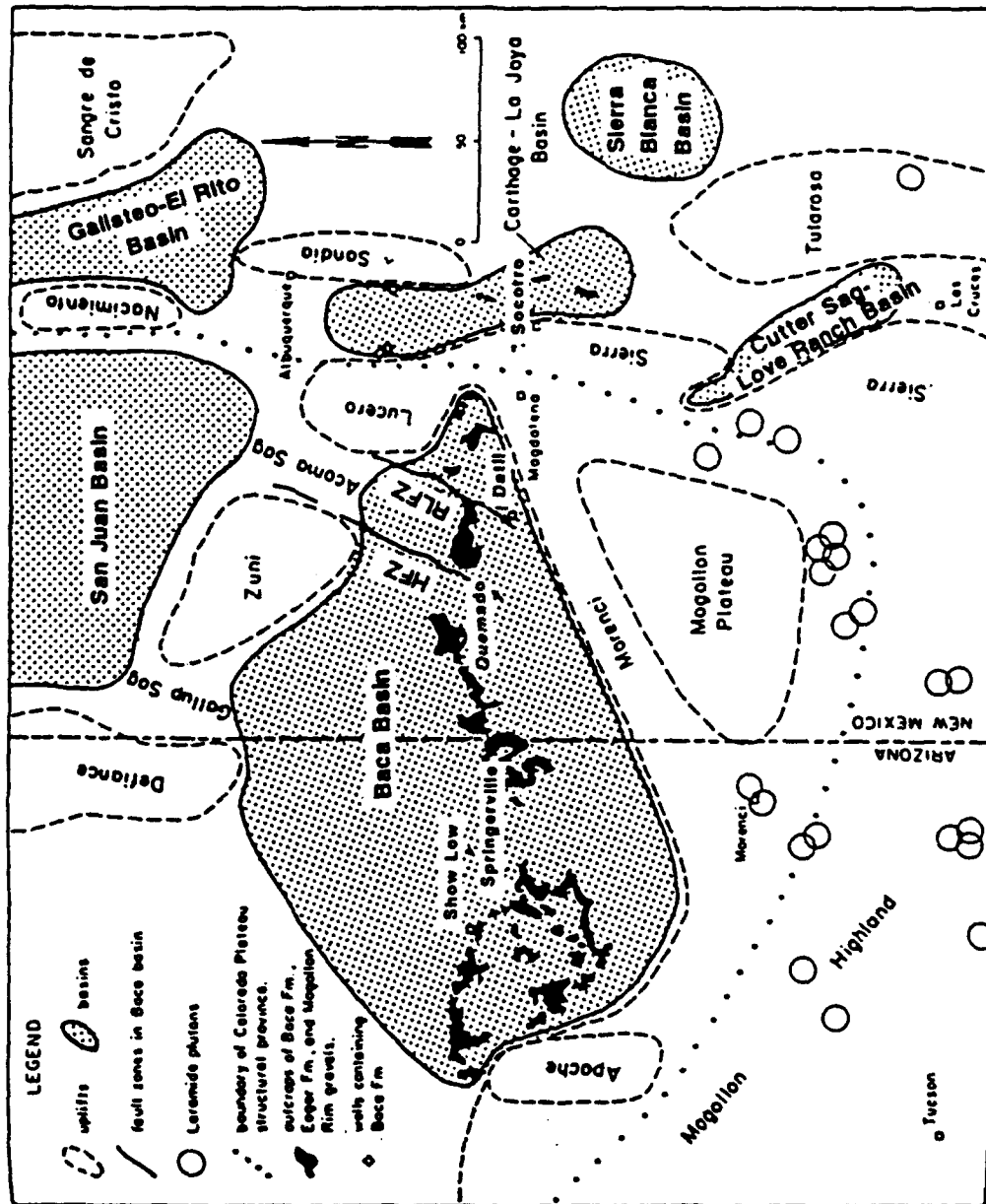


Figure 6. Map showing late Laramide tectonic configuration, including Eocene uplifts and basins, eastern Arizona and western New Mexico. Note the high angle between the north-northeast trending Hickman (HFZ) and Red Lake (RLFZ) fault zones and northwest trending Love Ranch basin. After Cather and Johnson (1986).

the structures further south, but are interpreted as Laramide in age (Cather and Johnson, 1986). But the primary motion is vertical thrusting, and a significant amount of crustal shortening is apparent in the region (Seager and Mack, 1986).

The timing of Laramide volcanism is in some debate within the literature. Coney (1978a) suggests a complicated west to east volcanic progression, then compressional deformation, followed by a retrograde motion of volcanism and plutonism. Seager and Mack (1986) suggest the presence of a volcanic arc that persisted throughout Laramide time. It stretched from southwestern New Mexico into east central Arizona. They conclude that volcanism postdates movement on basin-bounding faults, but is coeval to sediments shed from local highlands. Tectonic activity resulted in a progressively deformed and heated crust throughout Laramide time. Coney (1978a) infers that the thermal disturbance and complicated volcanism is the result of the breakdown of a underlying flat Benioff zone. This breakdown is coeval with cessation of subduction of the Farallon plate at the Pacific margin.

The end of Laramide time is generally regarded to be synchronous with initiation of mid-Tertiary volcanism. In New Mexico, Elston and others (1976a) identify this time at

an angular unconformity between the Cretaceous Mesaverde group and the Eocene Baca formation. The earliest mid-Tertiary volcanic flows and ash-falls are interbedded with these sediments, but do not affect Laramide drainage patterns (Seager and Mack, 1986; Cather and Chapin, 1989).

The Baca formation has been recognized as a stratigraphic equivalent to the Eager formation and Mogollon Rim gravels to the west (Cather and Johnson, 1986). These sediments were deposited in the Eocene Baca basin, one of a series of basins and uplifts actively forming at this time in eastern Arizona and western and central New Mexico (Figure 6). The proximal location of the Baca basin to the Mogollon-Datil volcanic field and preservation of its stratigraphic column has proven beneficial to timing the onset of mid-Tertiary volcanism. The sediments were deposited in a semiarid environment of alluvial fans, braided streams, and temporary lakes in a closed basin (Cather and Johnson, 1986). They are deposited unconformably on upper Cretaceous rocks eroded to a surface of little relief, creating a section up to 760 m thick. Paleocurrent directions indicate that the source areas are from surrounding Laramide uplifts. The Mogollon Highland to the south and southwest, the Sierra and Lucero uplifts to the east, and the Defiance and Zuni uplifts to the north all

contributed sediments to the Baca basin (Figure 7). In New Mexico, the sediments grade transitionally into the Spears formation, consisting of latest Eocene andesitic volcanoclastic material. In eastern Arizona, however, the Mogollon Rim gravels were eroded, possibly beginning in Oligocene time (Pierce and others, 1979). Thus, the stratigraphic record in Arizona and New Mexico shows the Colorado Plateau to be topographically low with respect to the region to the south until latest Eocene.

#### Mid-Tertiary

The Laramide orogeny resulted in a massive reorganization of the crust. This continued into post-Laramide time with the ascent of liquids into the upper crust, creating massive volcano-plutonic complexes throughout the western United States and Mexico (Elston and Bornhorst, 1979). The total volume of vented material was of sufficient magnitude that structural controls for each volcanic center were buried (Elston and others, 1976a). In all, more than  $1 \times 10^6$  km<sup>3</sup> of silicic material was vented over an area greater than  $1 \times 10^6$  km<sup>2</sup> in southwestern North America (Elston and Bornhorst, 1979; Christiansen, 1989; Elston and Abitz, 1989).

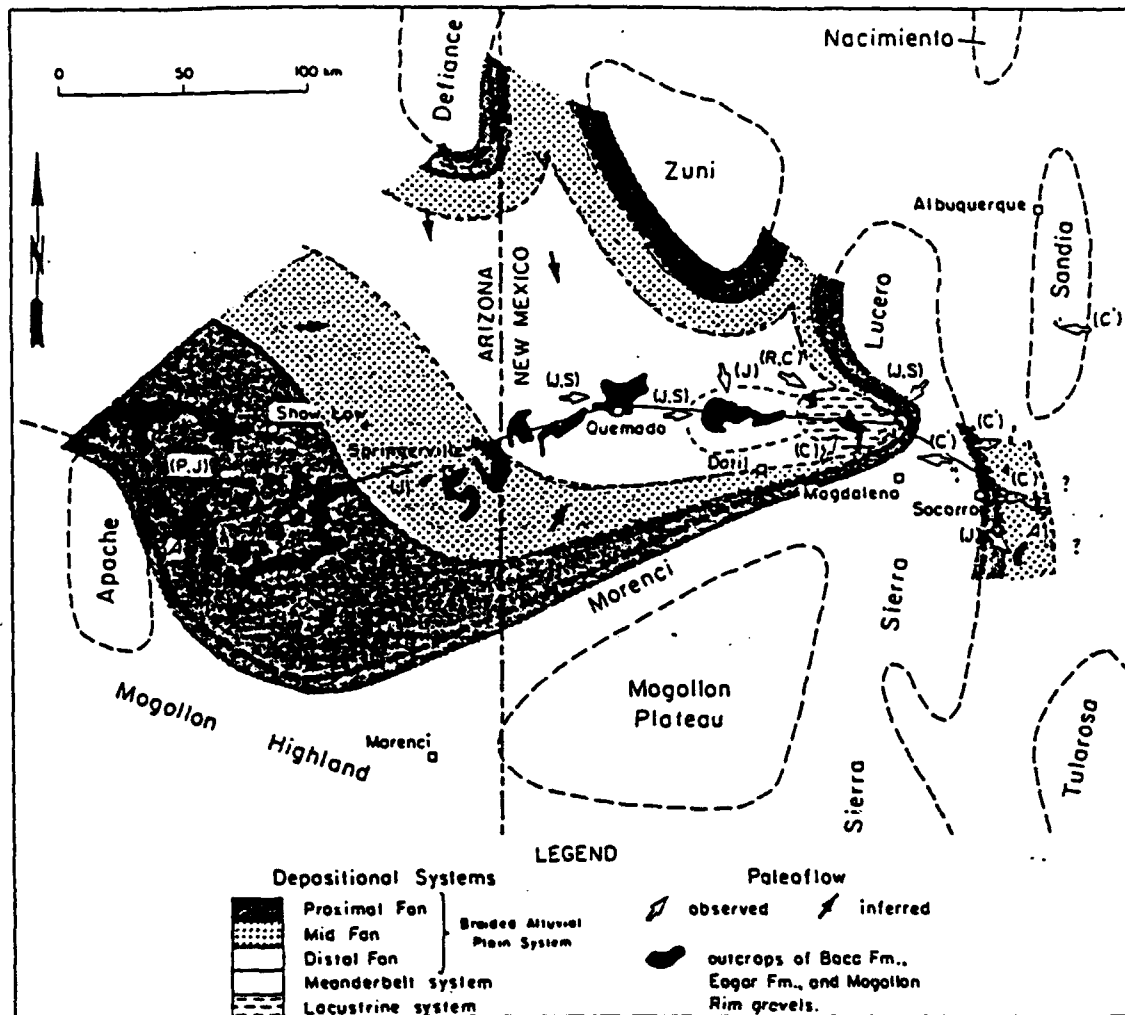


Figure 7. Map showing distribution of sediments off of the Laramide Mogollon highland and paleocurrent directions to the Mogollon Rim gravels, Eager fm and Baca fm. Southward-directed paleocurrent directions from the Defiance and Zuni uplifts show the southeastern Colorado Plateau to be a topographic low at this time. After Cather and Johnson (1986).

The surface features associated with these complexes are referred to in the literature as ignimbrite "flareups" (Elston, 1976; Coney, 1978a, 1978b). The exact cause of these events is unknown, although Coney (1978a) regards them as the result of the retrograde east-west sweep of igneous activity. These complexes developed during the mid-Tertiary, and in part owe their existence to an already heated crust (Coney, 1978a; Baldrige and others, 1989). Silicic volcanism occurred as far east as the Trans-Pecos volcanic field during this time (Barker, 1979). At the same time in southern Arizona, large metamorphic core complexes formed off the southern edge of the Colorado Plateau.

Within this province, loci for four mid-Tertiary volcano-plutonic complexes occur at the margins of the Colorado Plateau (Elston, 1989). The San Juan, Colorado (Lipman, 1989); White Mountains, Arizona; Marysville, Utah; and Mogollon-Datil, New Mexico volcanic fields (Elston and others, 1976a) contain batholithic volumes of extrusive material.

Of interest to this study is the Mogollon-Datil volcanic field, which lies within the transition zone between the Colorado Plateau, Basin-Range, and Rio Grande Rift tectonic provinces. Previous geologic and geophysical work yields inconclusive data to make a determination of the

relationship between this complex and the plateau. However, this complex created a volcanic display in the mid-Tertiary that rivals any volcanic activity over the history of the planet (Coney, 1978a), and its proximity to the Colorado Plateau is of importance to unravelling Cenozoic history in the region. A more detailed review of the Mogollon-Datil event is provided later.

#### Late Cenozoic

The mid-Tertiary period of ignimbrite flareup is correlated in space and time to the transition from Laramide compression to late Cenozoic extension. There is little debate that the stress field in the southwestern United States was strongly compressional during the Laramide, resulting in crustal shortening (Seager and Mack, 1986). Tension and crustal extension has been dominant in the late Cenozoic throughout the region (Seager and others, 1984; Henry and Price, 1986; Morgan and others, 1986). Elston and others (1976a) state that the high-silica volcanics were emplaced in a neutral stress field.

The late Tertiary brought block faulting, bimodal (mostly basaltic) volcanism, and extension in the southeastern Basin-Range and Rio Grande Rift provinces

(Coney, 1978a, 1978b; Morgan and others, 1986). Also, crustal thinning has occurred in both provinces (Warren, 1969; Cook and others, 1979; Olsen and others, 1979; Sinno and others, 1981, 1986; Daggett and others, 1986; Perry and others, 1988). Volcanic fields are associated with the southern margin of the Colorado Plateau in Arizona (Luedke and Smith, 1978) and the Jemez lineament in New Mexico (Aldrich and Laughlin, 1984). The tectonic style associated with this latest stage of deformation appears to be distinct from the previous ignimbrite episode, and the chemistry of the volcanics indicates a different source as well.

Many authors (e.g. Cather and Chapin, 1989) date the beginning of tension by the appearance of the bimodal volcanic suite. Thus, tension preceded faulting in the region (Price and Henry, 1984; Henry and Price, 1986). East-northeast extension apparently progressed from west to east across the region. Cather and Chapin (1989) date initiation of tension at 36 Ma in the Mogollon-Datil volcanic field, but not until 31 Ma in Trans-pecos Texas (Price and Henry, 1984; Henry and Price, 1986). Eocene extension is supported by Cather and Johnson (1986), who cite thickening of the Baca formation between the Hickman and Red Lake fault zones. These faults are therefore reactivated Laramide features, and now bound a shallow

Eocene graben. The timing of reactivation, however, is not well-constrained.

Seager and others (1984) have determined that two periods of extension have occurred in the Basin-Range and Rio Grande Rift immediately to the southeast of the Mogollon-Datil volcanic field. The first phase produced northwest-trending moderately deep basins and uplift of fault-block mountains. This may have reflected a back-arc environment about 29-28 Ma, during a westward progression of basaltic-andesite volcanism.

The latter phase of extension, from 9-3 Ma, may indicate accelerating or renewing of block faulting, now in a north-south trend. This is also associated in time with 1-2 km of regional uplift (Morgan and Swanberg, 1985), and is part of a west to east progression of block faulting which began at about 20 Ma in California. The driving force behind this phase of extension may be strike-slip tension generated by the San Andreas transform zone to the west (Seager and others, 1984), and other manifestations include lithospheric thinning, increased heat flow, and true basaltic volcanism, although true basalt is rare relative to basaltic andesite in New Mexico and Arizona (Baldrige and others, 1989).

An important point to note is that Basin and Range style faulting is not present in either the Colorado Plateau or the Mogollon plateau (Elston and others, 1976a; Coney, 1978a). This may indicate that the Mogollon plateau rests on the Colorado Plateau, but normal faulting occurs between the two as well (Dane and Bachman, 1965; Wilson and others, 1969).

On the Colorado Plateau, late Cenozoic tectonic activity has been confined to volcanism near its margins (Figure 8). In the study area, several volcanic centers have developed along a northeast trending line between the White Mountains-Springerville and Jemez Mountains volcanic fields (Luedke and Smith, 1978). This feature is referred to as the Jemez lineament (Aldrich and Laughlin, 1984). With the exception of the Zuni-Bandera field near Grants, New Mexico, Ander and Huestis (1982) found no gravity anomalies associated with these centers. Furthermore, Ander and Huestis presented magnetotelluric evidence that the gravity "root" of the Zuni-Bandera field is cold, and was probably emplaced before the Laramide orogeny. Thus, the recent volcanics along the lineament are probably derived from magma chambers beneath the upper crust, and are composed of a bimodal suite of alkalic and tholeiitic basalts (Ander and Huestis, 1982).

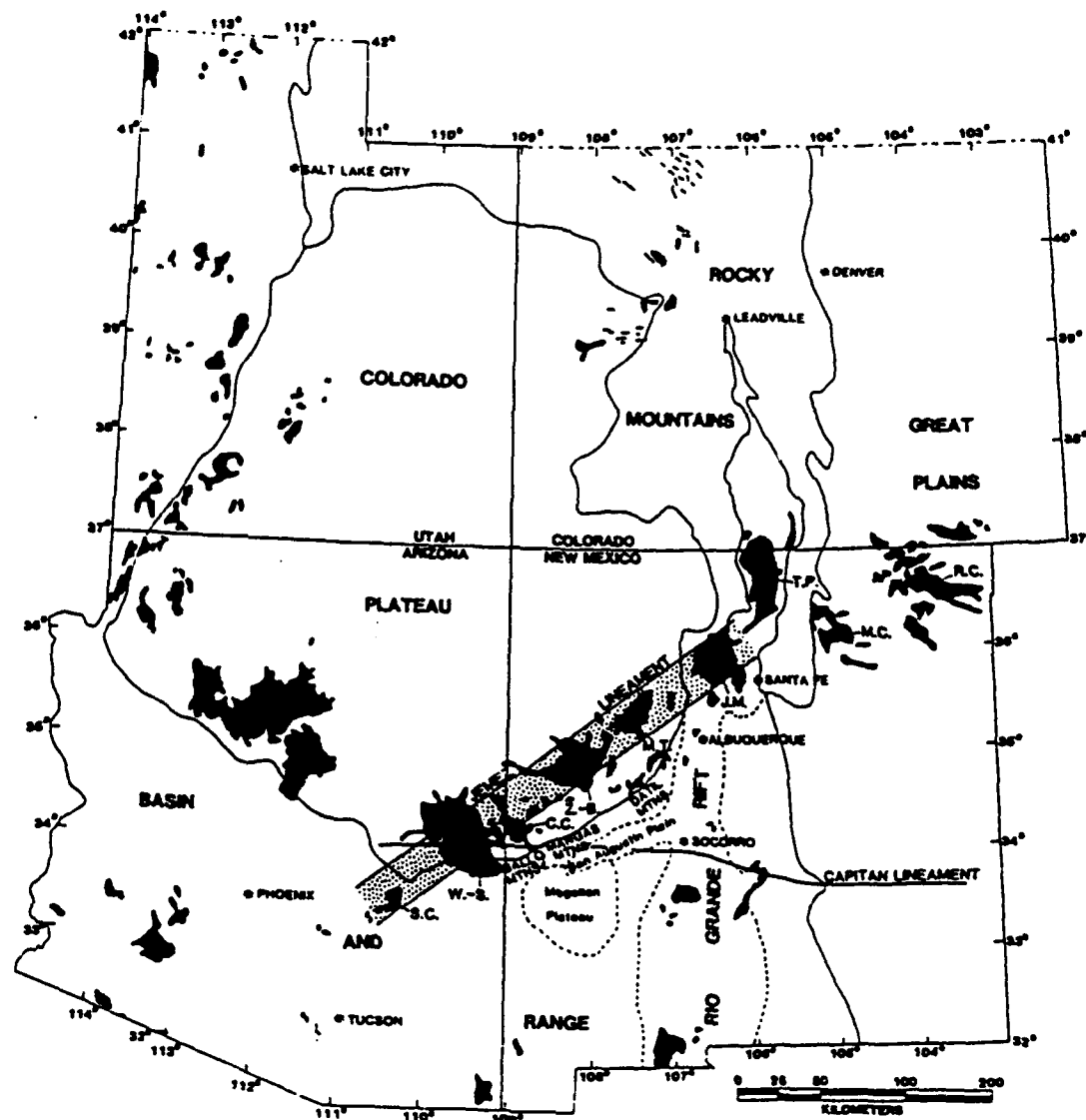


Figure 8. Map showing the Colorado Plateau and its relationship to surrounding provinces. The transition with the extensional provinces to the west, south, and southeast are marked by loci of several late Cenozoic volcanic fields. Labelled volcanic fields include: S.C., San Carlos; W.-S., White Mountains-Springerville; C.C., Catron County; Z.-B., Zuni-Bandera; M.T.-M.C., Mount Taylor-Mesa Chevato; J.M., Jemez Mountains; T.P., Taos Plateau; M.C., More County; and R.-C., Raton-Clayton. After Aldrich and Laughlin (1984).

## Present-Day Structure and Tectonics

### Colorado Plateau

The Colorado Plateau has remained relatively unaffected by tectonic activity with respect to the Basin and Range province and Rio Grande Rift throughout Phanerozoic geologic time. The base of the crust (Moho) under the plateau is estimated by seismic refraction experiments and surface wave studies to be 40-45 km below sea level (Roller, 1965; Topozada and Sanford, 1976; Keller and others, 1979a). However, crustal thickness is estimated to be 50 km by deep reflection profiling (Hauser and Lundy, 1989) and earthquake refraction data (Beghoul and Barazangi, 1989).

Upper mantle velocities determined by the seismic refraction surveys and surface wave dispersion studies are slow (7.8 km/sec at 40 km). Those found at 50 km (8.1 km/sec) are more typical of the stable North American craton. These data indicate that the Moho under the plateau may be transitional over a 10 km depth interval, and does not appear as a single reflector. The implications of this possible transition are not addressed or pursued in this study.

The seismic refraction study of Jaksha (1982) indicates a velocity of 8.0 km/sec at 33 km below the Mogollon-Datil volcanic field. This result must be viewed with caution because: 1) it has not been determined whether the Mogollon-Datil field is part of the Colorado Plateau; and 2) with an average of 18 km station spacing, these data lack the resolution of other work in the area. Both of these points are dealt with in the present study, as this line is reevaluated in light of new seismic information.

The slow seismic velocity at 40 km indicates that the upper mantle is presently hot. High electrical conductivities (Pedersen and Hermance, 1981) support this conclusion. Heat flow data (Reiter and others, 1975, 1979; Blackwell, 1978; Thompson and Zoback, 1979; Shearer and Reiter, 1981; Reiter and Clarkson, 1983; Swanberg and Morgan, 1985) show the interior of the Colorado Plateau to have moderate heat flow, about 1.5-1.8 HFU. This is bounded by a 100 km wide zone of increasing heat flow towards the Basin and Range and Rio Grande Rift (Lachenbruch and Sass, 1978; Swanberg and Morgan, 1985). The moderate surface heat flow does not predict deep temperature conditions implied by seismic refraction and electrical conductivity (Morgan and Swanberg, 1985). It is possible that the base of the crust

is presently the site of a thermal anomaly, but the thermal pulse has not yet reached the surface.

The present-day stress field of the Basin-Range and Rio Grande Rift provinces also appears to encroach on the margins of the Colorado Plateau (Humphrey and Wong, 1983; Aldrich and Laughlin, 1984). Geophysical studies at the Great basin-Colorado Plateau boundary in Utah (Keller and others, 1975) indicate lithospheric thinning and Basin and Range signatures inside the plateau margin. These studies indicate that the Basin and Range province is presently growing at the expense of the Colorado Plateau.

Despite this evidence for present day tectonism towards the margin of the Colorado Plateau, its free-air anomaly has a near-zero mean, indicating isostatic equilibrium (Keller and others, 1979a; Morgan and Swanberg, 1985). Inspection of the Bouguer gravity anomaly and topographic elevation (Thompson and Zoback, 1979) confirms that the Colorado Plateau must be isostatically compensated, and that the compensating material must be in the mantle.

#### Southern Arizona Basin and Range Province

Because of its elevation, southeast Arizona has been placed within the Mexican Highlands physiographic sub-

province of the Basin and Range tectonic province. This portion of the Basin and Range was uplifted in mid-Tertiary time along with the rest of the region, but not as much as the Colorado Plateau (Pierce and others, 1979).

There is evidence that the southern Arizona portion of the Basin and Range province has unique characteristics, and therefore may be differentiable from the rest of the province. For example, the free air gravity anomaly map shows a strong correlation with topography and surface geology (Aiken, 1978). This implies a homogeneous rigid lithosphere in isostatic equilibrium. A homogeneous crust is also inferred from heat flow data. Variability of all heat flow readings in southern Arizona ( $\pm 0.46$  HFU) is less than that for the entire Basin and Range ( $\pm 0.75$  HFU). Heat flow from wells greater than 650 m in depth show a southern Arizona heat flow of  $1.94 \pm 0.12$  HFU (Shearer and Reiter, 1981), which may be as little as 0.3 HFU higher than the Colorado Plateau. Shearer and Reiter state that the difference may be due to the greater volume of volcanics and plutons in the Basin and Range province, which implies a different lithospheric response to heating from below.

Some evidence exists for modification of the Basin and Range crust in recent time. Sinno and others (1981) suggest that crustal thinning in southern Arizona has occurred over

the past 5 Ma, roughly equivalent to the time that north-south structures were fully developed in the southern Rio Grande Rift (Seager and others, 1984) and commencement of regional uplift (Morgan and Swanberg, 1985). Late Quaternary faults increase in frequency towards the east side of the Basin and Range into the Rio Grande Rift, implying that Basin and Range-style faulting is still presently active in west Texas and southern New Mexico.

Seismic velocities display evidence of elevated upper mantle temperatures at the present time. This is based on studies showing anomalously low Pn values throughout southern Arizona: 7.67 km/sec in the southwest (Sinno and others, 1981) to 7.82 km/sec in the southeast (Gish and others, 1981). Beneath the Mogollon-Datil volcanic field, near the New Mexico-Arizona border, Gish and others (1981) found low (7.58 km/sec) Pn velocities. As will be discussed below, Pn velocity in the Rio Grande Rift are also low with respect to southeastern Arizona. The Basin and Range province of southeastern Arizona therefore has higher Pn velocities than in the surrounding extensional regions, but still reflects values that indicate a hot upper mantle.

The residual Bouguer gravity anomaly of Arizona is complicated by the overlap of shallow crustal and upper mantle heterogeneities (Aiken, 1978). This also appears to

be true for the Basin and Range as it enters southwestern New Mexico (DeAngelo and Keller, 1988). In order to interpret features of a given structural style or depth, bandpass filtering can be utilized (Aiken, 1978). However, Aiken also determined an almost exact correlation between a long-wavelength (800 km) regional anomaly and the elevation of gravity stations in southeastern Arizona. The long wavelength regional trend was therefore removed by cancelling the effects of topography, a procedure roughly equivalent to a high-pass filter.

Aiken (1978) and Sumner (1985) note that residual Bouguer gravity and magnetic trends are different between the Basin and Range and Colorado Plateau provinces. The trends are to the northwest in the Basin and Range, and to the northeast in the Colorado Plateau. They are separated by a northwest-trending 50 km-wide transition zone in which residual Bouguer gravity anomalies change by approximately 20 mgal (Aiken, 1978). Residual anomaly values are in general negative in the Basin and Range, and positive in the Colorado Plateau. These patterns are thought to be controlled by tectonic trends in the basement structure (Sumner, 1985).

The physiographic transition between the Basin and Range and Colorado Plateau provinces has been placed at the

Mogollon Rim (see e.g. Mayer, 1979; Pierce and others, 1979). Based on reversed seismic refraction profiling, Warren (1969) concludes that the Mogollon Rim lies above an abrupt change in crustal thickness of approximately 4 km in central Arizona. Additional thickening occurs from southwest to northeast as a result of a  $0.5^{\circ}$  dip on the Moho. However, other tectonic and geophysical indicators show that the boundary is more diffuse, and that a transition zone exists through which geophysical parameters change (Aiken, 1978; Brumbaugh, 1987).

The geological and geophysical evidence concerning faulting and stress, volcanism, heat flow, gravity and magnetic trends, and seismic data all point to the Basin and Range province as being a region of tectonic activity at present. Many questions remain concerning this province. Seismic investigations are currently being undertaken along the PACE (Pacific-Arizona Crustal Transect) in south-central Arizona (J. McCarthy, personal communication, 1989) and from Tyrone through Lordsburg to the Mexican border (S. Harder, personal communication, 1989).

## Rio Grande Rift

The Rio Grande Rift is a complex region with respect to structural style and evolution (Cook and others, 1979; Seager and Morgan, 1979; Morgan and Golombek, 1984; Olsen and others, 1987). It is a major continental rift system (Keller, 1986; Olsen and others, 1987). However, it was not recognized as such until the 1970s (e.g. Olsen and others, 1987; Keller and others, 1989). At that time, the extent of the rift was disputed, with some (e.g. Kelley, 1979) extending it southward only to about 33° N latitude, and others (e.g. Gries, 1979; Seager and Morgan, 1979; Smith and Jones, 1979) extending it as far southward as northern Mexico. Although it corresponds in style and timing with the Basin and Range province in southern Arizona, it has been shown to be a separate feature (Daggett and others, 1986; Sinno and others, 1986).

The region that defines the Rio Grande Rift is a zone approximately 1000 km long between central Colorado and northern Mexico (Kelley, 1979). It consists of a series of asymmetric grabens, and forms the eastern margin of the Colorado Plateau in New Mexico. South of the Colorado Plateau, its surface expression widens to include Basin and Range style block faulting in southern New Mexico, northern

Mexico and west Texas (Seager and Morgan, 1979; Olsen and others, 1987).

The Rio Grande Rift is a region of intense post-Laramide tectonic activity, but is enigmatic with respect to current tectonic deformation. For example, late Quaternary faults frequently appear throughout the rift (Seager and Morgan, 1979), yet contemporary seismicity is not differentiable from surrounding provinces (Jaksha and Sanford, 1986). Young volcanic centers with varying fluid compositions appear along the rift throughout New Mexico (Baldrige, 1979; Lipman and Mehnert, 1979; Warren and others, 1979; Zimmerman and Kudo, 1979), and mid- and upper-crust magma bodies have been identified (e.g. Sanford and others, 1977; Rinehart and others, 1979; Larsen and others, 1986). Yet the total volume of vented material is minor compared to the East African Rift (Olsen and others, 1987). Despite this seemingly controversial evidence, much geophysical data exists that shows the Rio Grande Rift to be an active tectonic feature, distinct from the provinces that surround it.

Quaternary faulting and volcanism are related to a change in lithospheric structure under the Rio Grande Rift. Many of these changes are related to heating at depth (Seager and Morgan, 1979). Heat flow readings exceeding 2.0

HFU are common. These values are thought to be caused by transport of fluids along through-going fracture systems in the crust (Reiter and others, 1979; Swanberg, 1979; Reiter and others, 1986). Heat flow values are also high near volcanic centers, yet are more intermediate away from them (Reiter and others, 1986). Due to the lag time necessary for conduction of heat, Seager and Morgan (1979) demonstrate that the intermediate background values do not preclude current heating at depth.

Further evidence for heating at depth comes from seismic velocity analysis. Sinno and others (1986) show intermediate crustal P-wave velocities within the rift when compared to Basin and Range (BRP) and Great Plains (GPP) provinces. They show upper-middle crust velocities of 5.9-6.1 km/sec in the Rio Grande Rift (RGR), as opposed to 5.8-6.0 km/sec in the BRP and 6.2 km/sec in the GPP. Middle crust values are 6.5 km/sec in the BRP, 6.6 km/sec in the RGR, and 6.7 km/sec in the GPP. They note that lower crust velocity differences between the BRP and RGR are near the error limit for their study, but the change in velocity could be caused by injection of basalt dikes under the rift. But upper mantle velocities are anomalously low under the RGR (7.7 km/sec as opposed to 8.0 km/sec under the adjacent BRP and 8.2 km/sec under the GPP). This implies a

significant amount of heat, and possible erosion of the mantle lithosphere.

The low Pn velocity found in seismic refraction studies for the upper mantle is also reflected in S-wave velocities determined from surface wave dispersion analyses. Keller and others (1979b) showed the Sn velocity to be about 4.4 km/sec (as opposed to 4.5 km/sec in the Colorado Plateau (CP) and 4.6 km/sec in the GPP), based on recordings from an earthquake in Chihuahua, Mexico. The travel path for that event, however, included a portion of the CP. A more complete analysis using surface waves recorded at World Wide Standardized Seismograph Network (WWSSN) stations at Albuquerque and El Paso (Sinno and Keller, 1986) found the Sn velocity to be 4.25 km/sec under the rift.

A local surface wave study in the Albuquerque-Belen basins (Schlue and others, 1986) shows two low velocity layers in the crust, with the Moho interpreted to be close to 38 km depth. The 19 km low velocity layer corresponds to the mid-crustal magma chamber identified by Sanford and others (1977). However, the 6 km low velocity layer and thickness of the crust were unusual results for this region. The near-surface low velocity layer was interpreted to be a possible newly-discovered magma chamber. However, Schlue and others (1986) point out that their resolvable data is

restricted to periods of 6-12 sec. The analysis of Sinno and Keller (1986) uses data resolvable between periods of 8-65 sec, and is in greater agreement with other geophysical data for the rift as a whole. But the discrepancy between the two studies should not be overly stressed, since dispersion between two recording points reflects the average velocity structure of the intervening material.

The studies of Keller and others (1979b) and Sinno and others (1986) also shows that the crust is thinner under the Rio Grande Rift than either side. The Moho in southern New Mexico lies approximately 27 km below sea level, and is at about 30 km and 50 km under the Basin and Range and Great Plains provinces, respectively. Thinned crust is supported by gravity analysis (Daggett and others, 1986), and appears to be thinnest under northwest Chihuahua, Mexico. Their gravity modeling also indicates that the upper mantle under the rift is less dense than would be expected, and they interpret the cause to be thermal expansion.

The combination of thinned crust, low-density upper mantle material, hot springs along deep (crustal penetrating?) faults, low rigidity and slow upper mantle velocities all point to the conclusion that heating is occurring at the base of the crust at the present time. At least one stage of lithospheric thinning occurred up to 8 Ma

ago (Perry and others, 1988), indicating that asthenospheric material has replaced mantle lithosphere in the region (Olsen and others, 1987; Perry and others, 1987). The total amount of thinning has not yet been established. Based on analysis of teleseismic data, Davis and others (1989) conclude that asthenospheric upwelling is presently occurring under the Rio Grande Rift. The amount of upwelling is greatest under the southern part of the rift.

In addition to crustal and lithospheric thinning, the Rio Grande Rift has been elevated along with the surrounding region (Kelley and Duncan, 1986). Superimposed on this uplift are areas of local uplift and subsidence (Reilinger and others, 1979). For example, the region near Socorro is undergoing active uplift, while downwarp is occurring in the immediate surrounding area (Larsen and others, 1986). Larsen and others suggest that the cause of this movement is the lateral flow of magma into the Socorro magma chamber combined with vertical fluid flow from depth.

These modifications to the lithosphere beneath the Rio Grande Rift and resulting geophysical signatures distinguish it from surrounding provinces (Sinno and others, 1986; Olsen and others 1987). However, it cannot be separated from adjacent regions within the context of post-Laramide tectonic events. For the purposes of the present

discussion, it is important to note the differences in velocity, gravity, crustal thickness and heat flow between the Colorado Plateau and the Rio Grande Rift in New Mexico. It is the transition between these provinces that is the target of this study.

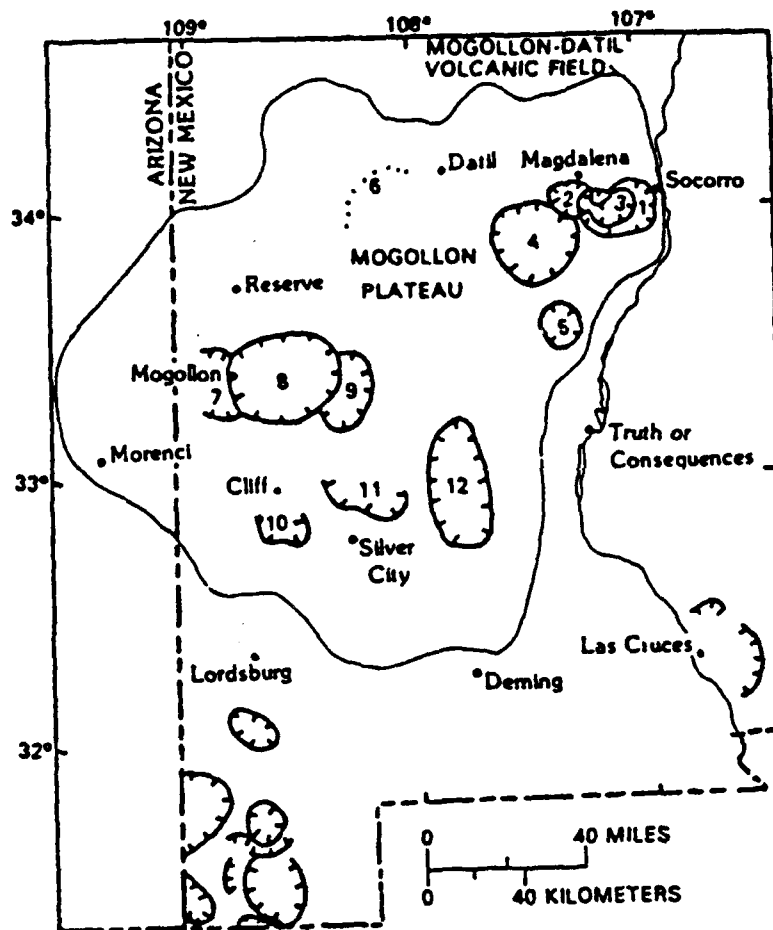
## MOGOLLON-DATIL VOLCANIC FIELD

### Introduction

The Mogollon-Datil volcanic field (MDVF) is located in west-southwest New Mexico, near the center of the present study (Figure 9). It is located in the transition zone between the Colorado Plateau, Basin and Range, and Rio Grande Rift provinces. Some associated volcanic centers appear to the south and southeast in the extensional provinces, but none are identified to the north and northwest on the plateau.

The MDVF is part of a province greater than  $1 \times 10^6 \text{ km}^2$  in area in which Laramide and post-Laramide volcanism is widespread (Figure 10). Elston (1989) considers it to be an outlier of the larger Mexican Sierra Madre Occidental to the south. They are now separated by the Mexican Highlands portion of the Basin and Range province (Figure 10).

Volcanism in the MDVF consists primarily of intermediate to silicic ash-flow tuffs and lava flows. These were vented by caldera-type volcanism as part of the ignimbrite flareup in western North America. At least 28 cauldrons have been identified (Figure 11), and up to 35 may exist (Elston, 1978).



#### CALDERAS

- 1 SOCORRO
- 2 MAGDALENA
- 3 SAWMILL CANYON
- 4 MT. WITHINGTON
- 5 NOGAL CANYON
- 6 CROSBY MTS. DEPRESSION(?)
- 7 MOGOLLON
- 8 BURSUM
- 9 GILA CLIFF DWELLINGS
- 10 SCHOOLHOUSE MOUNTAIN
- 11 TWIN SISTERS
- 12 EMORY

Figure 9. Sketch map of mid-Tertiary Mogollon-Datil volcanic field in southwestern New Mexico and far eastern Arizona. After Ratté (1989).

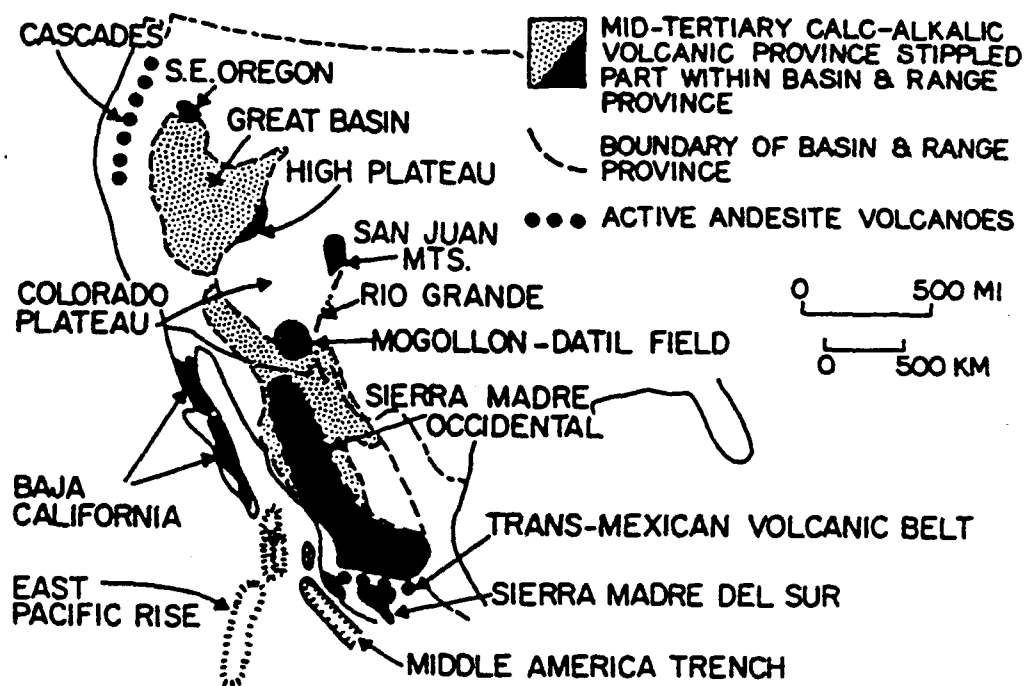


Figure 10. Map showing Mogollon-Datil volcanic field as part of a mid-Tertiary volcanic event that involved much of the western United States and Mexico. After Elston (1978).

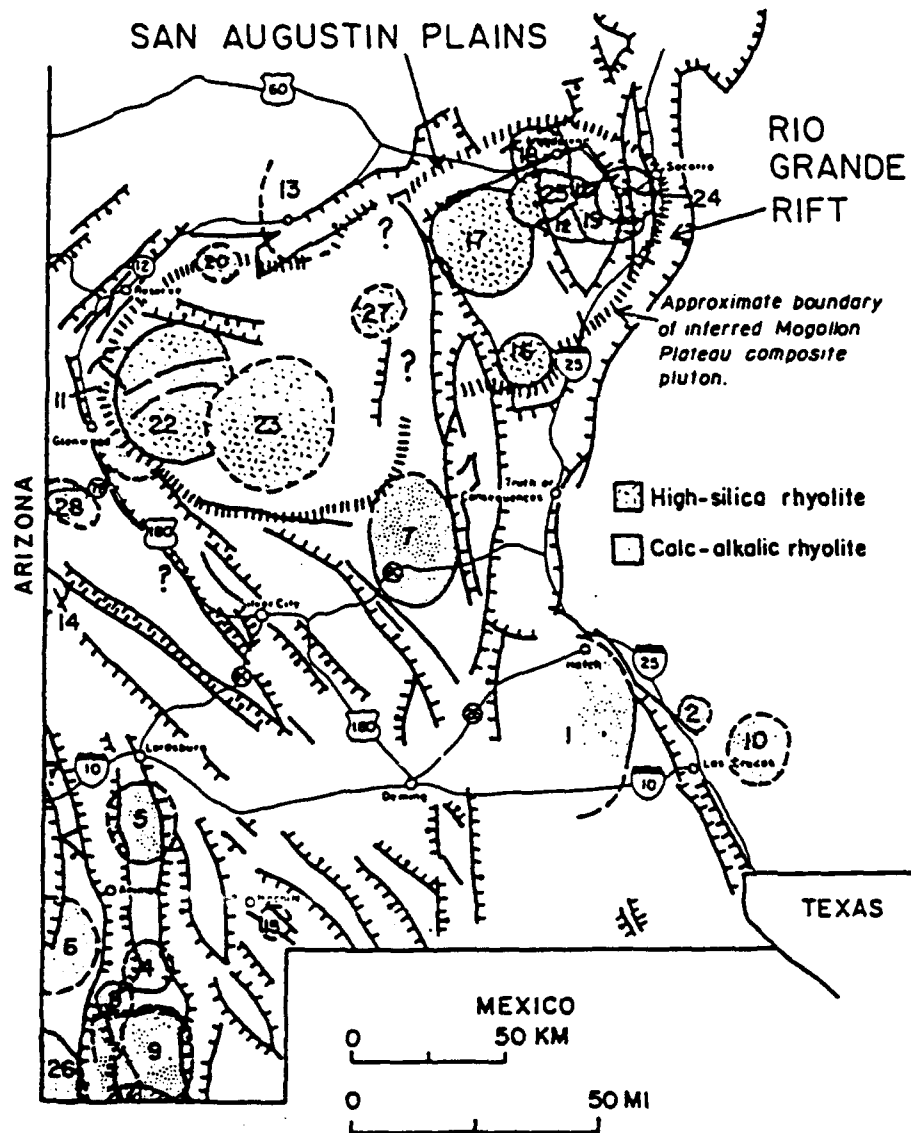


Figure 11. Intermediate to silicic ash-flow tuff cauldrons associated with the Mogollon-Datil volcanic field, southwestern New Mexico. For information on the numbered cauldrons, please refer to Elston (1978).

## General Geology

The MDVF consists of three volcanic suites (Elston and others, 1976a): 1) calc-alkalic andesite to rhyolite; 2) high silica alkali rhyolite; and 3) basalt and calc-alkalic basaltic andesite. These overlap in time and space, yet each appears to reflect different crustal and tectonic conditions at the time of extrusion (Figure 12).

The extrusives of the MDVF are found in and around a structural feature known as the Mogollon plateau (MP), described as a giant resurgent cauldron complex (Elston and others, 1976a). In its gross structure, the MP can be divided into three parts: 1) a broad, gently tilted interior platform showing relatively minor deformation with respect to its perimeter; 2) an encircling rim of uplifted material; and 3) an outlying graben system adjacent to the uplifts (Coney, 1976a; Elston and others, 1976a). The volcanic features on the plateau have been proposed to be the surface expression of an upper crustal granitic batholith (Elston and others, 1968, 1970, 1976a; Rhodes, 1976).

The volcanic units within the MP have been collectively termed the Datil group (Dane and Bachman, 1965). More recently, Cather and Chapin (1989) have informally expanded

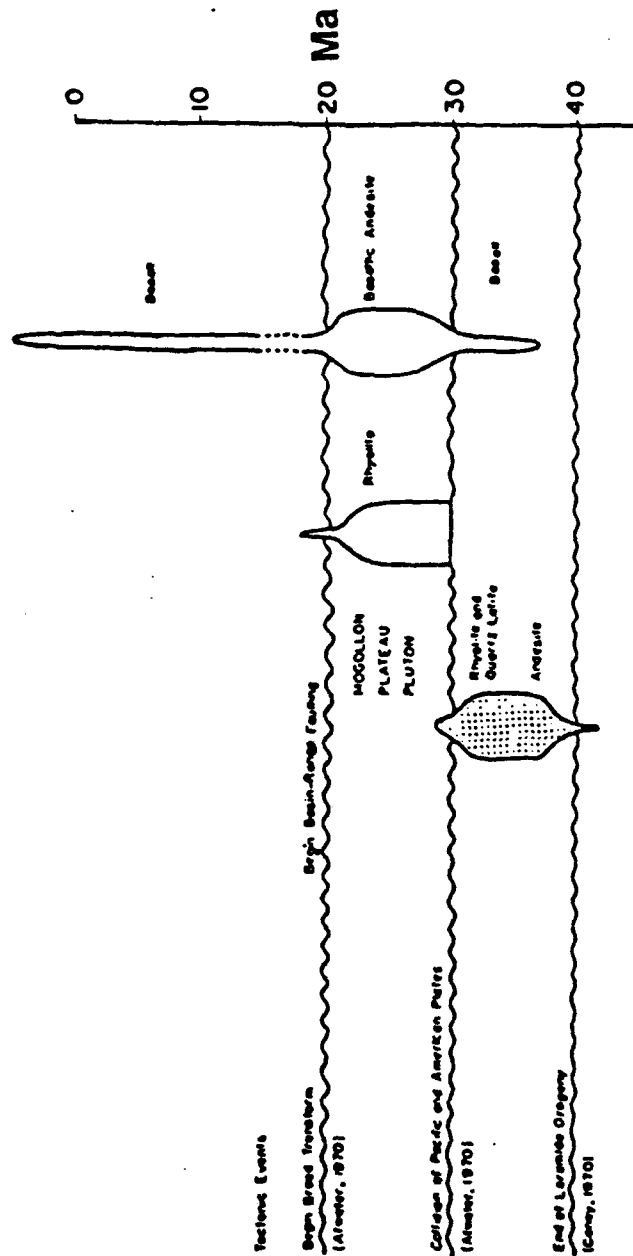


Figure 12. Timing and volume of post-Laramide volcanic activity in southwestern New Mexico and its relationship to tectonic events in the western United States. After Elston (1976).

the use of the term "Datil group" to include all sedimentation associated with mid-Tertiary volcanism in southwestern New Mexico. Their "lower" Datil group contains sediments included in the underlying Eocene Baca formation. The stratigraphic record indicates a smooth transition from the Baca formation, and the volcanics are grouped as andesite (with high  $K_2O$ ). The "upper" Datil group is composed entirely of volcanic deposits, now of bimodal composition. The two rock types representative of this group are mafic lavas, termed basaltic andesites, and silicic ash-flow tuffs. The transition is dated at 36 Ma and is thought to correspond to the change between Laramide extension and Cenozoic tension in the region.

#### Timing of Volcanism

Volcanism was initiated in mid-Tertiary time with the extrusion of the calc-alkalic andesite to rhyolite group (Elston and others, 1976a). Minor amounts of this suite began to vent at 43 Ma, with a significant increase in volume at 36 Ma (McIntosh, 1989). Source fluids for these rocks may have been derived from the remnants of a subducted slab, with probable upper mantle and/or lower crustal contamination. Elston and others (1976a) consider this

suite to be representative of Colorado Plateau margin-type volcanic material.

The last group of rocks to appear were the basalt and calc-alkaline basaltic andesites, erupted from 37-0 Ma. These are associated by Elston and others (1976a) to be typical of Basin-Range volcanism. They are thought to be of mantle origin, caused by the relaxation of the western North American plate after subduction ceased on its western margin (Elston, 1976; Elston and others, 1976a). Asthenospheric material was allowed to move into the lithosphere at liquidus temperatures during this time. Thus these groups are of different origin, although they intersect in space and time.

Overlapping both of these suites in time (32-21 Ma) are the rocks of the high silica alkalic rhyolite suite (Elston, 1976; Elston and others, 1976a; McIntosh, 1989). These form a distinctive group of rocks with respect to chemistry, location of volcanism, and possibly source location and composition. With minor exceptions, they occur entirely within the Mogollon plateau.

The bulk of magmatic activity occurred in late Eocene-early Oligocene time. McIntosh (1989) uses  $^{40}\text{Ar}/^{39}\text{Ar}$  chronology to show four major volcanic episodes, each separated by a hiatus, from 36.1 to 26.3 Ma. In general,

volcanic activity progressed from east to west and south to north. Three of the four episodes correlate in time to volcanism in the San Juan volcanic field in Colorado, implying consistent tectonic control on the east side of the mid-Tertiary Colorado Plateau.

### Mogollon Plateau

With the exception of about 2.5 km<sup>2</sup> of exposed underlying material, the MP is covered by volcanic rocks of Oligocene-Pliocene age (Coney, 1976a). The eruptive style for this structure is that of a series of overlapping flows, ash-falls, and pyroclastic and epiclastic debris (Elston and others, 1976a; Rhodes, 1976). The total thickness of the volcanic pile averages 3.1 km (Coney, 1976a; Rhodes, 1976). These units originate from overlapping resurgent cauldrons, ring-dike complexes and rhyolite domes.

Volcanic deposits within the MP unconformably overlie Precambrian crystalline rocks, Paleozoic-Mesozoic sedimentary rocks, and volcanic rocks of late Cretaceous to early Tertiary age (Krohn, 1976). The bulk of the volcanics on the MP is composed of high silica alkali rhyolite (Elston and others, 1976a).

There are several noteworthy geological and geophysical aspects of the Mogollon plateau:

1) With the exception of two minor centers of high silica extrusives (Red Mountain, Arizona, and the Mule Creek caldera, New Mexico), all of the high silica rocks are clustered in a region to the south of the Plains of St. Augustine and to the north of Silver City (Elston and others, 1976a).

2) There appear to be two types of felsic rocks within this suite: (a) A widespread, phenocryst-poor "framework lava"; and (b) A suite of phenocryst-rich lavas with varying composition that is spatially related to a source cauldron-"cauldron lava" (Rhodes, 1976). Sources for the framework lavas become younger as the center of the MP is approached, indicating a common, shrinking source region (Elston and others, 1976a).

3) During the time of high silica volcanism, the calc-alkalic and basalt to calc-alkalic basaltic andesite suites were not vented on the MP. Since they predate and postdate the rhyolite volcanism on the plateau, Elston and others (1976a) suggest that a geochemical barrier and/or thermal barrier were present under the MP from 32-21 Ma.

4) Gravity studies (Coney, 1976a; Krohn, 1976) show low values over the MP that cannot be completely explained by

surface geology. They interpret the anomaly to represent a mass deficiency in the upper crust.

5) The exterior grabens surrounding the MP are of Basin-Range type (Elston and others, 1976a). However, the grabens do not strike north-northwest as do other Basin-Range faults in the region. They appear to wrap around the MP. Elston and others (1976a) interpret this to be an indication of some type of barrier to faulting.

Taking these observations together, Elston and others (1976a) have deduced that a shallow granitic plutonic complex exists under the MP. Rhodes (1976) states that the framework lavas represent liquid from the main body of an individual batholith, but cauldrons represent areas above solitary, volatile-rich cupolas.

## DATA COLLECTION AND COMPILATION

### Seismic Refraction

Two previous seismic refraction studies were conducted across the Mogollon-Datil volcanic field (Figure 13). Jaksha (1982) reported on a partially reversed east-west profile between Morenci, Arizona and the White Sands Missile range, New Mexico. Harden (1982) collected data from an unreversed, north-northeast trending line between Tyrone and the Acoma Pueblo, New Mexico. Information from both of these studies were compiled for reanalysis in this study.

Between July 1987 and August 1989, the Harden (1982) line was reoccupied. The total number of stations deployed along this profile constituted a twofold increase of recorded data over the previous study, and an increase of approximately 125% over the MDVF as a whole.

Sources for this survey were quarry blasts at the Phelps Dodge open-pit copper mine at Tyrone, New Mexico. Since it was not possible to determine exact origin times from blast tickets provided by Phelps Dodge, a base station was installed on the mine property near the pit. Distance from the blasts to this base station never exceeded 3 km. Velocity of P-waves within the pit was determined to be 5.5 km/sec (S. H. Harder, personal communication, 1987)

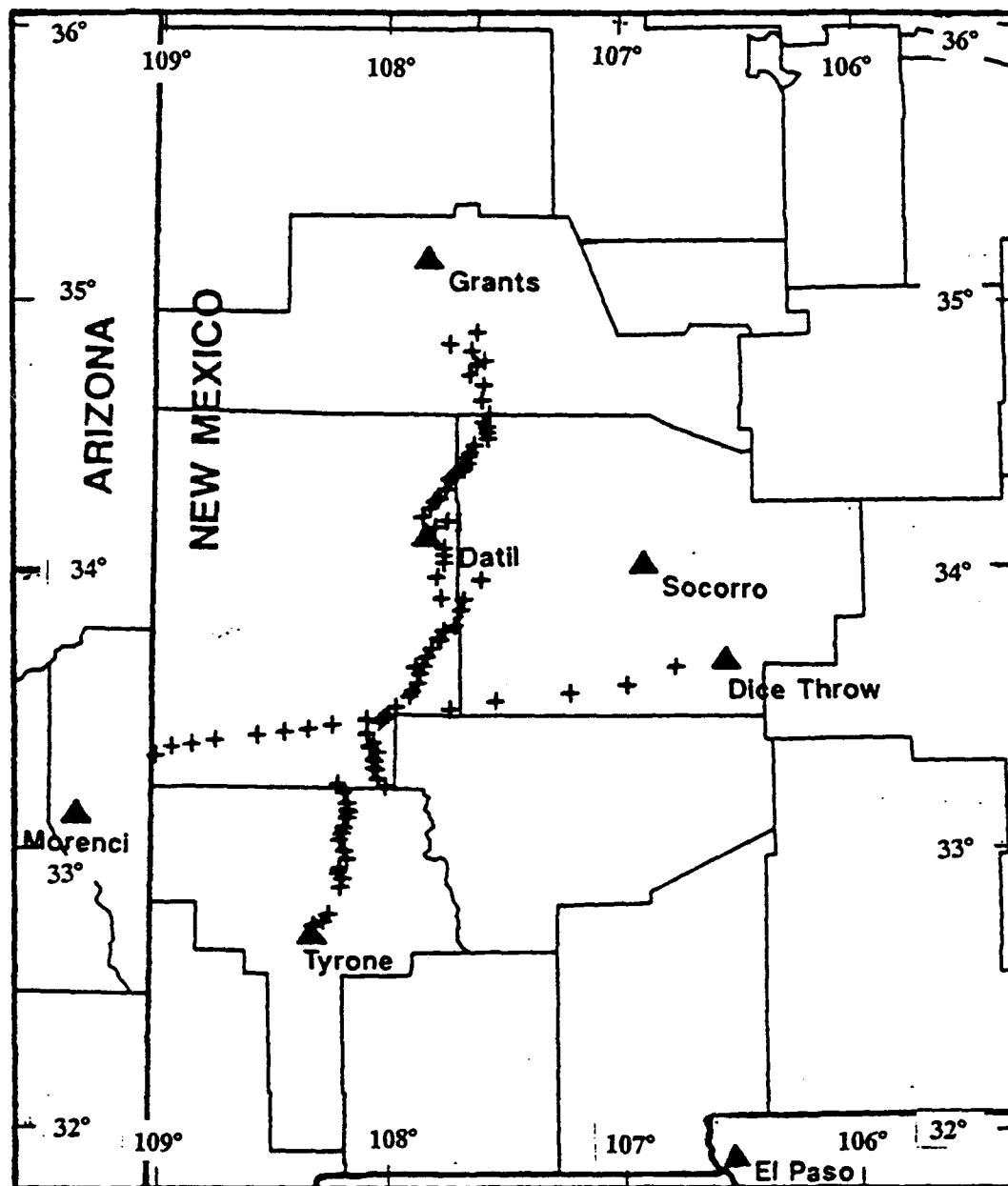


Figure 13. Location of seismic refraction lines used in the present study. The east-west trending line is from Jaksha (1982). Locations of seismic recording stations are indicated by a (+).

from a local study. With two exceptions, the base station was equipped with Sprengnether DR-100 recording instruments, with L4 geophones of 1 Hz natural frequency. These records were stored on cassette tape and later replayed with a DP-100 playback unit. The exceptions were two instances in which portable Sprengnether MEQ-800 analog recorders were used, records were stored on smoked paper and later visually inspected. Arrival time errors were never greater than .1 sec (smoked paper), and usually negligible (tape records). Source parameters are provided in Appendix I.

Stations were occupied by Sprengnether MEQ-800 portable seismograph stations. Portable FM tape recorders were connected to the MEQs to record the signal. Sprengnether S-7000 and L4 seismometers, both of 1 Hz natural frequency, were used in this study. Detailed data describing the stations are presented in Appendixes II and III.

In all, 59 distinct, good quality seismograms were recorded. Several sites were reoccupied in order to insure accuracy in source-receiver travel time and in order to insure good signal-to-noise ratios. In all cases where possible, the FM tapes were replayed into a DR-100 for digital sampling of the signal and then input as data files on the UTEP Department of Geological Sciences Hewlett-Packard HP-9000 computer. When data was unretrievable from

tape via this method, the signal was hand digitized, then resampled using a cubic spline routine. Signals used in this analysis were digitized at either .01 or .02 sec. An explanation of procedures for data retrieval is provided in Appendix IV. Each record was normalized to its greatest amplitude for display, so amplitudes of phases are not comparable from trace to trace. However, relative amplitudes are comparable within each trace in this study.

These records were then merged with the data from Harden (1982) to produce the record section shown in Figure 14, and the filtered record section in Figure 15. Arrivals of significant, recognizable phases were picked for each record and input to a ray tracing program for analysis.

Data from the Jaksha (1982) cross-line (Figure 16) was used in the present study for better control on three-dimensional structure. Arrivals were repicked from his record section, at an estimated error of less than 0.2 sec. A reversed profile for Pg and Pn from some of the stations was included in that study. The Pn branch was repicked with a similar estimated error as above, and used to constrain the upper mantle velocity and location of the Moho in this study.

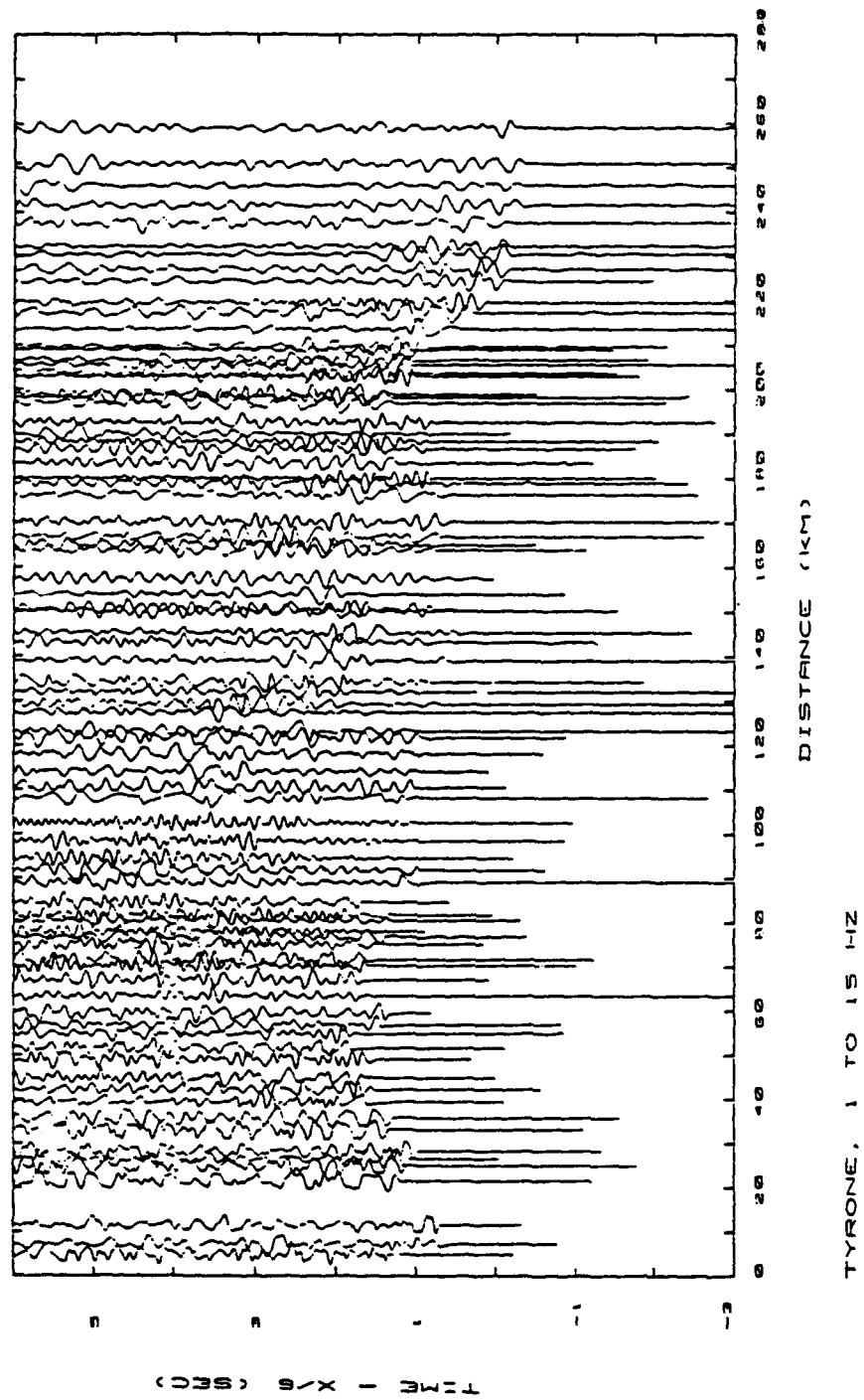


Figure 14. Seismic record section of the Tyrone-Acoma refraction line. Records were smoothed by a broad-band (1-15 Hz) filter.

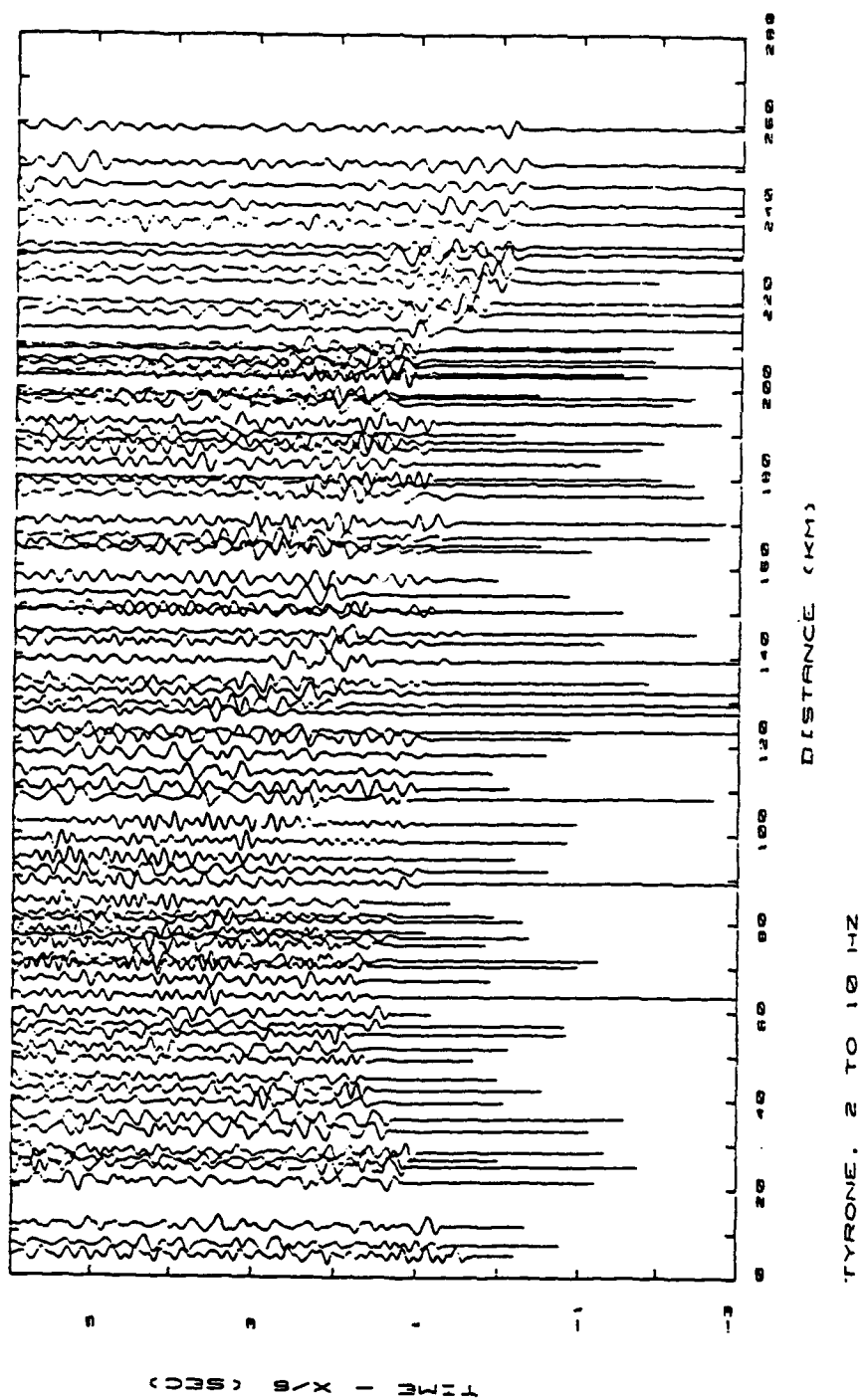


Figure 15. Filtered (2-10 Hz) record section, same data as in Figure 14.

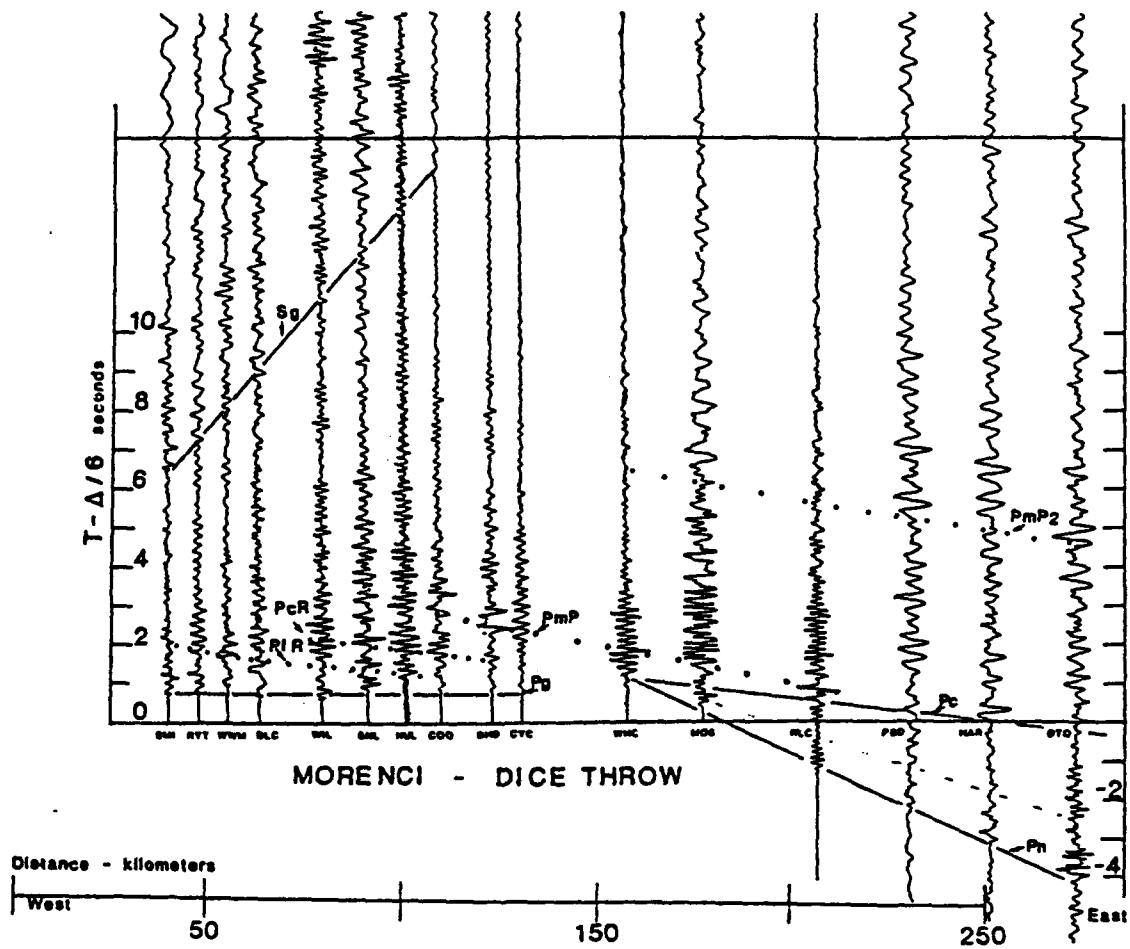


Figure 16. Seismic refraction line of Jaksha (1982), showing original picks used in that study.

## Gravity

The extensive gravity data base at the University of Texas at El Paso is well-documented (Daggett and others, 1986; Jenkins and Keller, 1989). This information source has been utilized in two ways: 1) to make gravity maps of the study area; and 2) to extract gravity profiles along each of the seismic refraction lines described above.

Complete Bouguer gravity anomaly values were retrieved from a region enclosed by  $31.0^{\circ}$  to  $36.5^{\circ}$  N latitude and  $105.5^{\circ}$  to  $112.5^{\circ}$  W longitude. A sea level datum and a density of  $2.67 \text{ gm cm}^{-3}$  were used in the Bouguer and terrain corrections for this study. The total number of available readings exceeds 40,000 in this area. Interpolated gravity values were derived at evenly-spaced (4 km) locations in the region, using the technique of minimum curvature (Briggs, 1974; Swain, 1976). To insure stability in frequency-domain filtering, a third-order polynomial surface was fitted to, and subsequently subtracted from the data (Figure 17). To separate trends for analysis, these data were then filtered using the technique of Peeples and others (1986).

Broad trends reflecting Moho-related features required a 125 km low-pass filter in the wave number domain in an area overlapping that of the present study (Daggett and

others, 1986). This filter has been applied and the results are shown in Figure 18. Upper crustal features in the study area are identified using a 15-125 km band pass filter (Figure 19).

Gravity profiles were extracted from the data base along strike of the seismic refraction lines used in this study. These consist of Bouguer anomaly values projected from gravity stations no more than 1 km from the profile. They are used in conjunction with the refraction lines for interpretation of the deep structure of the Mogollon-Datil volcanic field. Plots of the profiles are presented in the discussion section which follows.

#### Heat Flow

An extensive national heat flow data base has been provided for the present study (P. Morgan and J. Sass, personal communication, 1988). Data for Arizona and New Mexico have been extracted and are shown in Figure 20. This figure supports previous work which shows that: 1) the heat flow within the interior of the Colorado Plateau is relatively normal with respect to stable continental values; and 2) the heat flow in the Rio Grande Rift and Basin and Range provinces are above normal, with highest values

occurring near the boundary of the Colorado Plateau; 3) within these provinces, heat flow is highest near deep faults and late Cenozoic volcanism; and 4) groundwater circulation has complicated heat flow analysis in the region. These points are discussed in greater detail later.

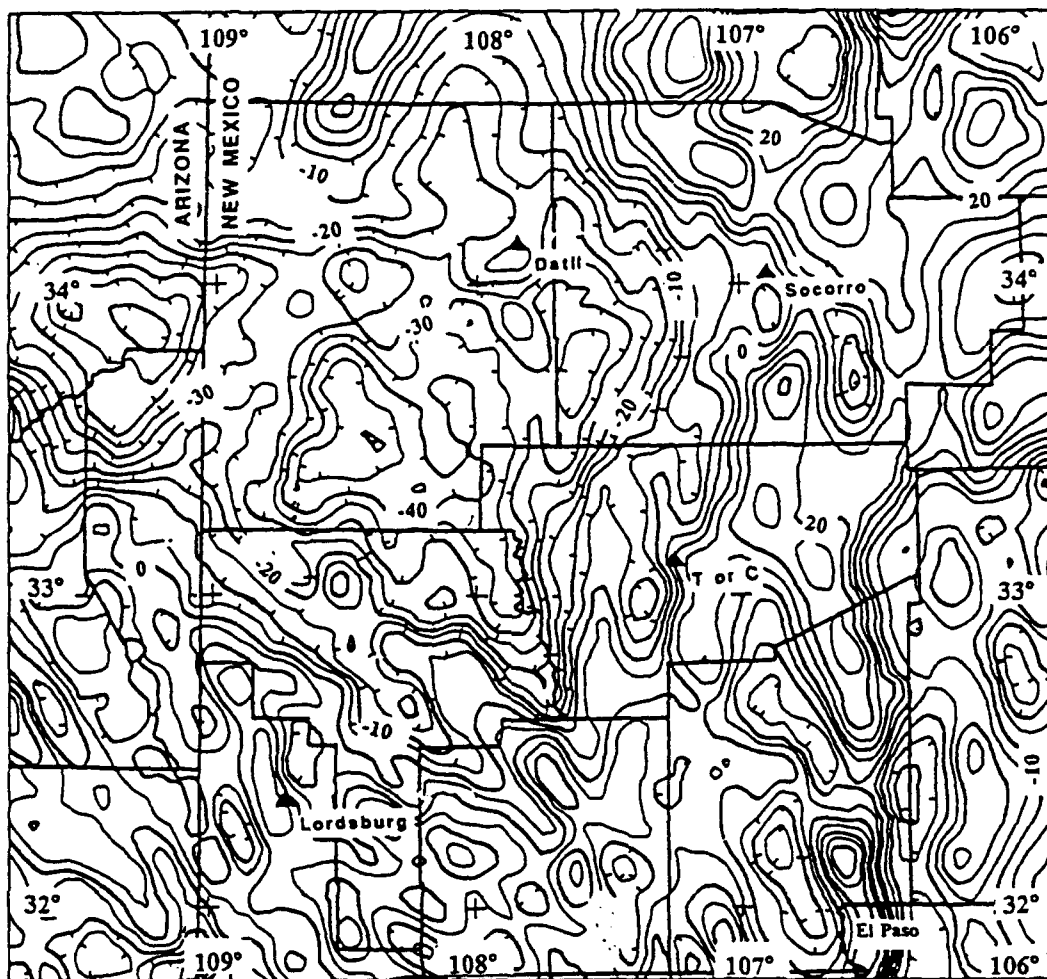


Figure 17. Bouguer gravity map of eastern Arizona and western New Mexico. A third-order polynomial surface fitted to the gridded values has been removed to produce this surface. Contour interval = 5 mgal.

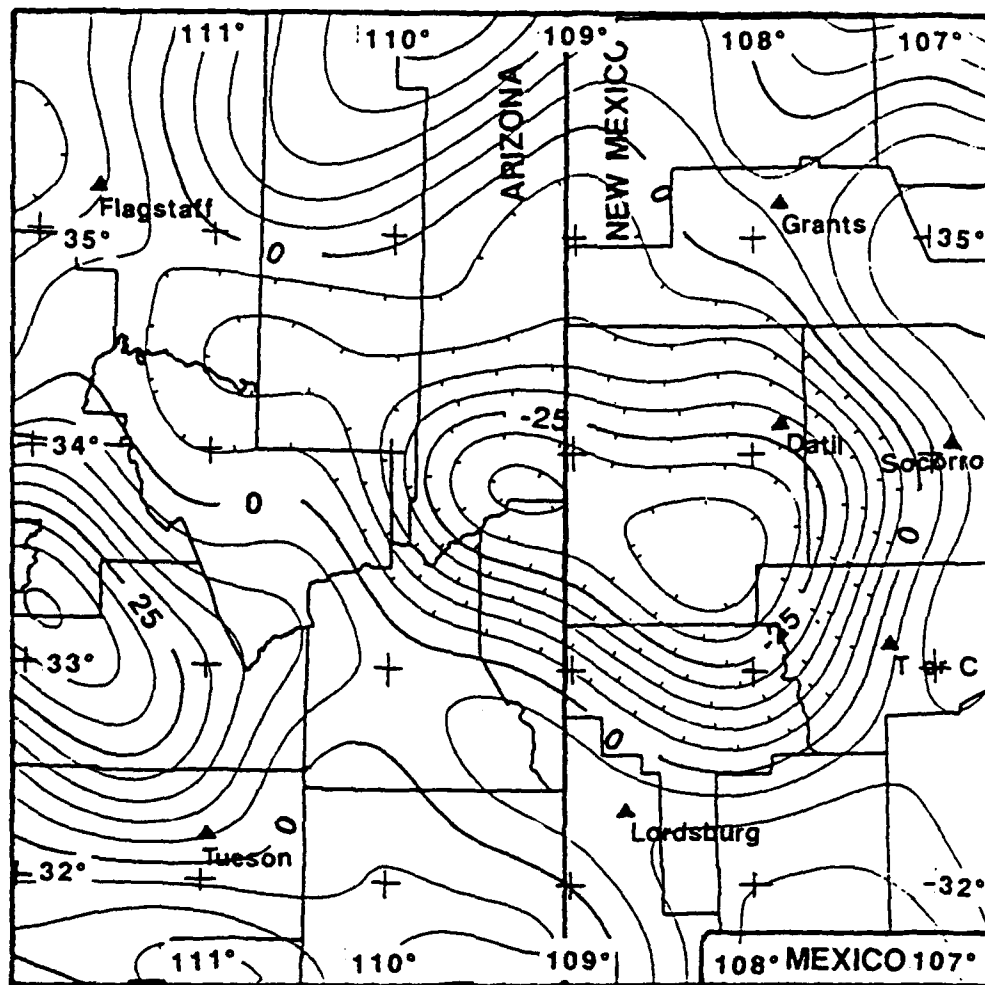


Figure 18. Regional Bouguer gravity anomaly map of eastern Arizona and western New Mexico constructed by a 125 km low-pass filter in the wave number domain. Contour interval = 5 mgal.



Figure 19. Regional Bouguer gravity anomaly map of eastern Arizona and western New Mexico constructed by a 15-125 km band-pass filter. Contour interval = 5 mgal.

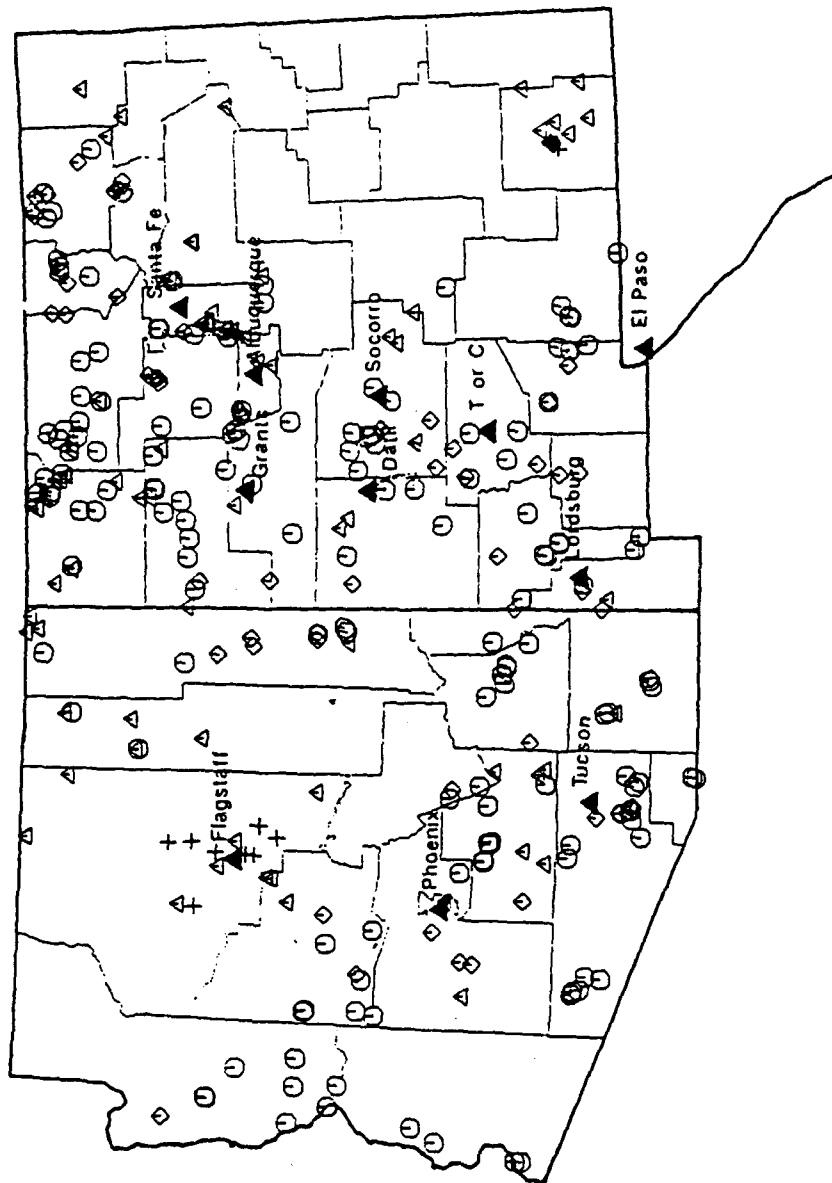


Figure 20. Heat flow readings in Arizona and New Mexico. Symbols indicate the corresponding range of heat flow values: pluses indicate  $\leq 0.8$  HFU; triangles correspond to 0.9 to 1.6 HFU; hexagons indicate 1.6 to 2.4 HFU; and diamonds correspond to values  $\geq 2.4$  HFU.

## DATA ANALYSES, MODELING AND DISCUSSION

### Seismic Refraction and Gravity Profiling

#### Technique

The Phelps-Dodge copper mine at Tyrone has been the source for several seismic refraction studies in southwestern New Mexico and southeastern Arizona (Figure 21). The crustal depth and velocity structure reported by Sinno and others (1986) was used as a constraint near Tyrone for the present study. The intersection of the Jaksha (1982) refraction line with this profile has proven beneficial in three ways: 1) resulting models must be consistent at the point of intersection, providing an additional constraint to layer thickness and velocity in each; 2) the ambiguity due to the lack of reversal of the N-S profile is reduced; and 3) they cross within the Mogollon plateau, a major target of this study.

Gravity profiles have been chosen to closely follow the seismic refraction lines described above. For each profile, gravity readings within 1 km were included by projection along a line perpendicular to its axis. Thus gravity data are used as an independent constraint to seismic model parameters. The objective of this analysis is to create an

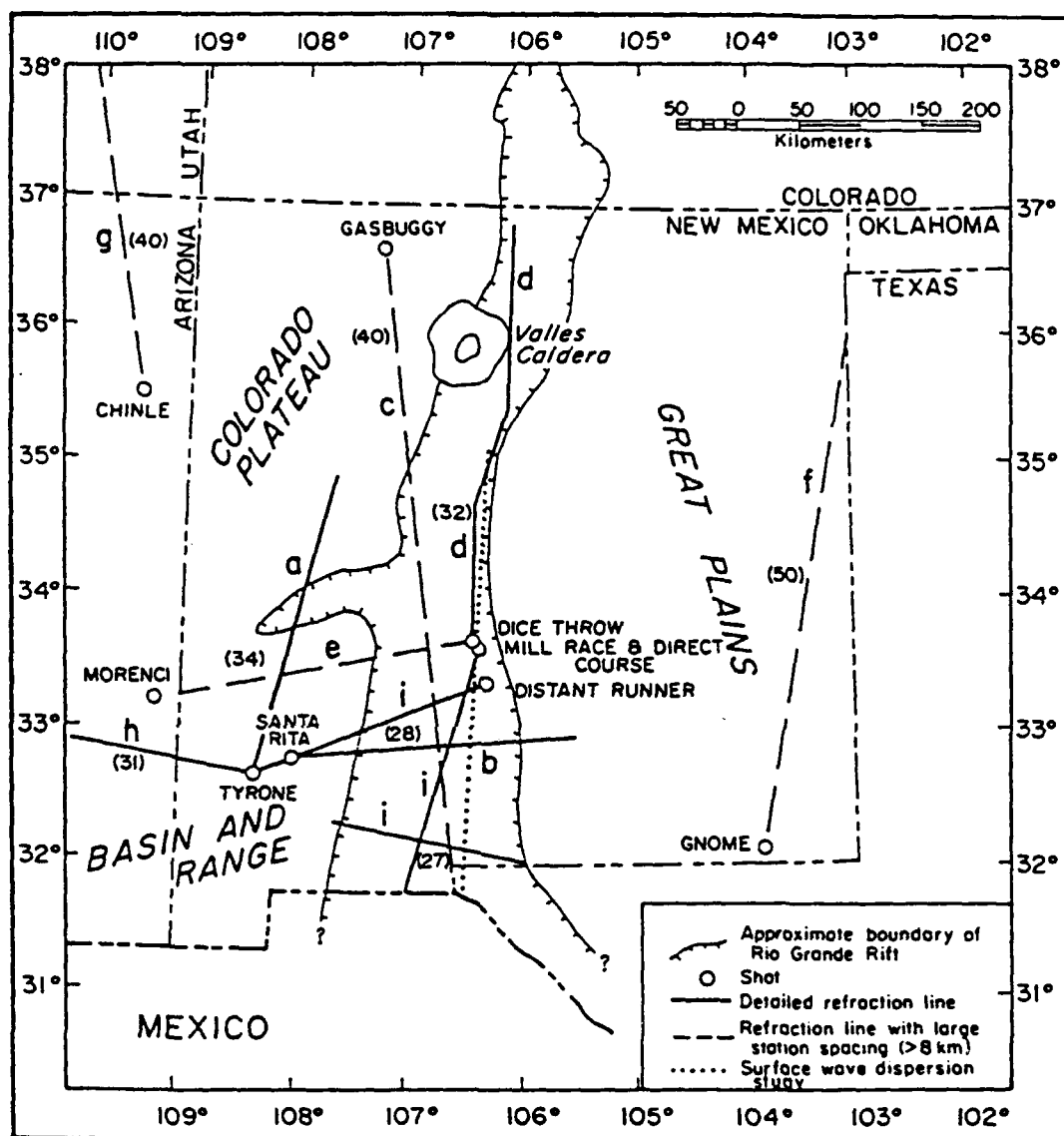


Figure 21. Location map for seismic analyses of the tectonic provinces and their boundaries in Arizona and New Mexico. Sources for refraction data: a (this study); b (McCullar, 1977; Cook and others, 1978); c (Toppozada and Sanford, 1976); d (Olsen and others, 1979); e (Jaksha, 1982); f (Stewart and Pakiser, 1962); g (Roller, 1965); h (Gish and others, 1981); i (Sinno and others, 1986).

earth model satisfying both of these data sets, the desired result being an image of present-day crustal structure.

The seismic modeling program used to determine earth structure is based on the algorithm described by Cerveny and Ravindra (1971). This technique, as applied by Leutgert (personal communication, 1989; see Hill and others, 1985), generates a model consisting of two-dimensionally varying earth structures. Many workers have used this ray-tracing technique, called asymptotic ray theory (ART), and it is well-described in the literature.

The computer program used to interpret the gravity profiles across the area is based on a 2.5 dimensional algorithm. The program is based on the technique of Talwani and others (1959) and Cady (1980). It was written by S. F. Lai at the University of Texas at Dallas, and modified extensively by D. Roberts (personal communication, 1989).

Depth to major velocity/density interfaces were the same for the seismic and gravity models at the point of intersection of the Tyrone-Acoma and Morenci-Dice Throw profiles, except for the near surface-upper crustal boundary. This exception is for the following reasons:

- 1) The seismic ray-tracing program is capable of including topography, while gravity data processing assumes reduction to a datum plane

effectively at the lowest station elevation. The Bouguer correction results in a D.C. shift equal to the portion of the correction due to material between this elevation and sea level.

2) Gravity and seismic stations do not coincide. Therefore, the gravity readings may reflect very local structure that does not influence the seismic ray path.

3) Near-surface inhomogeneities within the Mogollon plateau may cause minor disagreements between the two data sets.

The near surface structure is smoother in the seismic model than in the gravity model because of limitations in the ART approach. Because of computer time limitations, it was not possible nor desirable to model highly complex shallow structures. The near surface structure in the gravity models is more complex than required by either the gravity or seismic data, but this complexity reflects known geologic features. Thus, the gravity models should be considered large scale geologic cross-sections.

Known geologic information was used to create the initial model and constrain its evolution. When alterations to structure were suggested for a particular profile (gravity or seismic, Tyrone-Acoma or Morenci-Dice Throw)

during modeling, the effects on the other profiles were examined. Thus every modification required running two ART and two Talwani programs to observe its effect. More than 250 repetitions of these computer programs were run before a satisfactory earth structure was derived. The final model satisfies both refraction and gravity observations, ties to nearby results (Olsen and others, 1979; Gish and others, 1981; Sinno and others, 1986) and is compatible with surface geologic features.

#### Refraction Observations

Observed arrivals for major crustal velocity interfaces are shown respectively for the data of Jaksha (1982) and the present study in Figures 22 and 23. For this discussion, the following notations are used to identify different phases:  $P_g$  and  $P_n$  are critically refracted P waves from the top of the upper crust and upper mantle respectively; and  $P_{gR}$  and  $P_{cR}$  indicate reflections from the top of the upper and lower crust respectively.  $P_mP$  corresponds to the P-wave reflection from the M-discontinuity.

The Jaksha profile (Figure 22a) shows  $P_g$  to be a first arrival to a distance of 155 km, after which the  $P_n$  branch

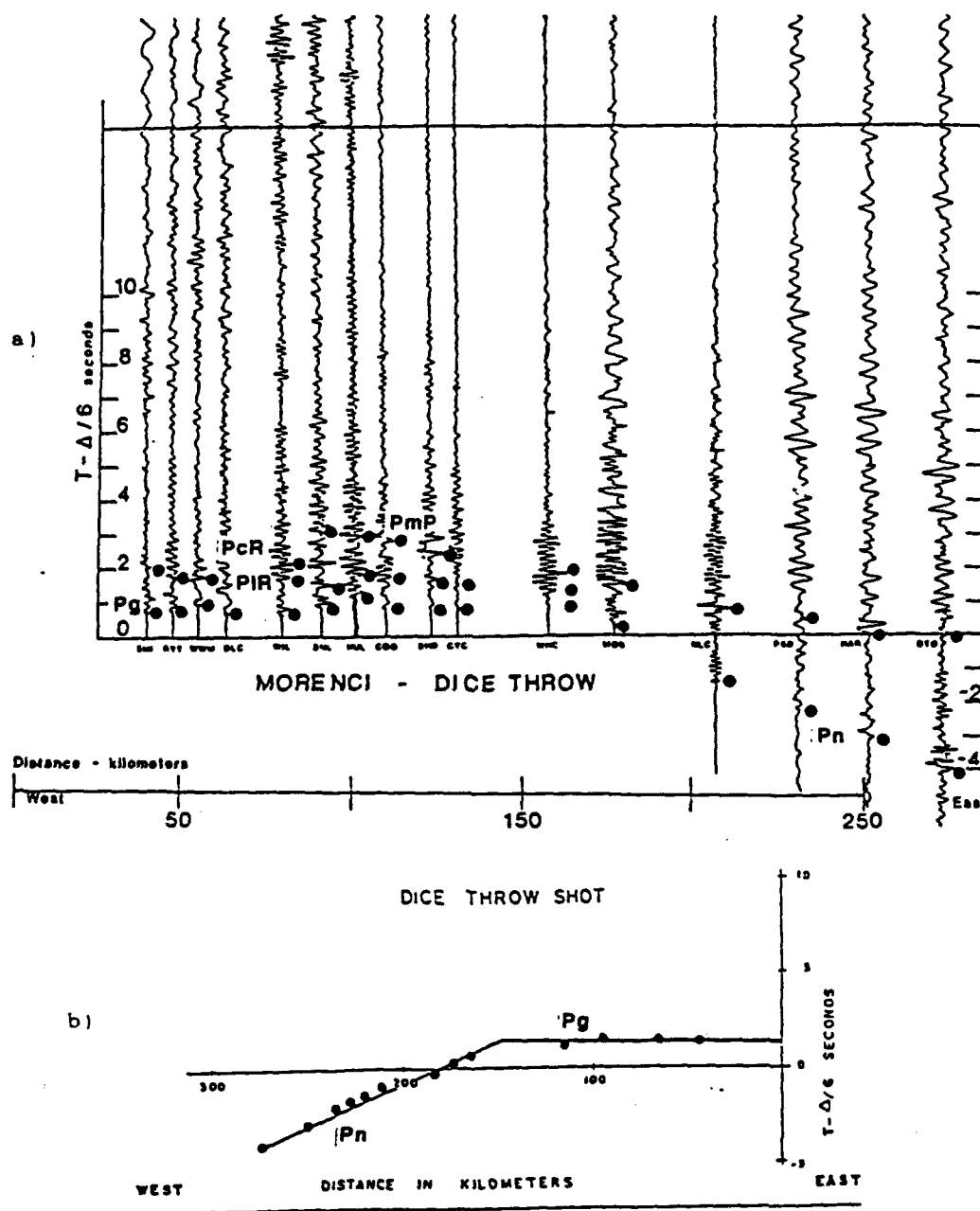


Figure 22. a) Repicked arrivals for Jaksha (1982) Morenci-Dice Throw refraction line.  
 b) Arrival picks for reversed Pn branch.

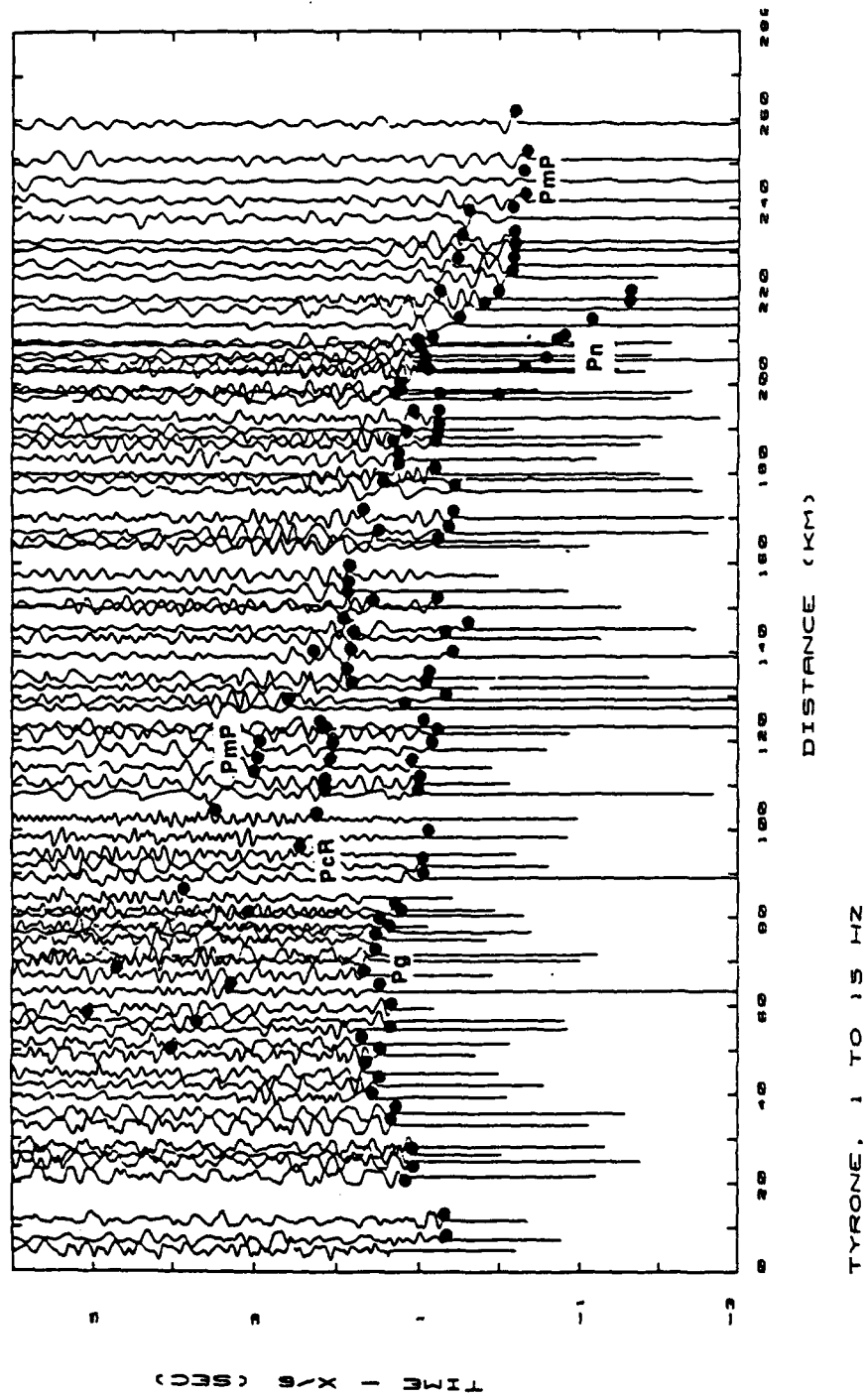


Figure 23. Arrival picks for Tyrone-Acoma refraction line.

becomes the first arrival. PgR, PcR and PmP never become first arrivals on this line, yet their arrival times combined with gravity data and the intersection with the Tyrone-Acoma line (this study) are important contributors to determining crustal structure. Upper mantle velocity structure and placement of the Moho is supported by the use of the reversed Pn branch (Figure 22b).

The density of seismic readings along the Tyrone-Acoma profile gives confidence to location and timing of arrivals. Analysis of Figure 23 shows several items of interest throughout the profile. Pg arrivals are delayed in the interval from 30 km to 85 km, indicating slow upper crustal velocities. Chatter in the Pg data is interpreted to be caused by topography and near-surface inhomogeneities in the volcanic pile within the southern Mogollon plateau.

PgR does not appear as a distinct arrival on the Tyrone-Acoma line. Possible reasons for this include: 1) The upper crust-middle crust interface does not produce a strong reflector; 2) The delay in Pg arrivals may have interfered with the identification of PgR; and 3) The time shifts due to near surface effects make reliable phase correlation impossible. PcR never occurs as a first arrival in this region, yet it gives valuable information that provides a constraint to the gravity model derived for this

profile. Pn becomes the first arrival at approximately 170 km, and ceases to be observed beyond 220 km.

The most striking feature in the Tyrone-Acoma profile is the time shift in PmP arrivals from 210 km to 225 km. Across this interval, PmP arrivals step almost 1.5 sec forward on the reduced ( $T - X/6$  sec) travel time plot. Early arrivals indicate that: 1) seismic rays now pass through faster material; and/or 2) the distance traveled has been shortened. A change of fundamental importance within the crust has created this step, and must be accounted for in the final integrated model.

#### Gravity Observations

Gravity profiles for both refraction lines are shown in Figure 24. A gravity low is apparent in the center of the Jaksha line (Figure 24a). It is approximately 80 mgal lower than the west end and 70 mgal lower than the east end (disregarding the Rio Grande graben anomaly at 270 km distance). By itself, this low does not constrain the density difference or depth of the causative anomalous body. However, the half wavelength (about 250 km) suggests a deep, possibly Moho-related feature. A depression or sag is observed within this low from about 50 km to 165 km. This

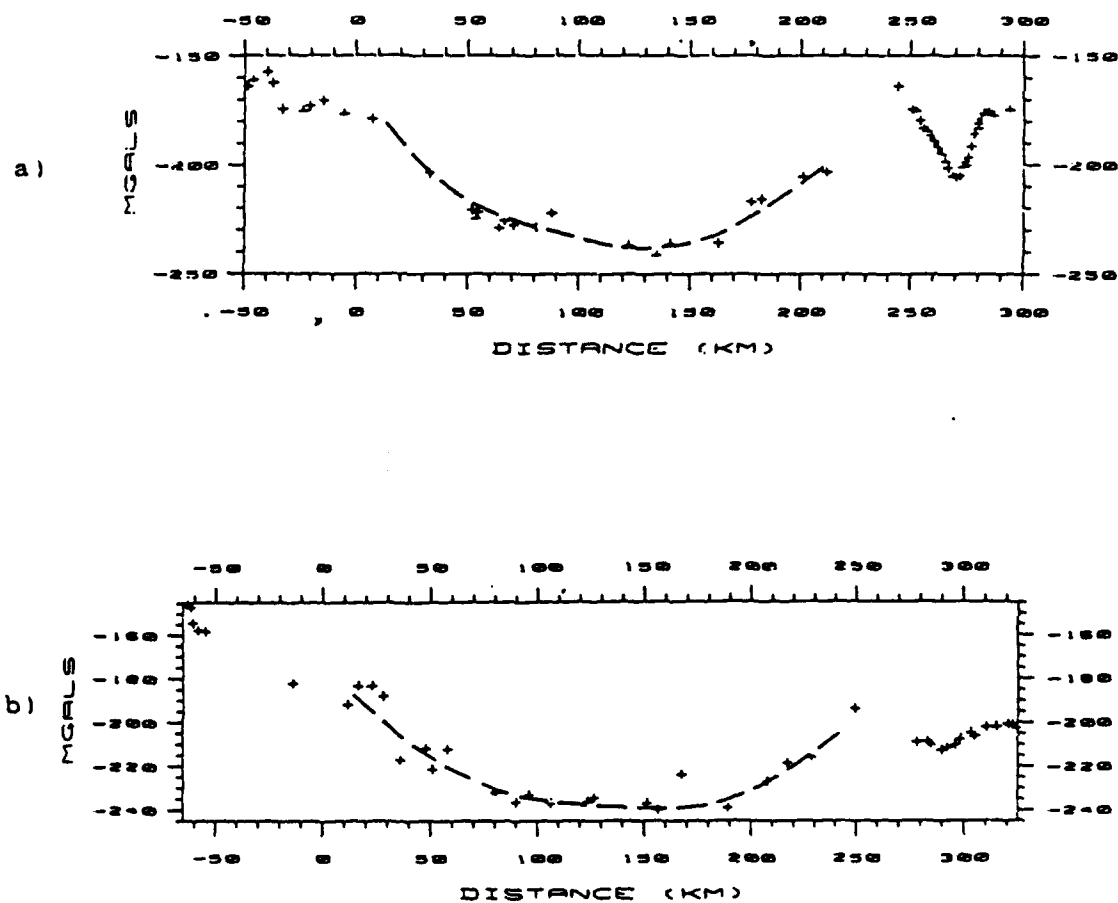


Figure 24. a) Gravity field for profile along Jaksha (1982) refraction line.  
 b) Gravity field for profile along Tyrone-Acoma refraction line.

feature, about 115 km in half wavelength, may be caused by an upper crustal anomalous body. The Tyrone-Acoma gravity field also displays a low in the center of the profile (Figure 24b). Values in the center of this feature are nearly 100 mgal lower than those at the south end, and nearly 50 mgal lower than the north end. Thus, it is superimposed on a slope in the regional gravity field that becomes more negative to the north. Along the Morenci-Dice Throw line, a subtle depression is observed from 50 km to 200 km within the larger negative anomaly.

#### Model Generation and Evolution

Jaksha (1982) used a flat-lying, homogeneous layered model to interpret his results for the Morenci-Dice Throw profile. His model was approximately duplicated using ART modeling and the result is shown in Figure 25. Although this structure is adequate in reproducing observed arrivals, it yields a Bouguer anomaly field that does not match observed values (Figure 26). Since the gravity field indicates greater complexity within the crust and upper mantle, alternative models were generated.

The first alternative is one in which the gravity anomaly is derived entirely by crustal thickening (Figure

27). This model shows that a near-surface pluton is not necessary to satisfy gravity observations. The resulting model was then used in the ART seismic ray-tracing program, and the result is shown in Figure 28.

For the Morenci-Dice Throw profile, it appears from seismic and gravity data that crustal thickening is a viable explanation of geophysical anomalies in the region. The maximum thickness of the crust does not exceed 37 km along this line, which is intermediate between the Colorado Plateau and Basin and Range/Rio Grande Rift provinces. The effect of the upper mantle density change under the Rio Grande Rift is to slightly thin the crust at that point. However, crustal thinning would still be observed even if the upper mantle density were made homogeneous, and the outcome of the analysis is unchanged.

The margins of crustal thickening correspond approximately to the -20 mgal contour line of the low-pass gravity map in Figure 18. If this association holds in southwestern New Mexico, the thickened crust is present nearly as far south as Silver City. Therefore, a model based purely on thickened crust indicates that the region between Morenci and Dice Throw is part of the transition zone.

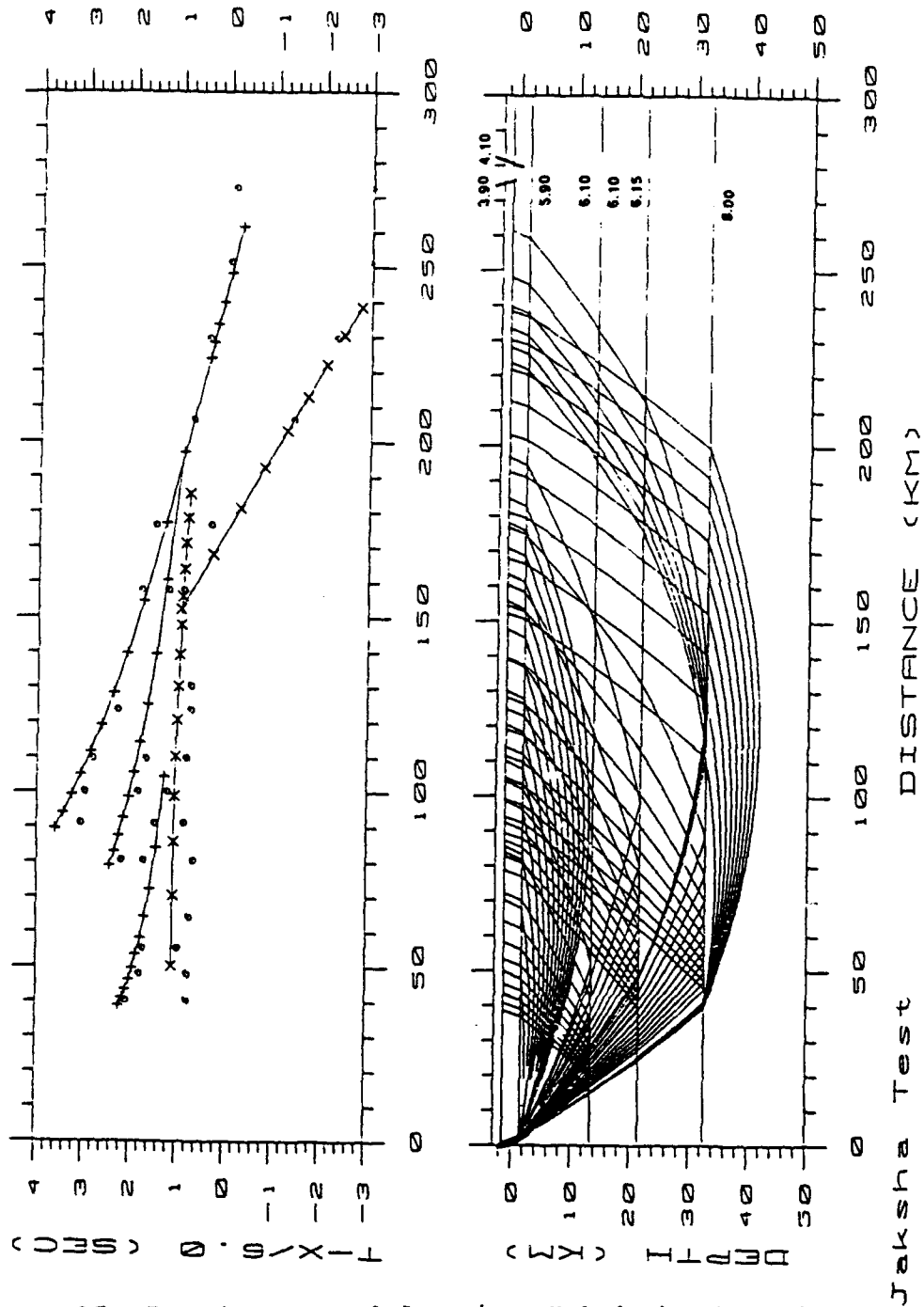


Figure 25. Ray trace model using Jaksha's (1982) interpretation of crustal structure from the Morenci-Dice Throw refraction line. Velocities are in km/sec. Symbols: o = observed arrivals; + = calculated reflection arrivals; x = calculated refraction arrivals.

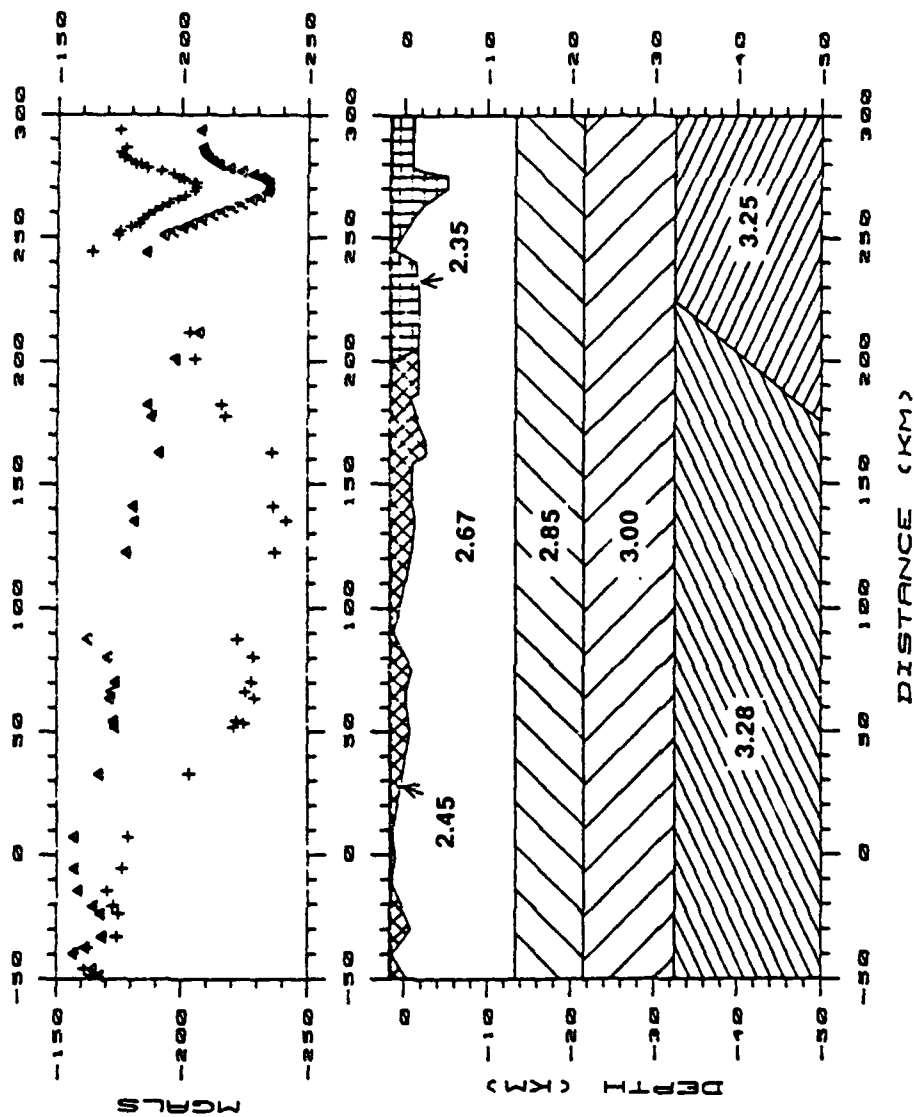


Figure 26. Gravity profile based on Jaksha's (1982) earth model. Pluses (+) indicate observed values; triangles reflect model-calculated gravity field. The flat-lying structure obviously does not fit the observed data. Values for density are in  $\text{gm/cm}^3$ .

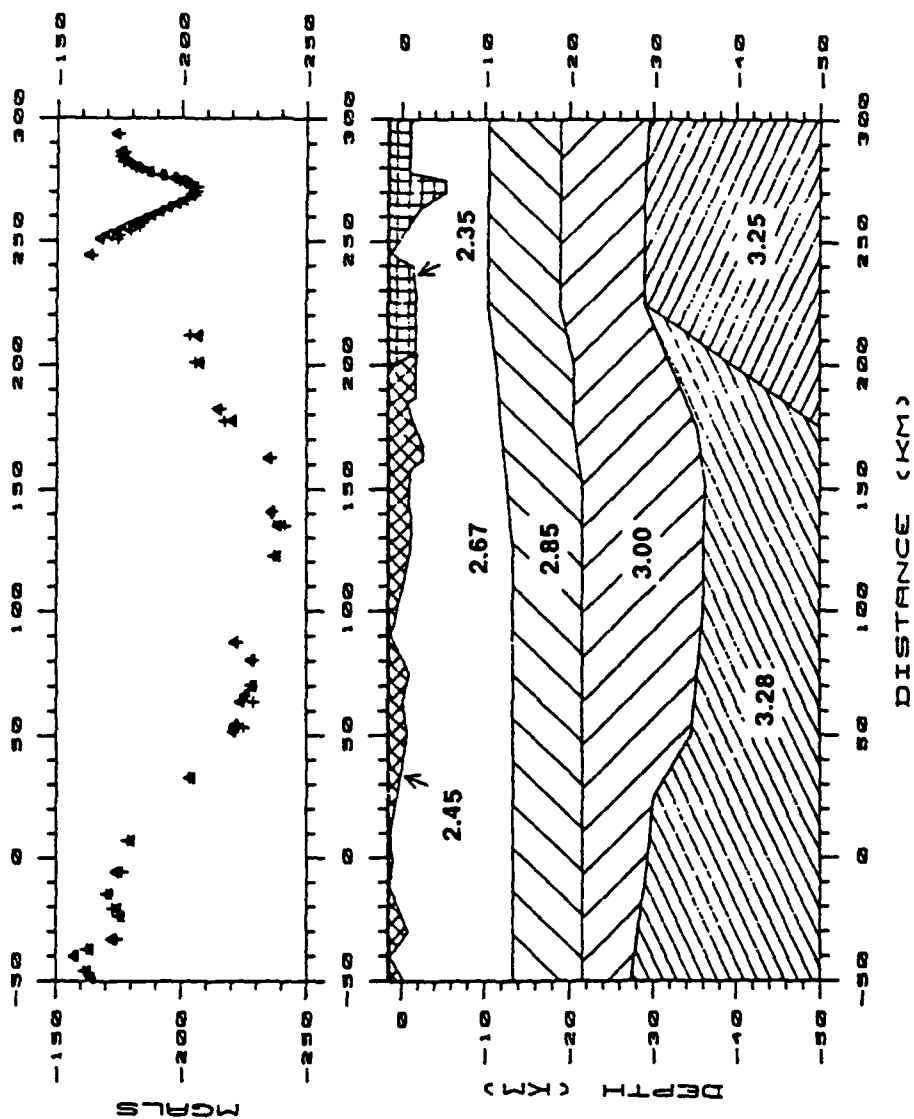


Figure 27. Gravity model for thickened crust showing the fit of predicted values to observed data along the Jaksha (1982) refraction line. Pluses (+) indicate observed values; triangles reflect model-calculated gravity field. Crustal thickening is sufficient to account for the observed anomaly. Values for density are in  $\text{gm/cm}^3$ .

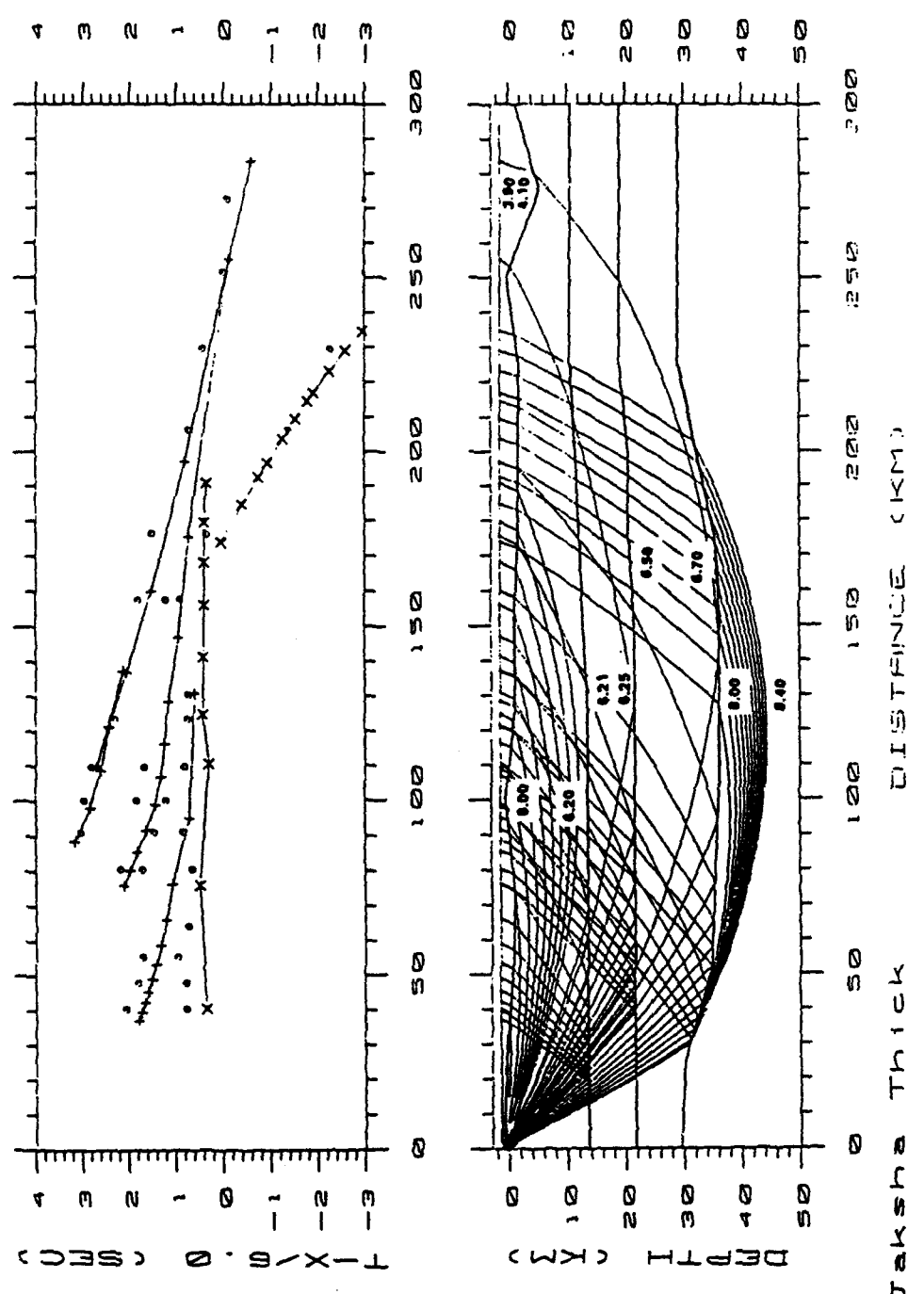


Figure 28. Thickened crust seismic ray-tracing model for the Jaksha (1982) refraction line using re-picked arrivals for this study. Symbols: o = observed arrivals; + = calculated reflection arrivals; x = calculated refraction arrivals. Velocities are in km/sec.

The second alternative investigates whether a near-surface pluton could account for the gravity anomaly instead of crustal thickening. Of primary concern for this model is the tradeoff between density contrast and volume. The density of a granitic pluton is almost always lower than that of the displaced country rock (Bott and Smithson, 1967), usually within the range of  $-0.05$  to  $-0.18$  gm/cm<sup>3</sup>. Bott and Smithson find that the departure is rarely more than  $-0.2$  gm/cm<sup>3</sup>. For the present study, the density contrast of the pluton is set equal to  $-0.1$  gm/cm<sup>3</sup> with respect to country rock (in a lateral sense), a conservative value within their range.

The volume of the plutonic complex must now be considered. E. A. Anthony (personal communication, 1989) states that venting of a pluton into a caldera volcanic complex may remove from 10-90% of the original volume of the magma. If the plutonic complex of Rhodes (1976) and Elston and others (1976a) covers the same lateral extent as the outline of the caldera complex, the thickness of the underlying magma chamber can be calculated using the formula for the gravitational attraction of a cylinder. Given an average thickness of 3.1 km of volcanic pile, 90% removal of liquid from the underlying chamber yields an approximately 0.33 km thick pluton. This pluton is too thin to have

significant effect on the gravity field or the wide angle seismic measurements. Venting of 10% of the magma chamber yields a residual pluton about 27.9 km thick. Since this represents almost the entire thickness of the crust, the 10% scenario was also discarded for this study.

Two models were therefore developed with plutons of intermediate thicknesses: 1) 50% of the magma was vented to the surface, leaving a 3.1 km thick pluton in the subsurface; and 2) 20% of the magma was removed, yielding a 12.5 km thick pluton. The top of each pluton was set at 4.5 km below the present surface, primarily to leave room for the volcanic pile that presently exists in the area.

Figure 29 displays the 3.1 km pluton in the upper crust, and shows that the gravity anomaly produced is insufficient for observed readings. This model would require either a greater density contrast with respect to the country rock, or a component of crustal thickening to supply mass deficiency with depth. Figure 30 shows that the mass deficiency of a pluton about 12.5 km thick is sufficient to reproduce the gravity low between Morenci and Dice Throw.

Three paradigms were generated for the Tyrone-Acoma line that used the Morenci-Dice Throw thickened crust, 3.1 km and 12.5 km plutonic models as guides. Depth to major

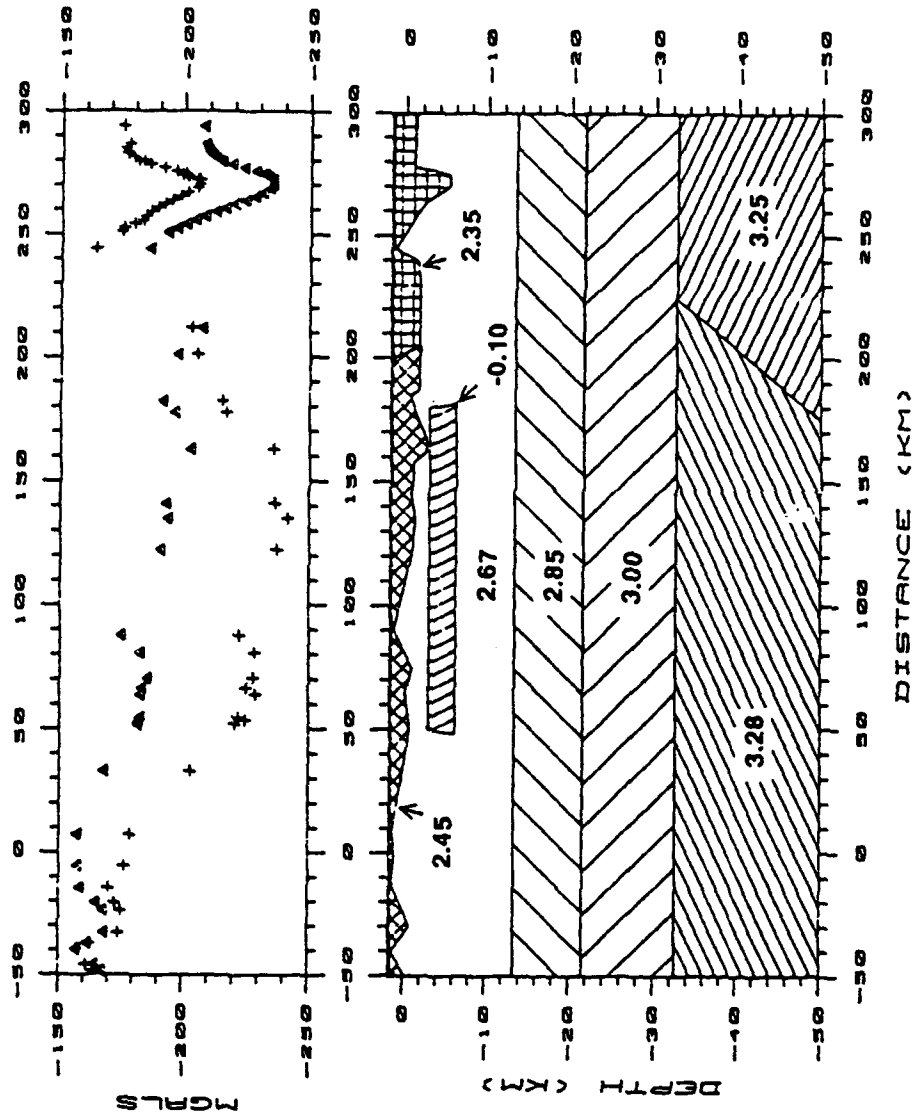


Figure 29. Gravity model along Jaksha's (1982) refraction profile, including a 3.1 km thick pluton (50% model). Values for density are given in  $\text{gm/cm}^3$ , except for the granitic pluton which displays a density contrast with respect to its country rock.

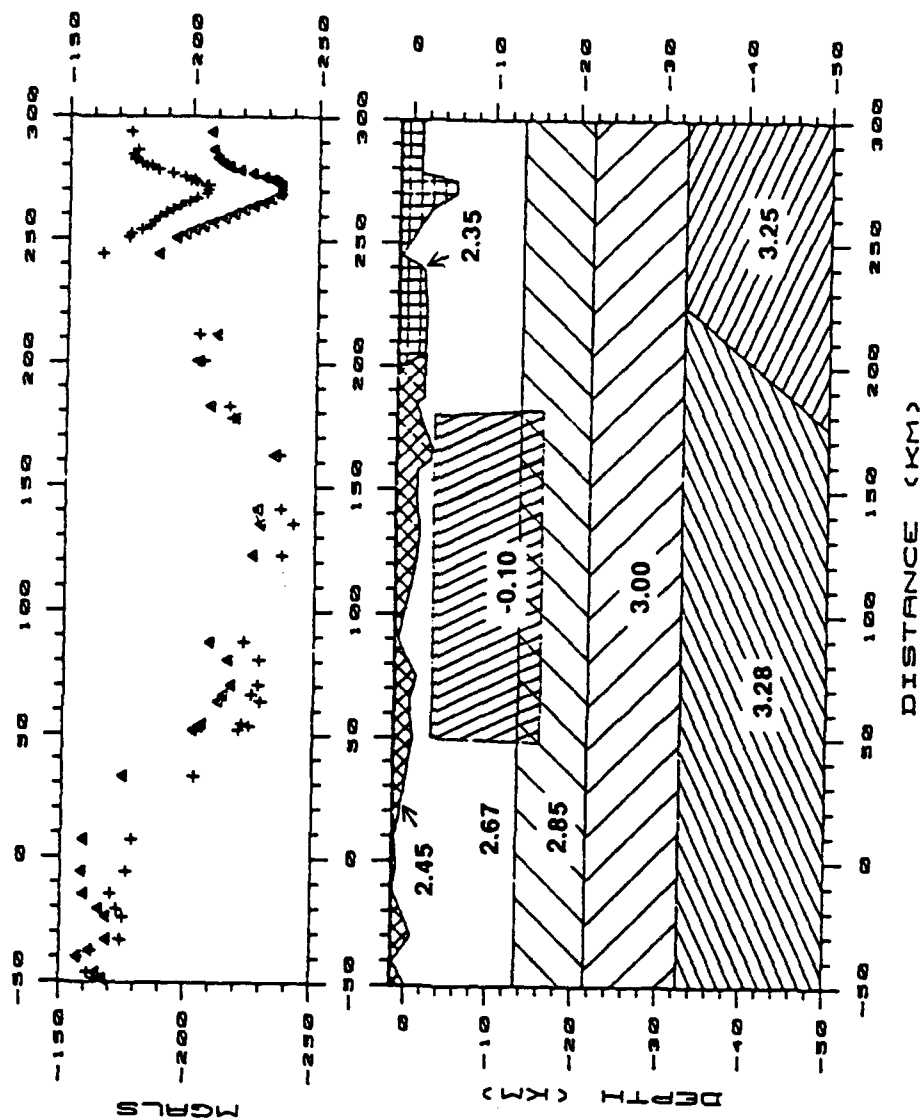


Figure 30. Gravity model along Jaksha's (1982) refraction profile, including a 12.5 km thick pluton (20% model). Values for density are given in  $\text{gm/cm}^3$ , except for the granitic pluton which displays a density contrast with respect to its country rock.

interfaces, velocity and density were matched at the intersection point of these two profiles. That point is in Corduroy Canyon, approximately 80 km from Tyrone and 125 km from Morenci. Crustal structure and velocity were also constrained near Tyrone by the previous work of Sinno and others (1986). These models were then tested by gravity and seismic data on the Tyrone-Acoma line.

The calculated gravity results along the Tyrone-Acoma line for the two plutonic models are shown in Figures 31 and 32, respectively. The north end of the pluton in these models is placed 220 km from Tyrone, the edge of the sag in gravity values. In these figures, the northern extent of the pluton, as mapped by Elston and others (1976a) and suggested by Krohn (1976), is 150 km north of Tyrone. Again, the 3.1 km pluton is insufficient to account for the entire gravity anomaly. The 12.5 km pluton creates a gravity field which is relatively close to the observed readings. However, it is clear from this analysis that the gravity low extends further north along the profile than predicted by Elston and others (1976a). Reconciling this problem requires extending the low-density body or increasing the thickness of the crust to the north.

The model showing the anomaly along the Tyrone-Acoma refraction line due to crustal thickness alone is presented

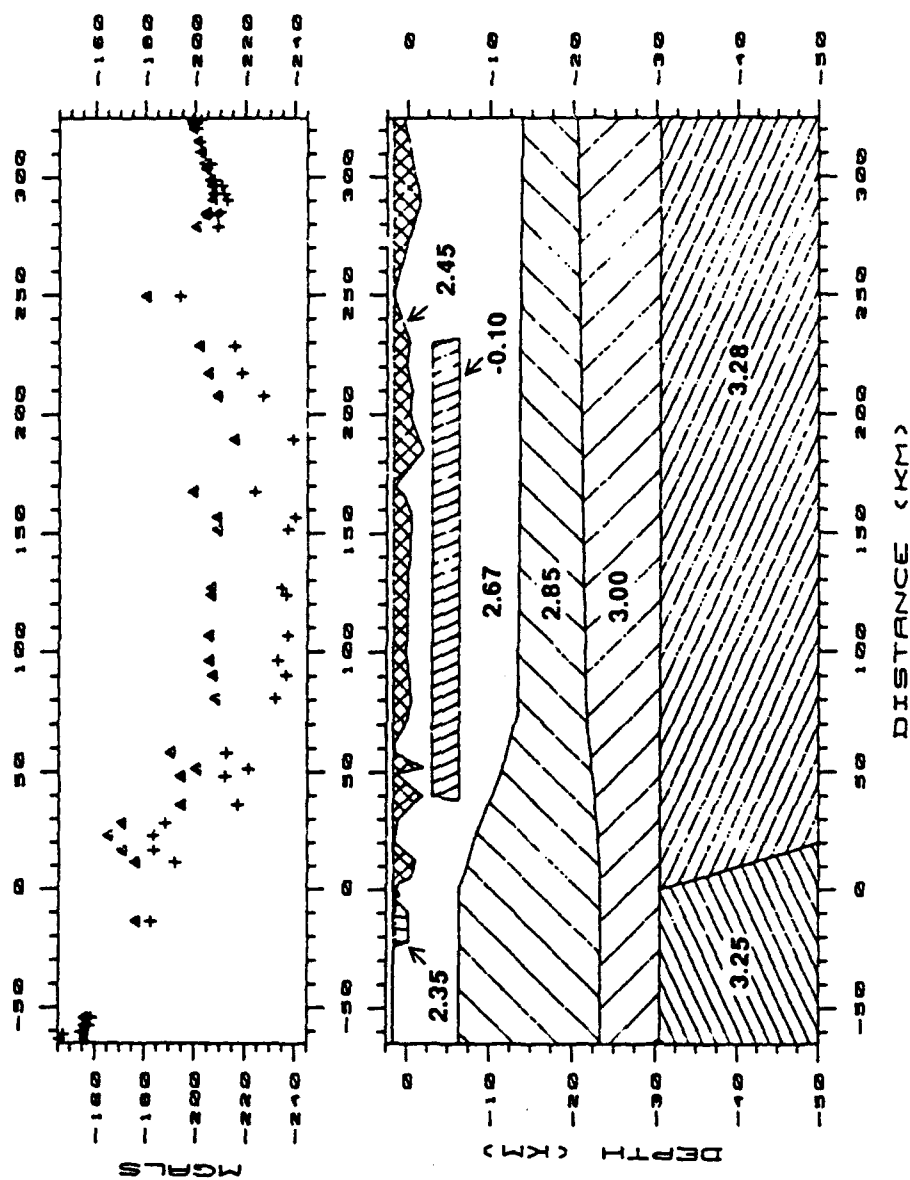


Figure 31. Gravity profile along the Tyrone-Acoma refraction line with a 3.1 km thick buried pluton. Pluses (+) indicate observed values; triangles reflect model-calculated gravity field. Values for density are in  $\text{gm/cm}^3$ , except for the granitic pluton which displays a density contrast with its country rock.

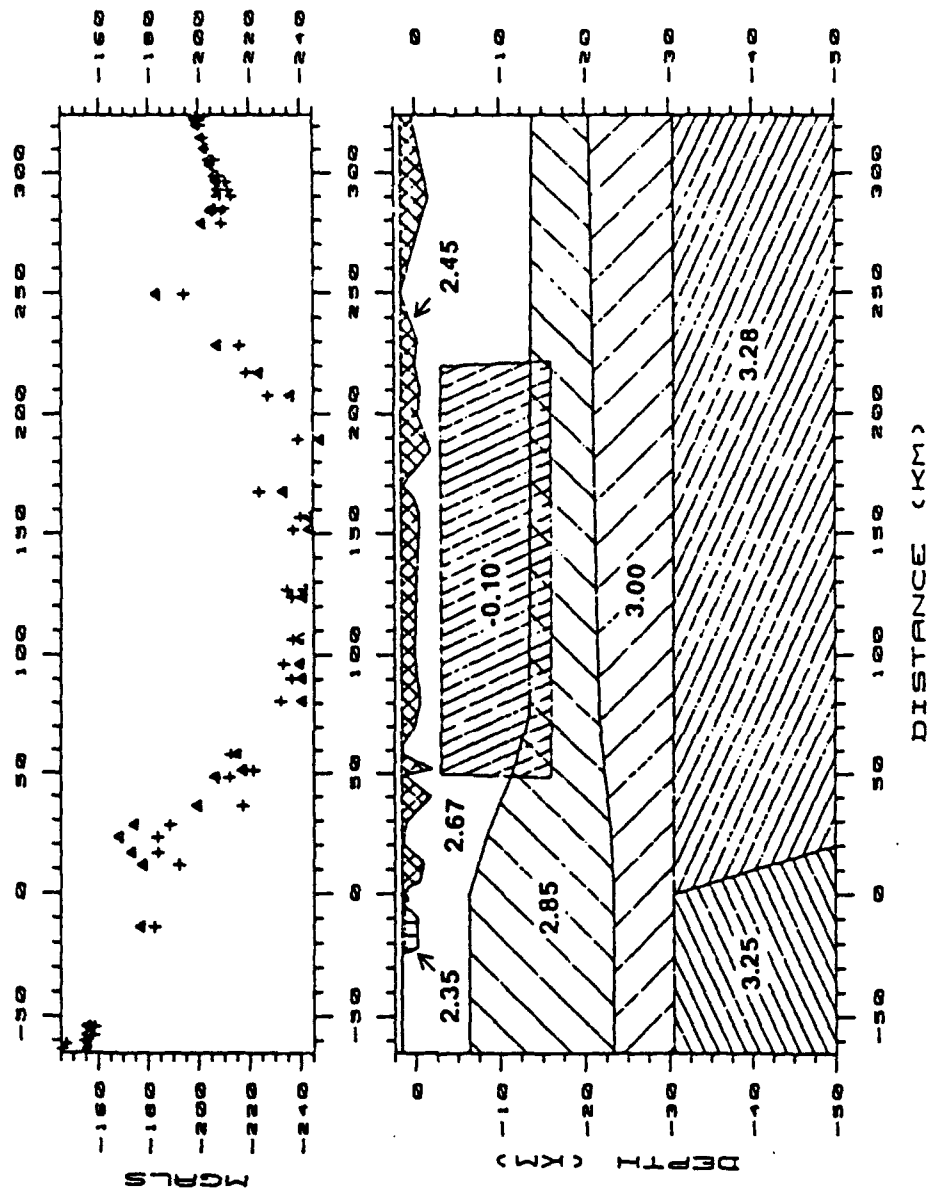


Figure 32. Gravity profile along the Tyrone-Acoma refraction line with a 12.5 km thick buried pluton. Values for density are in  $\text{gm/cm}^3$ , except for the granitic pluton which displays a density contrast with its country rock.

in Figure 33. Based on gravity analysis alone, the crustal thickening and 12.5 km thick pluton models provide equally acceptable solutions to available data. The validity of each model is tested by the use of the ART ray-tracing program and comparing the outcomes to observed arrival times.

From Figure 34, the rays arriving just before the shift in PmP arrival reflect off the Moho about 100 km from Tyrone. If the travel-time anomaly is caused by thinning of the crust, it must begin just beyond 100 km from Tyrone. As shown in Figure 35, extreme thinning to 23 km is required to recreate this step. However, such thinning produces a discrepancy between the predicted and observed gravity fields (Figure 36) of almost 50 mgal. Clearly, the gravity field does not support crustal thinning of such magnitude along this profile.

The time step in the PmP arrivals must therefore be produced by lateral velocity variations within the crust. A 1.5 sec shift in arrival times suggests a significant feature. With an average velocity of 4 km/sec in the near-surface layer and a thickness of 3 km, the travel time for a vertical seismic ray through the section is 0.75 sec. If this layer is removed and replaced by upper crustal material

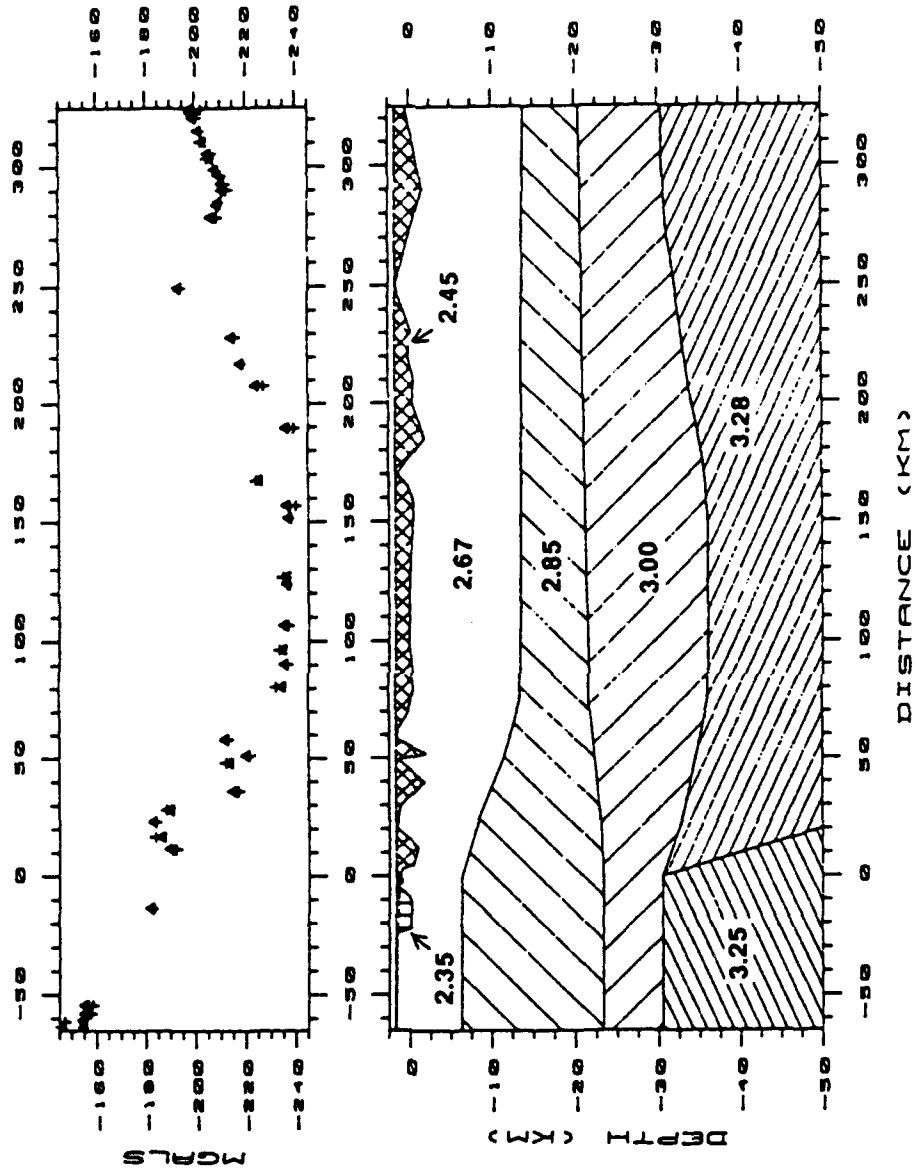


Figure 33. Gravity model along the Tyrone-Acoma refraction line involving crustal thickening alone. Values for density are in  $\text{gm/cm}^3$ .

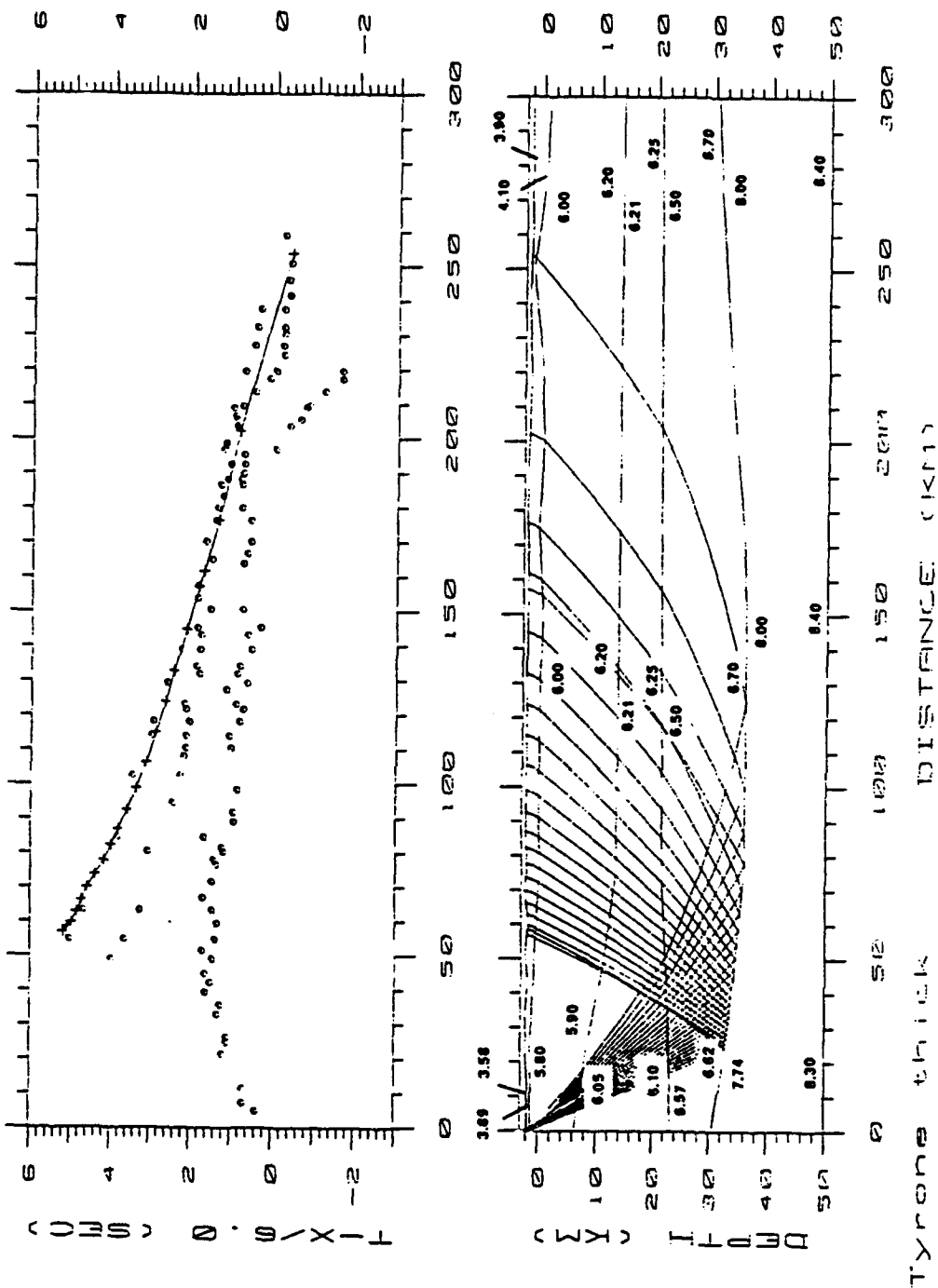


Figure 34. Seismic ray-tracing model along the Tyrone-Acoma line for a crust thickened to produce the observed gravity anomaly. Here, PmP arrivals do not recreate the observed time shift at 210 km. Velocities are in km/sec. Symbols: o = observed arrivals; + = calculated reflected arrivals; x = calculated refracted arrivals.

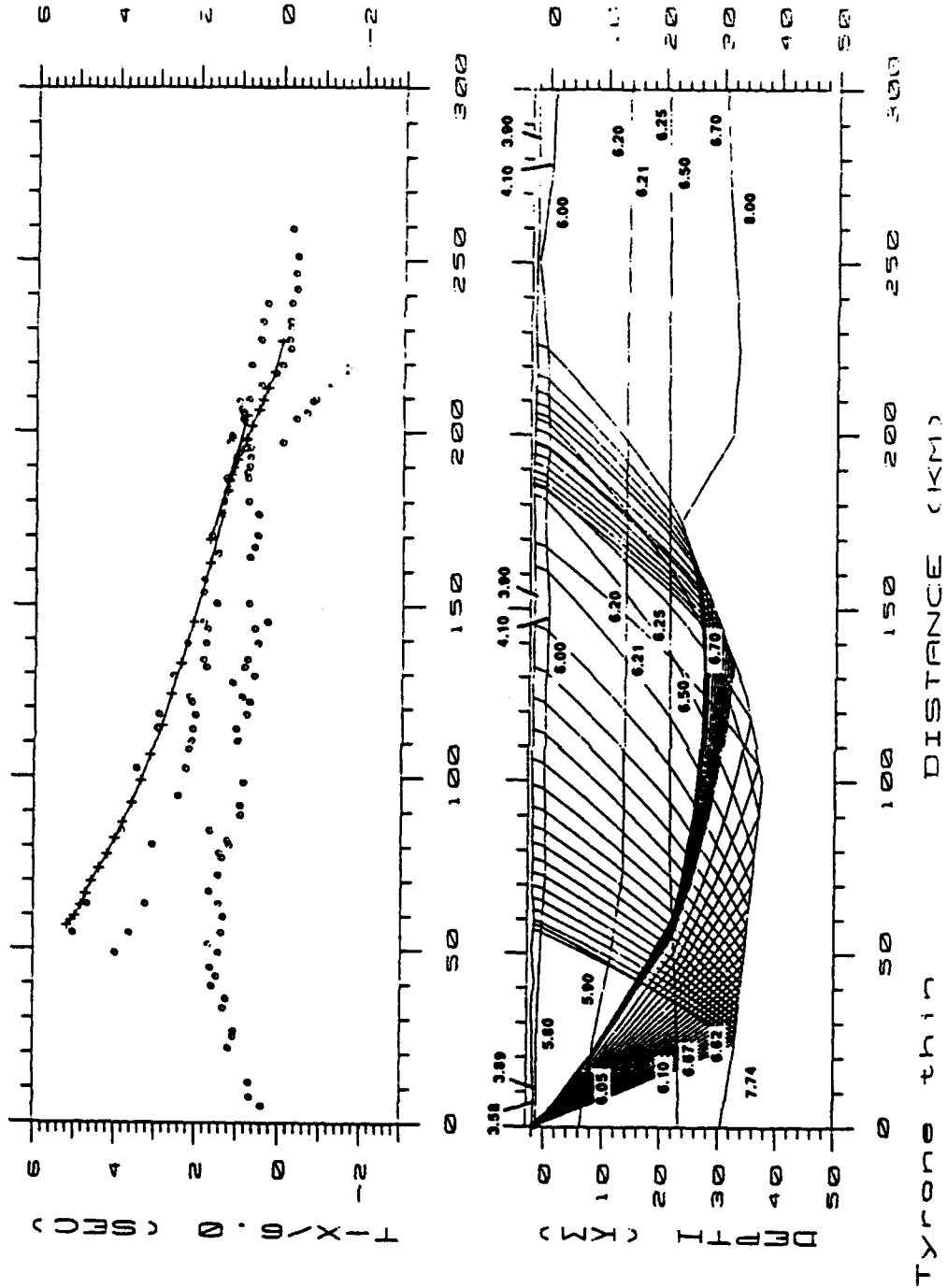


Figure 35. Ray-trace model of the Tyrone-Acoma line, attempting to model step change in PmP by crustal thinning. Even by thinning to 23 km, the step is not reproduced. Velocities are in km/sec. Symbols: o = observed arrivals; + = calculated reflected arrivals.

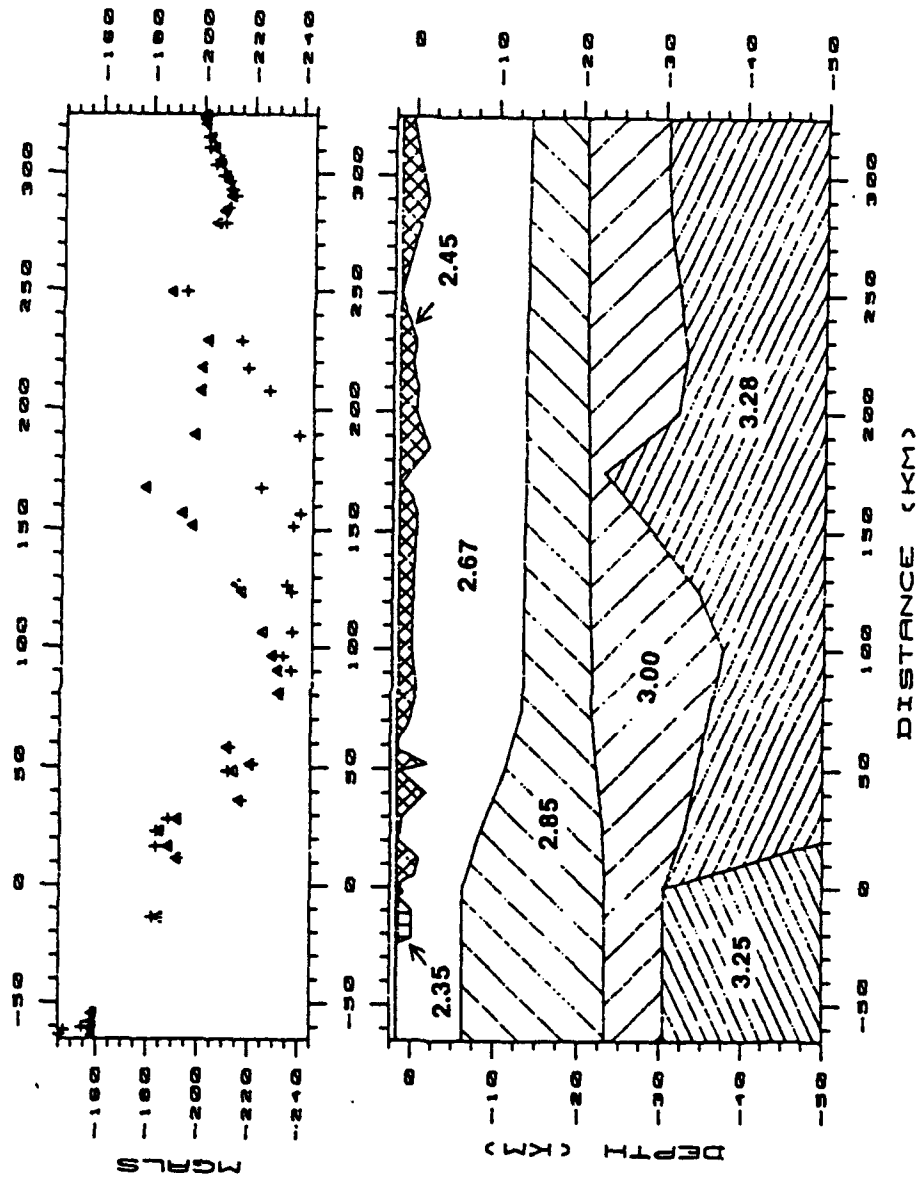


Figure 36. Gravity profile along the Tyrone-Acoma refraction line showing crustal thinning to 23 km. This model is unsupported by the regional gravity field. Values for density are in gm/cm<sup>3</sup>.

with a velocity of 6 km/sec, a difference in travel time of only 0.25 sec is expected. To create a time shift of 1.5 sec, the near-surface layer must have a velocity of 1.67 km/sec, which is unrealistic. As a result, the PmP arrival time step change cannot be caused by variations in the near-surface layer alone, and must be the result of deeper changes within the crust. This can be accomplished by thickening the lower crustal layers in the north at the expense of the upper crustal layer, but by doing so the gravity field again would be raised.

The presence of a near-surface plutonic complex under the Mogollon plateau could create the time shift in PmP. It has been mentioned earlier that granitic batholiths are less dense than their surroundings. This implies that seismic velocity within a pluton is slower than the country rock. The 1.5 sec step could then indicate the point where the pluton no longer affects the ray path, suggesting that the plutonic complex extends approximately 50 km north of Elston and others' (1976a) boundary. This position also corresponds to the north end of the sag superimposed on the regional Bouguer gravity low at that point.

The emplacement of such a large plutonic complex has profound significance on the overall structure of the crust.

Of critical importance is the question: Where did the displaced upper crustal material go?

Bott and Smithson (1967) correctly point out that when a pluton is inserted into the upper crust, a like volume of material is displaced regardless of where the source is derived. Forceful, or active, injection of fluids imply that country rock is uplifted, pushed aside, or is displaced downward by stoping. If the primary displacement is upward, then the 20% model should create a structural high of 12.5 km under the Mogollon plateau relative to its surroundings. No structural high of this magnitude has been reported in the region. If displacement is primarily outward, significant compressive features should be seen in the area surrounding the Mogollon plateau. However, southwestern New Mexico switched from regional compression to tension during the time of emplacement, and there are no outward-radiating indications of stress from the Mogollon plateau in the mid-Tertiary. Instead, radially-directed tension cracks occur in a wide region around the Mogollon plateau, with the center of the pattern somewhere to the southwest of Magdalena (Elston and others, 1976a). Furthermore, they report that the calderas formed in a neutral field, and presumably the pluton emplacement occurred in the same field.

Therefore, stoping must be the dominant factor in movement of country rock during emplacement of the proposed mid-Tertiary pluton in southwest New Mexico. Elston and others (1976a) propose that the source region for these fluids was in the lower crust. Melting was due to heat from asthenospheric basalts that pooled at the base of the crust.

With these geological constraints applied, the key feature of the final model became apparent: A near-surface pluton, extending through the Plains of St. Augustine, must be present in the crust. It must be sufficiently thick to produce a fundamental velocity change throughout the crust via stoping, and account for (at least) the sag within the regional Bouguer gravity low. It must also satisfy both the Tyrone-Acoma and Jaksha (1982) refraction and gravity data. The final integration of these data sets proved to be difficult and time-consuming, since perturbing one model had a cascading effect on the other three.

For the Tyrone-Acoma profile, the placement of the Moho and upper mantle velocities for distances >100 km from Tyrone were addressed by further analysis of gravity and seismic data. Gravity data suggested continued thickening of the crust and/or pluton. An attempt was made to model Pn data by upper mantle velocity changes alone as a test for pluton thickening. Reasonable velocity gradients that

yielded 8.0 km/sec values at 50 km were, however, insufficient to reproduce the Pn branch of the record section (Figure 37). Crustal thickening is therefore required to account for Pn arrivals under the northern part of the pluton. From gravity data, continued thickening to the north under the Colorado Plateau is supported. This implies that the Mogollon-Datil volcanic field currently overlaps the southeastern margin of the Colorado Plateau. The relationship between the magmatism and the southeastern margin during emplacement in mid-Tertiary time remains unresolved.

The bottom of the pluton in the final model is estimated to be at 10 km, as shown in Figure 38. The stopping effect is shown in this model as a depression recorded by the intermediate crustal boundaries. The northern boundary of the depression is more abrupt than that to the south, and may imply a major fault of crustal thickness in that region. However, no reflections from such a fault were observed in the seismic data, and further work is necessary to justify such a conclusion. A major crustal fault and an abrupt sag under the pluton both produce the same effect: they bring faster velocity material nearer to the surface north of the boundary. This feature, as well as

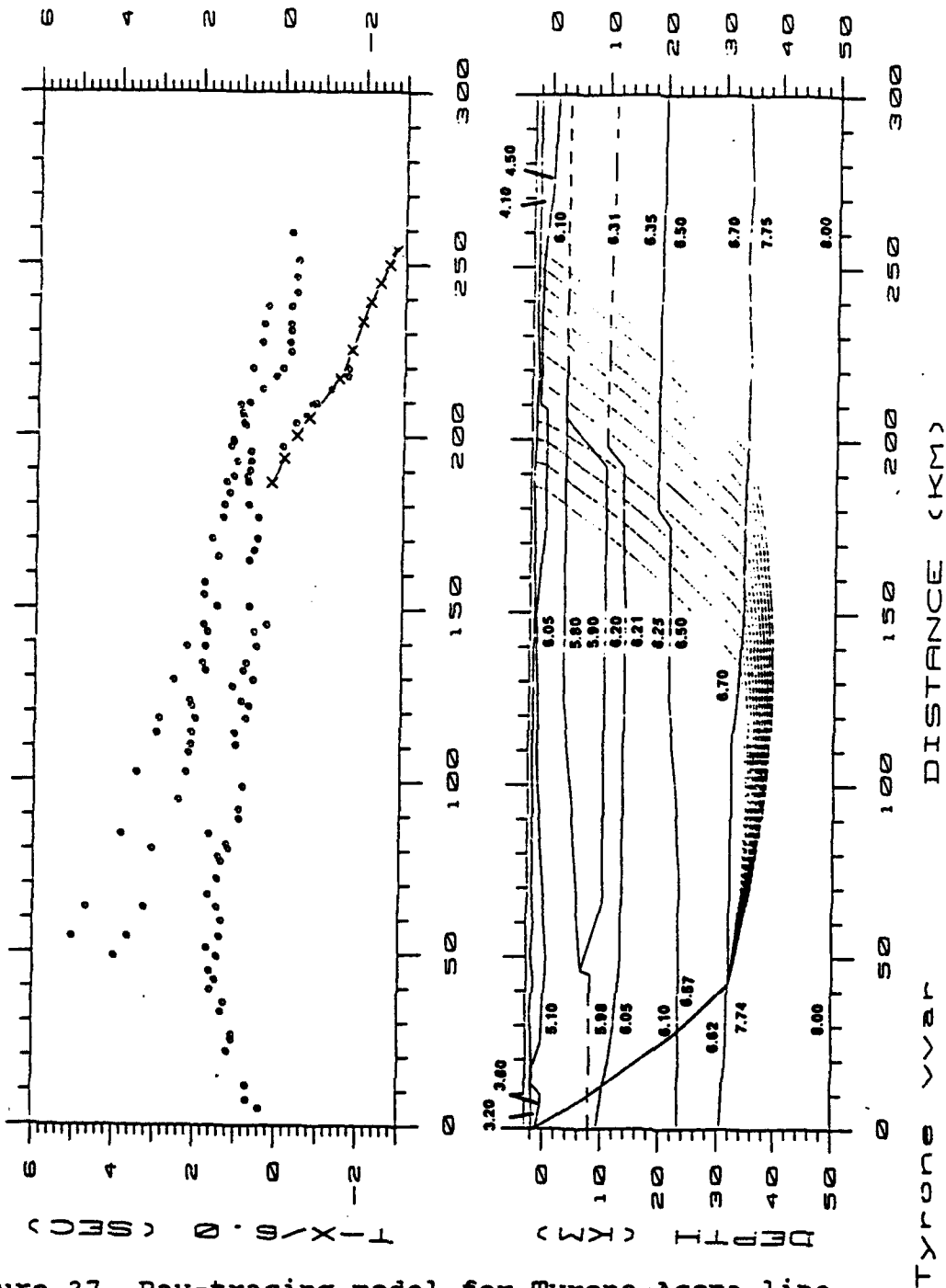


Figure 37. Ray-tracing model for Tyrone-Acoma line attempting to match Pn branch by upper mantle velocity anomalies alone. Velocities are in km/sec. Symbols: o = observed arrivals; + = calculated reflected arrivals; x = calculated refracted arrivals.

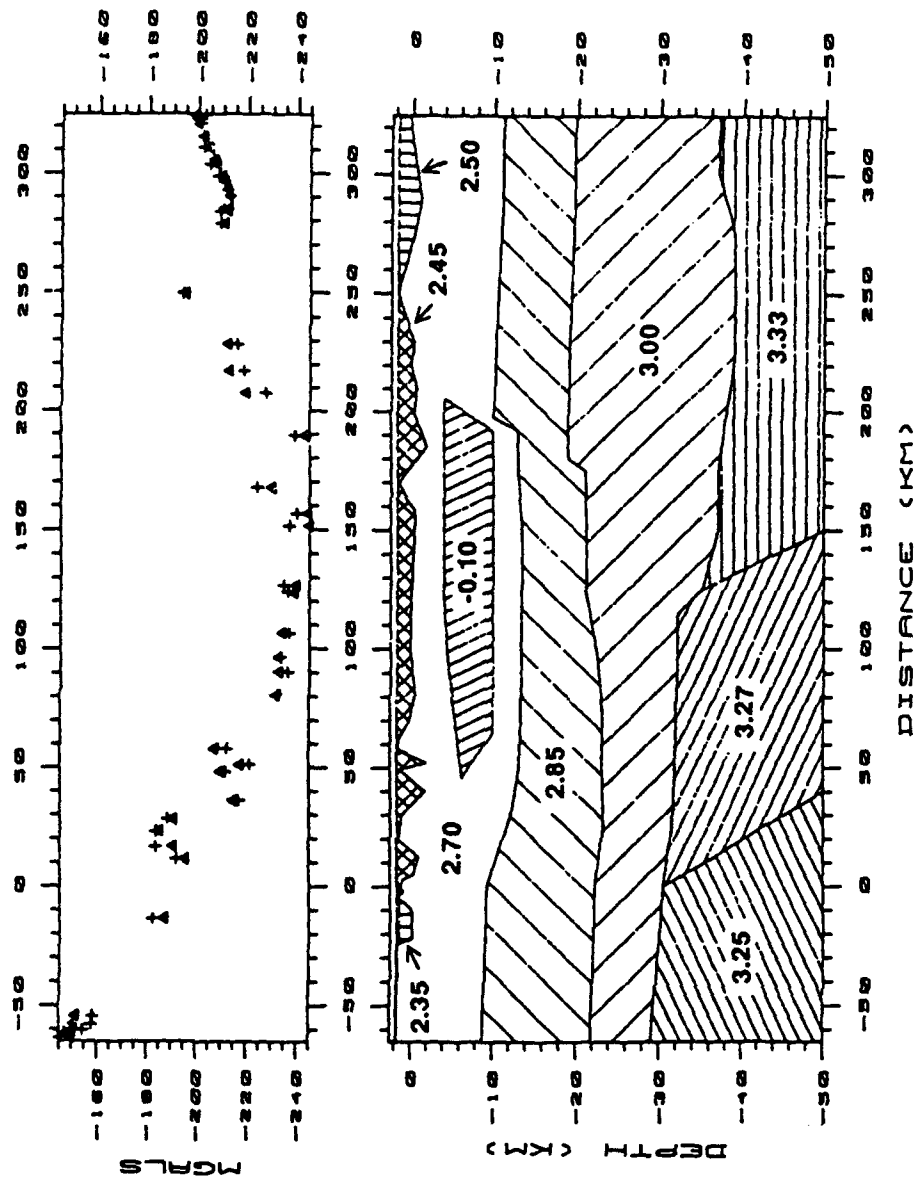


Figure 38. Gravity profile for Tyrone-Acoma refraction line, final model. Values for density are in gm/cm<sup>3</sup>, except for the granitic pluton which displays a density contrast with its country rock.

the presence of the pluton, is necessary to create the change in arrival time of the PmP phase (Figure 39).

To insure the viability of the model developed for the Tyrone-Acoma data, it was applied to the Morenci-Dice Throw profile. Results are shown in Figures 40 and 41. Assuming the east-west line is along the strike of crustal structure, the pluton is modeled as a slab. It is observed that the models are compatible in all major respects, including the reversed Pn branch for the Morenci-Dice Throw study (Figure 42). This model is therefore preferred over the model of crustal thickening alone.

The model that results from combined analysis of seismic and gravity data, along with present day knowledge of the geology in the region, strongly supports a complex history. The use of both data sets yields placement of major crustal boundaries with an error estimated at  $\pm 2$  km. At the north end of the Tyrone-Acoma profile, the use of gravity alone suggests a possible thinning of the crust (Figure 38). However, thinning can be avoided by increasing the thickness of the upper and middle crust layers at the expense of the lower crust.

The time of emplacement of the near-surface plutonic complex is placed in the mid-Tertiary, mainly because of the assumption that it is the source for the overlying

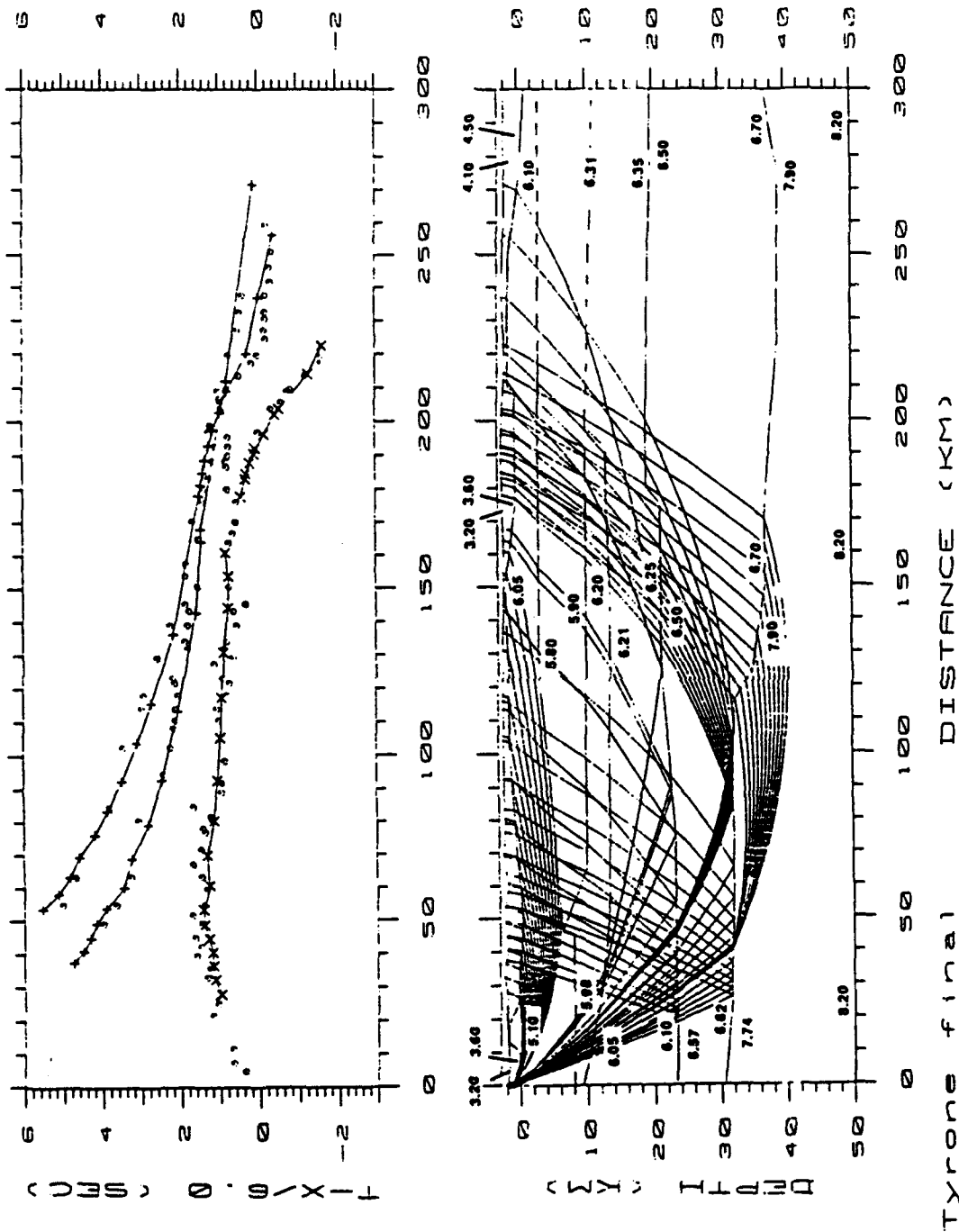


Figure 39. Ray-tracing model for Tyrone-Acoma line, final configuration. Velocities are in km/sec. Symbols: o = observed arrivals; + = calculated reflected arrivals; x = calculated refracted arrivals.

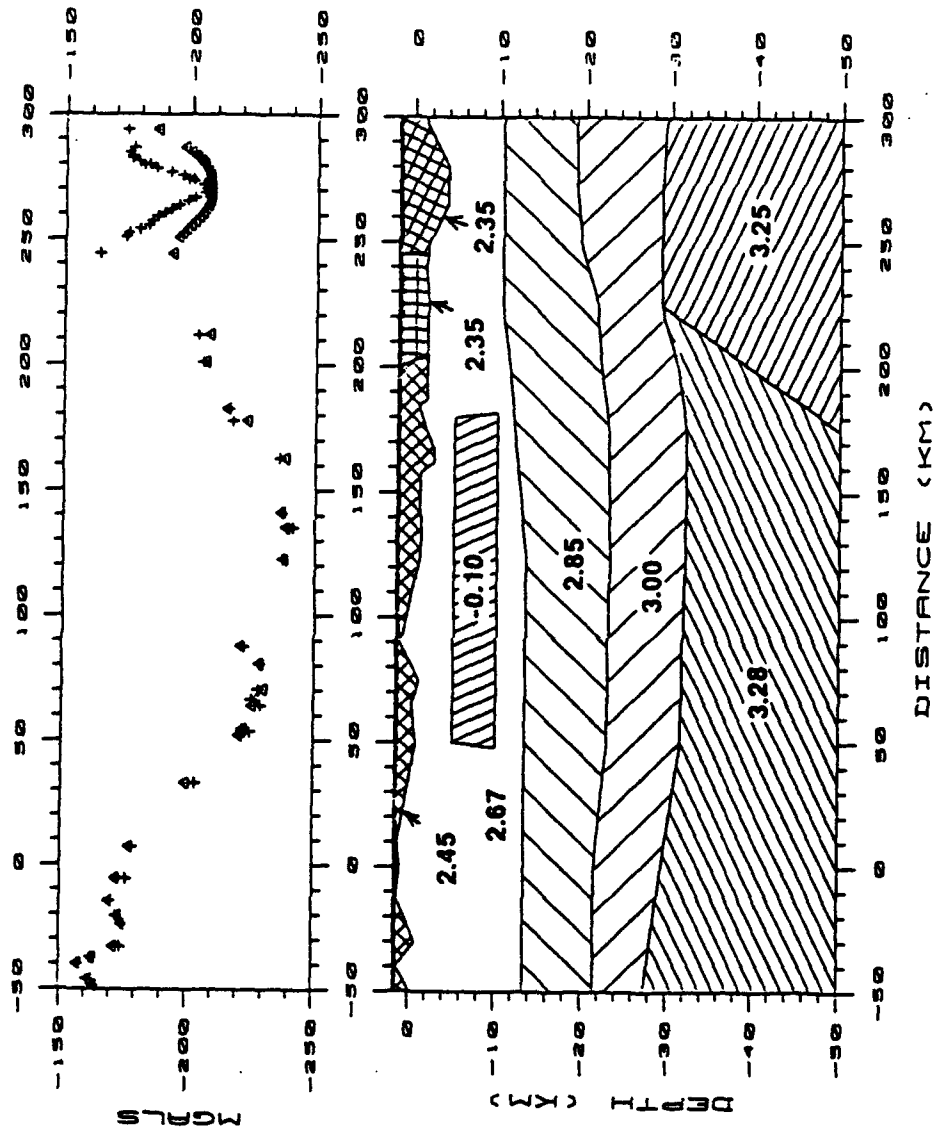


Figure 40. Gravity profile for Jaksha (1982) cross-line, including the final model. Values for density are in  $\text{gm/cm}^3$ , except for the granitic pluton which displays a density contrast with its country rock.

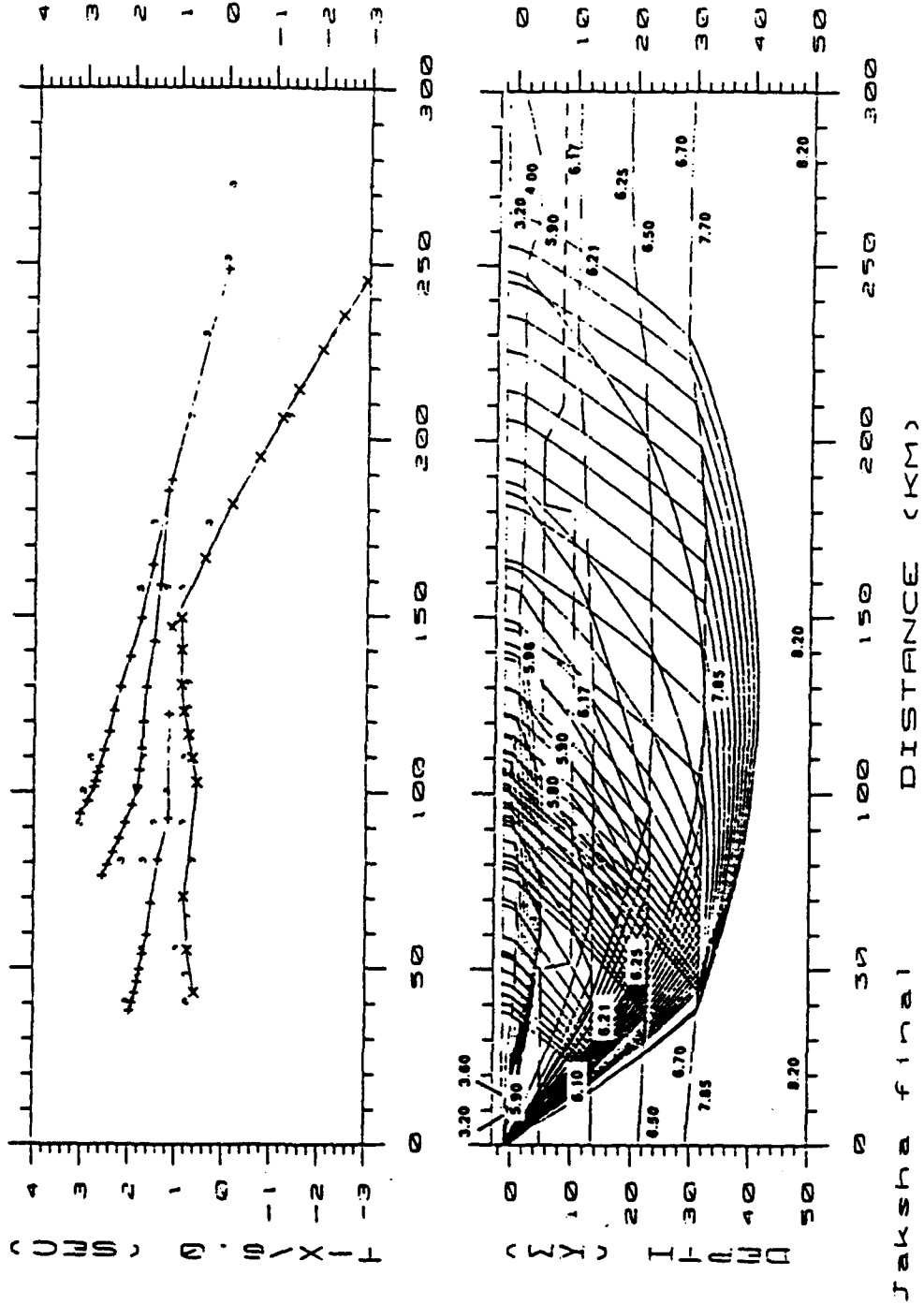


Figure 41. Ray-tracing model for the Jaksha (1982) cross-line, final configuration. Velocities are in km/sec. Symbols: o = observed arrivals; + = calculated reflected arrivals; x = calculated refracted arrivals.

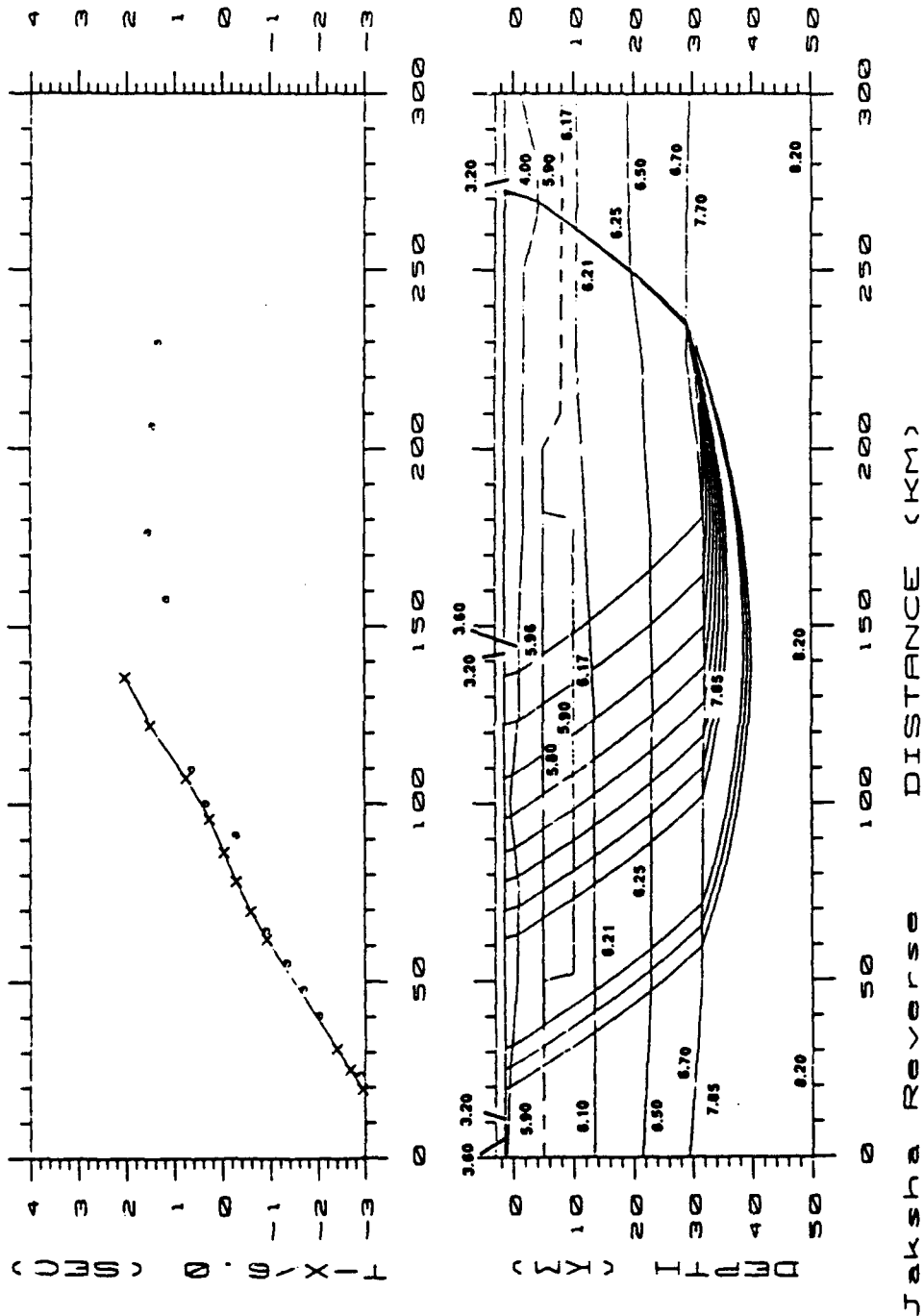


Figure 42. Ray-tracing model for the Jaksha (1982) cross-line, reversed Pn branch, final configuration. Velocities are in km/sec. Symbols: o = observed arrivals; x = calculated refracted arrivals.

volcanics. Within the constraints provided by these geophysical models, we can conclude that the history for southwestern New Mexico in mid-Tertiary time was one of large-scale reorganization of the crust:

- 1) Magmas formed from excess heat in the lower crust worked their way to the near-surface portion of the upper crust. Movement must have been rapid, as Elston and others (1976a) find little evidence of crustal contamination.
- 2) It is commonly held that a basaltic source rock yields 10% of its volume to acidic fractionation (Cox and others, 1979). The lower crust was therefore either reduced in total volume, or the loss of magma to the upper crust was replaced by cooling basaltic fluids at the base of the crust. If the lower crust has been reduced in total volume, it is possible that this region was part of the Colorado Plateau prior to the heating event. If the fluid loss was replaced by new magma, the Mogollon-Datil volcanic field may have formed off the Colorado Plateau. The solution to this problem remains undetermined by this study.
- 3) The crustal column between the near-surface pluton and the base of the crust was displaced downward by stoping. This implies that a negative

density anomaly was introduced at all levels of the crust in this column, and slower-velocity material is pushed downward throughout this region.

4) Venting of the near-surface pluton, especially with caldera collapse, provided a near-surface stoping effect, completing a total reorganization of the crust.

5) If the initial heating event is caused by the introduction of asthenospheric fluids at the base of the crust, it is implied that the upper mantle section of the lithosphere has been disturbed in addition to the crust. Presumably these magmas came from depth, and implies a stoping effect in the upper mantle. Then the mid-Tertiary events in southeastern Arizona and southwestern New Mexico actually represent reorganization of the entire lithosphere.

THERMAL MODELING OF THE LITHOSPHERE,  
ARIZONA AND NEW MEXICO

The present structure of the crust, along with known geology, suggests a complex tectonic history in southeastern Arizona and southwestern New Mexico. Although the nature and chemistry of the volcanism has changed over time, the continued activity indicates heating at depth at least since the mid-Tertiary. The model describing present day crustal structure as derived in the above section must be understood with respect to preceding events.

The complex nature of observed heat flow in the Colorado Plateau, Basin and Range and Rio Grande Rift provinces and their transition zones is introduced in a previous section in this report. However, a brief review is necessary for the present discussion. This section describes a two-dimensional temperature model that attempts to recreate the present-day lithospheric thermal structure by a finite difference method. In addition, it calculates heat flow and isostatic uplift over the model. By comparison to modern heat flow and elevation the input parameters can be constrained, and reasonable physical paradigms can be investigated.

Heat flow values for Arizona and New Mexico were extracted from a national data base (P. Morgan and J. Sass, personal communication, 1988) and are plotted in Figure 20. This map demonstrates that high heat flow values are associated with the boundary of the Colorado Plateau. This relationship implies that: 1) a thermal pulse is spatially associated with the boundary, i.e. in the Basin and Range and Rio Grande Rift (Seager and Morgan, 1979); or 2) faults or other conduits allowing hot fluids to be transported to the surface are associated with the plateau margin (Swanberg, 1979).

The Colorado Plateau displays heat flow values near or slightly above those found in stable continental regions (Blackwell, 1978; Lachenbruch and Sass, 1978; Bodell and Chapman, 1982; Reiter and Clarkson, 1983). This heat flow is highly variable, however, and care must be taken in the interpretation of available data (Reiter and Clarkson, 1983). Shearer and Reiter (1981) and Sass and others (1982) discuss the influence of groundwater circulation on heat flow values in the San Francisco volcanic field on the plateau margin in Arizona. Significant hydrothermal effects are also noted in the Rio Grande Rift (Reiter and others, 1978). This concern is typical of the problems in much of the western United States (Blackwell, 1978; Sass and others,

1982). Figure 43 shows that the transition between the Colorado Plateau and the extensional provinces to the south and east is complex. It appears to be at least 100 km wide in Arizona and New Mexico (Bodell and Chapman, 1982; Swanberg and Morgan, 1985).

The recent uplift of the region indicates some heat has been taken up by thermal expansion. However, Morgan and Swanberg (1985) and Hinojosa (1989) show that thermal expansion is insufficient for the total amount of uplift under the Colorado Plateau. In fact, Morgan (1983) states that a surface heat flow anomaly should not develop until after lithospheric thinning has stopped. It has been shown in a previous section that geophysical data indicate that the upper mantle is hot under the plateau, even though the surface heat flow indicates lower temperature at depth. This tends to support Morgan's (1983) study, but does not address the present elevation and uplift of the plateau. The causes and consequences of the geophysical data and present day tectonic state of the Colorado Plateau are beyond the scope of this study.

Heat flow values have been separated into "deep" values and "shallow" values within the Basin and Range province in Arizona (Shearer and Reiter, 1981) and the Colorado Plateau (Reiter and Clarkson, 1983). In Arizona, temperature

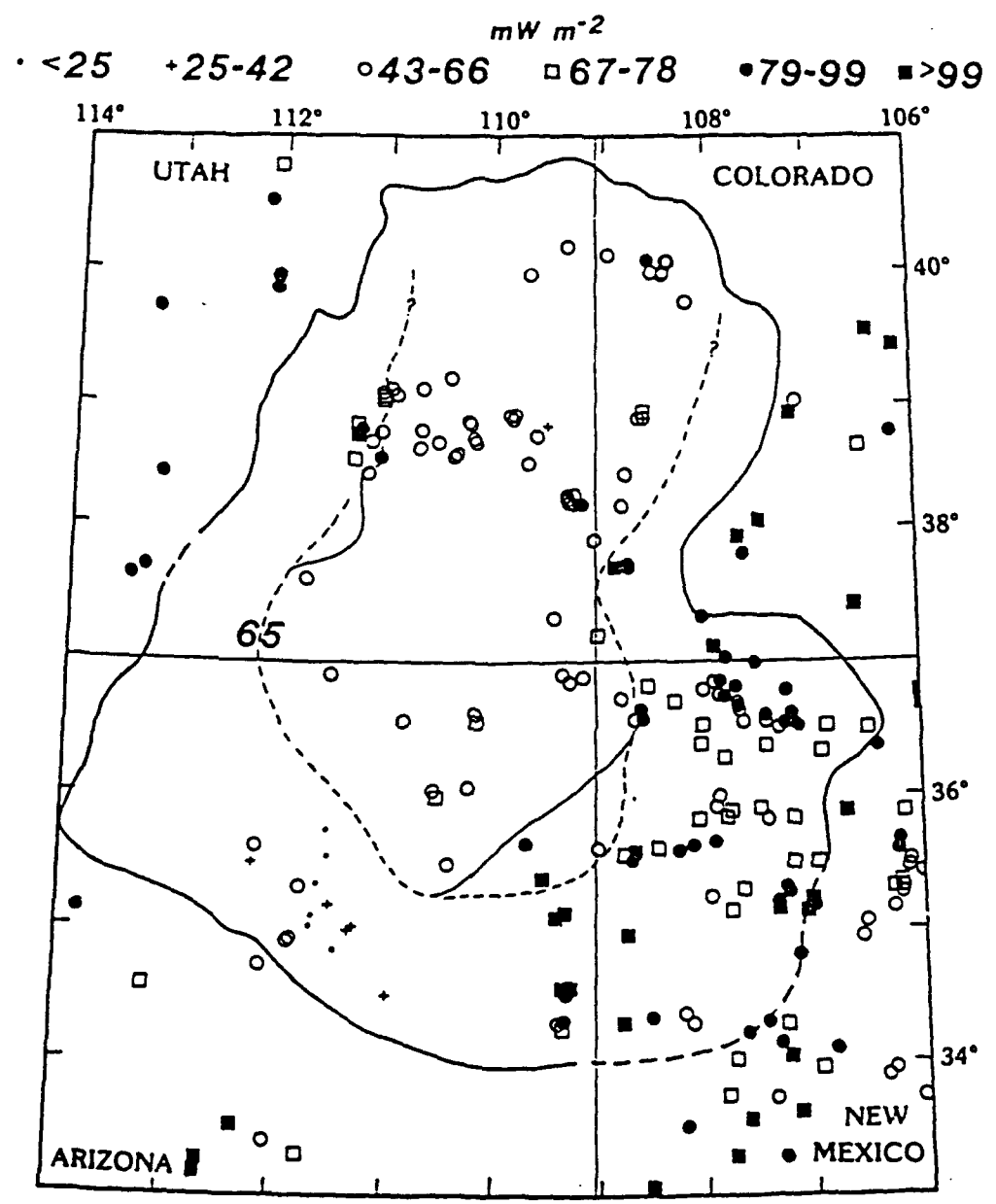


Figure 43. Heat flow data for the Colorado Plateau and adjacent areas. After Swanberg and Morgan (1985).

gradients measured at depths >650 m ("deep") yield more consistent values (i.e. smaller variance) than the province as a whole. The heat flow/heat generation regression for deep data yields a reduced heat flow (intercept) of 1.71 HFU for the Arizona Basin and Range. The "shallow" heat flow, determined from well data, is  $1.94 \pm 0.12$  HFU. The low standard error is suggested to indicate a uniform radiogenic layer, which in turn implies a homogeneous crust (Shearer and Reiter 1981). For the Colorado Plateau, data from depths >750 m also display much lower lateral variability than near-surface measurements (Reiter and Clarkson, 1983). Furthermore, Reiter and Clarkson find a higher heat flow mean in the deep data (1.53 HFU) than in shallow measurements (1.31 HFU). Greater lateral consistency in the deep values imply an equal radiogenic contribution to the heat flow, and also consistent upper mantle temperatures. Within the limits of statistical analysis, Shearer and Reiter (1981) show that the difference between the mean heat flow of the Colorado Plateau and Basin and Range provinces may be as little as 0.3 to 0.5 HFU. This implies that their tectonic history is more similar than previously thought, and that the crust has responded differently in each province. However, the deep data are sparse in both

provinces, and conclusions based on them should be viewed with caution.

The Rio Grande Rift and Basin and Range provinces display high heat flow near faults and volcanic centers, and intermediate to slightly elevated heat flow elsewhere (Reiter and others, 1975, 1978; Shearer and Reiter, 1981; Reiter and Clarkson, 1983). However, Swanberg (1979) states that the Rio Grande Rift displays consistently high heat flow values along its axis (Figure 44). High heat flow in the rift is thought to be caused by tectonic and magmatic sources in the crust and upper mantle (Edwards and others, 1978). Heat flow values exceeding 3.0 HFU appear to the west of El Paso, but are not found near the Colorado Plateau in New Mexico.

For a continental rift with dimensions near those of the East African Rift in Kenya, surprisingly little volcanism has occurred within the Rio Grande structure (Baldrige and others, 1984). Magma compositions in and near the rift are highly variable and do not necessarily reflect their tectonic setting. Sources are also varied in depth of origin for the extrusives found in and around the rift (Baldrige and others, 1987; Perry and others, 1987, 1988; Elston, 1989). Because of the small total volcanic volume, however, Baldrige and others (1984) conclude that no major thermal pulse is present in the upper mantle

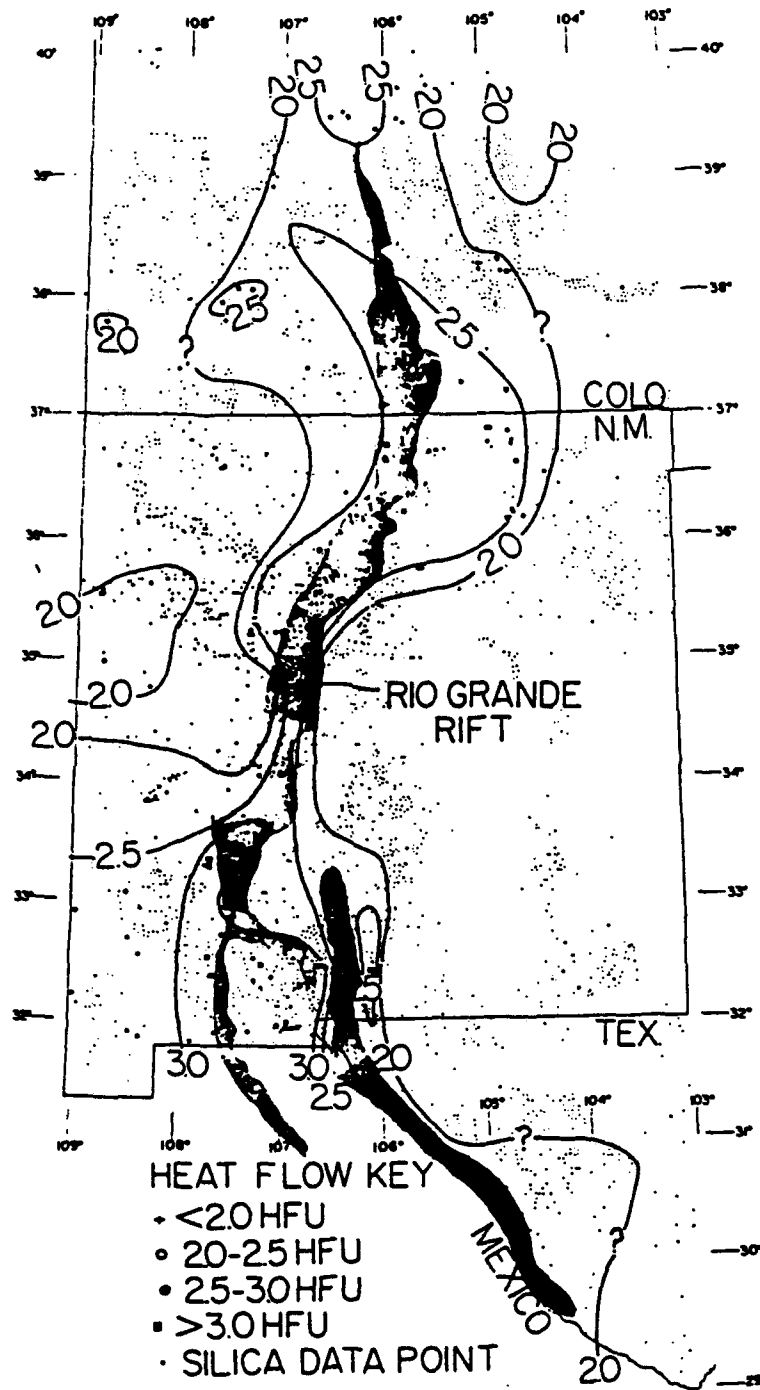


Figure 44. Heat flow along the Rio Grande Rift and adjacent areas. After Swanberg (1979).

beneath the Rio Grande Rift. Although pooling at mid-crustal depths appears to occur along the rift (e.g. Sanford and others, 1977), the volume of such bodies appears to be minor or is undetectable by available heat flow data.

Although the highest heat flow values in the Rio Grande Rift occur near deep faults and volcanic centers, the higher heat flow trend along its axis (Swanberg, 1979) indicates a more fundamental thermal disturbance. The lack of extensive volcanism and plutonism (Baldrige and others, 1984) may be the result of a crustal composition that resists melting at this time. Sparse earthquake activity (Jaksha and Sanford, 1986) implies little voluminous movement of magma in the crust. For this study, it is assumed that a thermal disturbance is present in the upper mantle, and that the small volcanic volume indicates the primary transport of thermal energy is conductive.

A two-dimensional finite difference conductive heat transfer program has been created in an attempt to analyze the phenomena described above. Its derivation is presented in the following section, and the resulting program HF2D is presented in Appendix V. It is applied as a cross-section of the Colorado Plateau boundary, and is assumed to be infinite in the y-direction. The origin of the model is placed at the physical axis of high heat flow readings ( $z =$

0), and temperature perterbations are symmetric about the z-axis of the model in the x-direction.

## Derivation of the Algorithm

The analytical form of the two-dimensional heat flow equation (HF2D) is:

$$\frac{\delta T}{\delta t} = K \left( \frac{\delta^2 T}{\delta x^2} + \frac{\delta^2 T}{\delta z^2} \right)$$

Where      T = Temperature  
               t = Time  
               K = Thermal diffusivity  
               x = Distance in horizontal direction  
               z = Distance in vertical direction

It is desirable that the discrete form of this equation be unconditionally stable. An equation that satisfies this form is the alternating-direction implicit (ADI) method described by Anderson and others (1984). This equation splits the forward step in time into two "half-steps", taking the following form:

$$\text{Step 1} \quad \frac{T_{i,j}^{n+1/2} - T_{i,j}^n}{\Delta t/2} = K \left( \hat{\delta}_x^2 T_{i,j}^{n+1/2} + \hat{\delta}_z^2 T_{i,j}^n \right)$$

$$\text{Step 2} \quad \frac{T_{i,j}^{n+1} - T_{i,j}^{n+1/2}}{\Delta t/2} = K \left( \hat{\delta}_z^2 T_{i,j}^{n+1/2} + \hat{\delta}_x^2 T_{i,j}^{n+1} \right)$$

Where 
$$\hat{\delta}_x^2 T_{i,j}^n = \frac{T_{i+1,j}^n - 2T_{i,j}^n + T_{i-1,j}^n}{(\Delta x)^2}$$

$$\hat{\delta}_z^2 T_{i,j}^n = \frac{T_{i,j+1}^n - 2T_{i,j}^n + T_{i,j-1}^n}{(\Delta z)^2}$$

n = Time from which this step is being made

n+1/2 = Intermediate, or "half-step"

n+1 = Next time step

i, j = x and z points on a grid of dimension

N x N

This method is second order accurate with a truncation error of:  $O [ (\Delta t)^2, (\Delta x)^2 \text{ and } (\Delta z)^2 ]$ .

for step 1,

$$T_{i,j}^{n+1} - T_{i,j}^n = \frac{K\Delta t}{2} \left( \frac{T_{i+1,j}^n - 2T_{i,j}^n + T_{i-1,j}^n}{(\Delta x)^2} + \frac{T_{i,j+1}^n - 2T_{i,j}^n + T_{i,j-1}^n}{(\Delta z)^2} \right)$$

Let  $a = \frac{K\Delta t}{2(\Delta x)^2}$  and  $b = \frac{K\Delta t}{2(\Delta z)^2}$

Then we find that for step 1,

$$-aT_{i+1,j}^{n+1/2} + (1+2a)T_{i,j}^{n+1/2} - aT_{i-1,j}^{n+1/2} = bT_{i,j+1}^n + (1-2b)T_{i,j}^n + bT_{i,j-1}^n$$

For step 2,

$$T_{i,j}^{n+1} - T_{i,j}^{n+1/2} = a(T_{i+1,j}^{n+1/2} - 2T_{i,j}^{n+1/2} + T_{i-1,j}^{n+1/2}) + b(T_{i,j+1}^{n+1} - 2T_{i,j}^{n+1} + T_{i,j-1}^{n+1})$$

or

$$-bT_{i,j+1}^{n+1} + (1+2b)T_{i,j}^{n+1} - bT_{i,j-1}^{n+1} = aT_{i+1,j}^{n+1/2} + (1-2a)T_{i,j}^{n+1/2} + aT_{i-1,j}^{n+1/2}$$

For the present discussion, we will apply the following boundary conditions:

$$\frac{\delta T}{\delta x} \quad x = 0, L \quad = 0 \quad \text{Heat flow through the lateral edges is set} = 0$$

$$T \quad z = 0 \quad = 0 \quad \text{Temperature at the surface is set} = 0$$

$$T \quad z = H \quad = f(x) \quad \text{Temperature at the base is some function of } x$$

Numerically, the lateral change in temperature at any point can be defined as:

$$\frac{\delta T_{i,j}}{\delta x} = \frac{T_{i+1,j} - T_{i-1,j}}{2\Delta x}$$

Since the heat flow = 0, then  $T_{i+1,j} = T_{i-1,j}$ . This step is necessary for step 1, when the points  $T_{i,j}$  and  $T_{n,j}$  are evaluated. The matrix notation for the first step is:

$$\begin{bmatrix} (1+2a) & -2a & 0 & \cdot & \cdot & \cdot & 0 \\ -a & (1+2a) & -a & \cdot & \cdot & \cdot & \cdot \\ 0 & -a & (1+2a) & -a & \cdot & \cdot & \cdot \\ \cdot & \cdot & \cdot & \cdot & \cdot & \cdot & \cdot \\ \cdot & \cdot & \cdot & \cdot & \cdot & \cdot & 0 \\ \cdot & \cdot & \cdot & \cdot & -a & (1+2a) & -a \\ 0 & \cdot & \cdot & \cdot & 0 & -2a & (1+2a) \end{bmatrix} \cdot \begin{bmatrix} T_{1,j} \\ T_{2,j} \\ T_{3,j} \\ \cdot \\ \cdot \\ \cdot \\ T_{n,j} \end{bmatrix} = \begin{matrix} n+1/2 \\ \\ \\ \\ \\ \\ \end{matrix}$$

$$\begin{bmatrix} T_{1,j+1} & T_{1,j} & T_{1,j-1} \\ T_{2,j+1} & T_{2,j} & T_{2,j-1} \\ T_{3,j+1} & T_{3,j} & T_{3,j-1} \\ \cdot & \cdot & \cdot \\ \cdot & \cdot & \cdot \\ T_{n,j+1} & T_{n,j} & T_{n,j-1} \end{bmatrix} \cdot \begin{bmatrix} b \\ (1-2b) \\ b \end{bmatrix}$$

Where the superscripts  $n$  and  $n+1/2$  refer to the time step for these temperature values. This equation increments  $i$  from 1 to  $N$  while holding  $j$  constant. After the  $i$ -loop terminates,  $j$  increases by 1 and the process repeats. Since  $T_{i,1}$  and  $T_{i,N}$  are held fixed (upper and lower boundary conditions), they are not necessary in the outer loop. Thus the matrix equation takes the form  $\bar{A} \tilde{x} = \tilde{y}$  where  $\bar{A}$  is an  $N \times N$  matrix,  $\tilde{x}$  is the  $N \times 1$  vector of temperatures for row  $j$  at time step  $n+1/2$ , and  $\tilde{y}$  is the  $N \times 1$  vector of temperature-spatial parameters at time step  $n$ . Noting that  $\bar{A}$  is a tridiagonal matrix, much computer time can be saved in calculating  $\bar{A}^{-1}$  by using program TRIDAG (Press and others, 1986; also see Appendix V).

The second step requires that  $i$  be held constant while  $j$  increments from 2 to  $N-1$  (For the same reason as in step 1). However, the right-hand side of equation (3) depends on the value of  $i$ . For  $i = 1$  and  $i = N$ , the heat flow = 0 boundary condition must be applied for  $T_{0,j}$  and  $T_{N+1,j}$ .

Thus:

For  $i = 1$

$$\begin{bmatrix} -b & (1+2b) & -b & 0 & \cdot & \cdot & 0 \\ 0 & -b & (1+2b) & -b & \cdot & \cdot & \cdot \\ \cdot & \cdot & \cdot & \cdot & \cdot & \cdot & \cdot \\ \cdot & \cdot & \cdot & \cdot & \cdot & \cdot & 0 \\ \cdot & \cdot & \cdot & \cdot & -b & (1+2b) & -b \end{bmatrix} \begin{bmatrix} T_{1,1} \\ T_{1,2} \\ T_{1,3} \\ \cdot \\ T_{1,n} \end{bmatrix} =$$

$$\begin{bmatrix} T_{2,2} & T_{1,2} \\ T_{2,3} & T_{1,3} \\ T_{2,4} & T_{1,4} \\ \cdot \\ T_{2,n-1} & T_{1,n-1} \end{bmatrix} \cdot \begin{bmatrix} 2a \\ (1 - 2a) \end{bmatrix}$$

Note that the left-hand matrix is no longer square, it is of dimension  $(N-2) \times N$ . Also, the right-hand side combines to form an  $(N-2) \times 1$  vector. However, it is noted that the top and bottom elements in the  $T^{n+1}$  vector (left-hand side) are points at which the temperature never changes (boundary conditions). Thus the  $\bar{A}$  matrix can be made square and tridiagonal, and the right-hand side becomes  $N \times 1$ , by the following modifications:

$$\begin{bmatrix}
 1 & 0 & 0 & \cdot & \cdot & \cdot & 0 \\
 -b & (1+2b) & -b & \cdot & \cdot & \cdot & \cdot \\
 0 & -b & (1+2b) & -b & \cdot & \cdot & \cdot \\
 \cdot & \cdot & \cdot & \cdot & \cdot & \cdot & \cdot \\
 \cdot & \cdot & \cdot & \cdot & \cdot & \cdot & 0 \\
 \cdot & \cdot & \cdot & \cdot & -b & (1+2b) & -b \\
 0 & \cdot & \cdot & \cdot & 0 & 0 & 1
 \end{bmatrix} \cdot \begin{bmatrix} T_{1,1} \\ T_{1,2} \\ T_{1,3} \\ T_{1,4} \\ \cdot \\ \cdot \\ T_{1,N} \end{bmatrix} =$$

$$\begin{bmatrix}
 T_{1,1} \\
 2aT_{2,2} + (1-2a)T_{1,2} \\
 2aT_{2,3} + (1-2a)T_{1,3} \\
 2aT_{2,4} + (1-2a)T_{1,4} \\
 \cdot \\
 2aT_{2,N-1} + (1-2a)T_{1,N-1} \\
 T_{1,N}
 \end{bmatrix}^{n+1/2}$$

Again, this is in the form  $\bar{A} \tilde{x} = \tilde{y}$  where  $\bar{A}$  is  $N \times N$ , and  $\tilde{x}$  and  $\tilde{y}$  are both  $N \times 1$ . A similar derivation for  $i = N$  yields:

$$\begin{bmatrix}
 1 & 0 & 0 & \cdot & \cdot & \cdot & 0 \\
 -b & (1+2b) & -b & \cdot & \cdot & \cdot & \cdot \\
 0 & -b & (1+2b) & -b & \cdot & \cdot & \cdot \\
 \cdot & \cdot & \cdot & \cdot & \cdot & \cdot & \cdot \\
 \cdot & \cdot & \cdot & \cdot & \cdot & \cdot & 0 \\
 \cdot & \cdot & \cdot & \cdot & -b & (1+2b) & -b \\
 0 & \cdot & \cdot & \cdot & 0 & 0 & 1
 \end{bmatrix} \cdot \begin{bmatrix} T_{n,1} \\ T_{n,2} \\ T_{n,3} \\ T_{n,4} \\ \cdot \\ \cdot \\ T_{n,n} \end{bmatrix} = \begin{matrix} \\ \\ \\ \\ \\ \\ \end{matrix}$$

$$\begin{bmatrix}
 T_{n,1} \\
 (1-2a)T_{n,2} + 2aT_{n-1,2} \\
 (1-2a)T_{n,3} + 2aT_{n-1,3} \\
 (1-2a)T_{n,4} + 2aT_{n-1,4} \\
 \cdot \\
 (1-2a)T_{n,n-1} + 2aT_{n-1,n-1} \\
 T_{n,n}
 \end{bmatrix}^{n+1/2}$$

Finally, for  $i$  from 2 to  $N-1$ :

$$\begin{bmatrix}
 1 & 0 & 0 & \cdot & \cdot & \cdot & 0 \\
 -b & (1+2b) & -b & \cdot & \cdot & \cdot & \cdot \\
 0 & -b & (1+2b) & -b & \cdot & \cdot & \cdot \\
 \cdot & \cdot & \cdot & \cdot & \cdot & \cdot & \cdot \\
 \cdot & \cdot & \cdot & \cdot & \cdot & \cdot & 0 \\
 \cdot & \cdot & \cdot & \cdot & -b & (1+2b) & -b \\
 0 & \cdot & \cdot & \cdot & 0 & 0 & 1
 \end{bmatrix} \cdot \begin{bmatrix}
 T_{1,1} \\
 T_{1,2} \\
 T_{1,3} \\
 T_{1,4} \\
 \cdot \\
 \cdot \\
 T_{1,N}
 \end{bmatrix} =$$

$$\begin{bmatrix}
 T_{1,1} \\
 2aT_{2,2} + (1-2a)T_{1,2} \\
 2aT_{2,3} + (1-2a)T_{1,3} \\
 2aT_{2,4} + (1-2a)T_{1,4} \\
 \cdot \\
 2aT_{2,N-1} + (1-2a)T_{1,N-1} \\
 T_{1,N}
 \end{bmatrix}^{n+1/2}$$

Since  $i$  is held constant while  $j$  increments, this calculates one row at a time. The result is the 2D temperature profile at time  $n+1$ .

### Consequences of Lithospheric Heating

An increase in temperature at the base of the lithosphere appears at the surface after a certain lag time, which is a function of the average thermal diffusivity of the rock column. If the transport of heat is conductive, the result will be an increase in surface heat flow. In addition, an increase in temperature will result in a thermal expansion of the rock material. This expansion changes the density of the material, with the change being a function of the coefficient of thermal expansion. As a result, an increase in elevation in response to isostatic uplift can be calculated. Program HF2D has been designed to yield these quantities for a homogeneous two-dimensional model.

### Surface Heat Flow

The surface heat flow is the product of the geothermal gradient and the thermal conductivity of the rock material.

To obtain the gradient at a given horizontal position, the program takes the difference between the top two points in the model divided by the distance between them. The result is a set of heat flow values as a function of distance from the z-axis in the model.

### Isostatic Uplift

The isostatic uplift at a given point is the integrated change in density along the underlying rock column. The integration algorithm chosen for use in this program is the 1/3 Simpson's rule, determined for an odd number of points. The result is a set of values for uplift in kilometers as a function of distance from the z-axis in the model.

### Consequences of the Model

Within certain restrictions discussed below, any of the data sets calculated in this program can be compared to the present day values found in New Mexico and Arizona. In this way, each provides constraints on the amount, extent and duration required for a thermal pulse at the base of the lithosphere. However, these values taken together and compared to present day observations of heat flow and

elevation will provide an optimum constraint to determine the Cenozoic thermal history of Arizona and New Mexico.

### Discussion

A series of thermal perturbations have been applied to a steady-state, stable continental temperature gradient in order to determine a reasonable thermal history in the area. The present day heat flow anomaly associated with the Rio Grande Rift can be viewed as symmetric over a significant distance along its axis in New Mexico (Figure 44). Because the surface heat flow falls off towards both the Colorado Plateau and Great Plains provinces, the perturbation is in the form of a gaussian 'bell' curve described by:

$$T = C \times \exp(-a \times d^2)$$

Where T = Temperature

C = Amplitude of curve at distance  $x = 0$

a = Power coefficient, which determines the width of the bell

d = Offset distance in km.

In order to minimize spatial error in this analysis, only half of the bell curve is used in the calculation. The x-values can then be placed twice as close as if the whole bell curve is used. This is allowable because of the

symmetry inherent in the problem. The symmetry also implies that the lateral heat flow across the axis of the bell is zero, a condition required for the mathematical derivation. For the present analysis, therefore, the axis of the gaussian perturbation coincides with the axis of high heat flow readings along the Rio Grande Rift in central New Mexico. The program assumes that the thermal pulse is infinite in extent along the line perpendicular to the bell curve.

These thermal pulses have been applied at both 100 km and 30 km depth to calculate their effect on heat flow and isostatic uplift. However, crustal thinning has taken place both in the Basin and Range province (Gish and others, 1981; Sinno and others, 1981; this study) and Rio Grande Rift (Daggett and others, 1986; Sinno and others, 1986; this study). Since the lower crust has been replaced by mantle (asthenosphere ?) material, a convective component has been added in those regions, which is not addressed by program HF2D. This has a direct effect on the isostatic uplift calculations, which are based on thermal expansion alone. Therefore, for the cases in which heating is confined to the base of the lithosphere (100 km depth), the calculated values for isostatic uplift are not correlatable to observations from the Basin and Range and Rio Grande Rift in

Arizona and New Mexico. However, since the entire region has been uplifted, the isostatic uplift calculated by HF2D may have a broad meaning to the discussion. That is, uplift has occurred over the entire region, affecting all three provinces. The calculation of isostatic uplift can therefore be used as a general constraint to subsurface temperatures and their effect on surface heat flow. Also, all of the values created in the program should have quantifiable meaning for perturbations at 30 km, since they involve only the crust.

The initial estimates for temperature and density are similar for all models run in this study, and are presented in Figures 45 and 46 respectively. The initial steady-state temperature gradient includes a radioactive contribution for the top 10 km, underlain by a linear increase in temperature to the bottom of the lithosphere. After the program started calculating temperature evolution, the near surface radioactive contribution was removed. This resulted in an effective downwarp in elevation and lowering of the surface heat flow over the entire model, which was overcome by increasing the thermal pulse at depth. In this way, the maximum thermal perturbation could be calculated for the observed uplift and heat flow values. The density

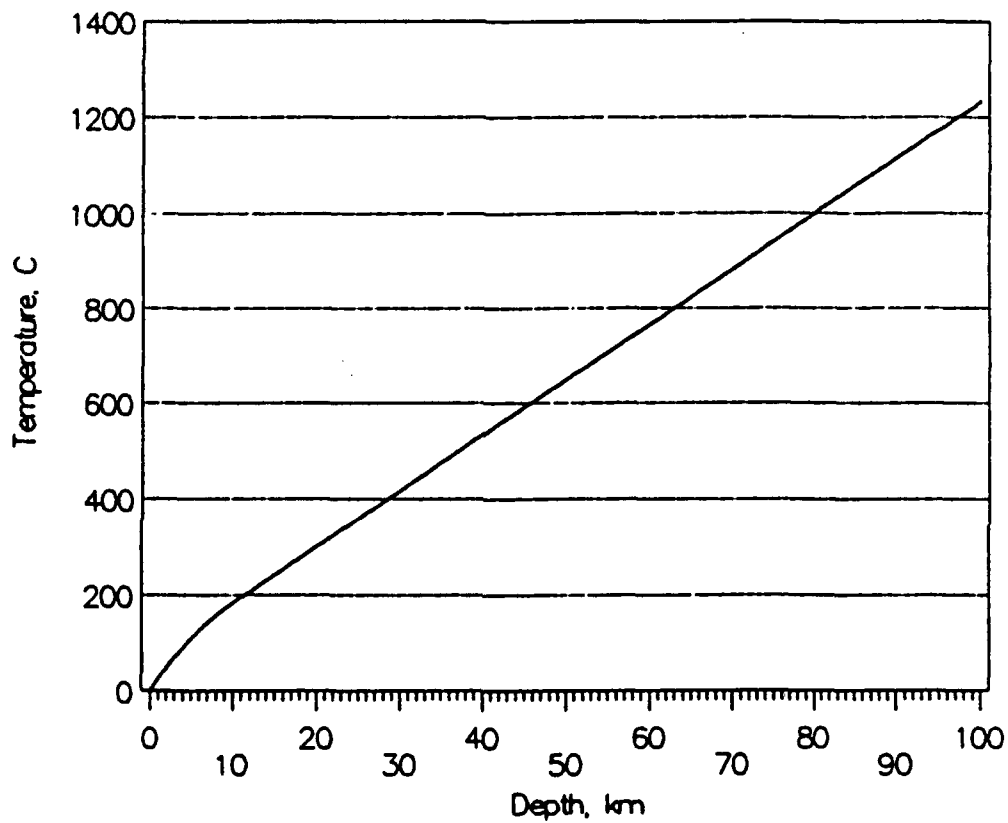


Figure 45. Initial temperature distribution for program HF2D. This is a typical steady-state temperature gradient with a 10 km thick radioactive layer in the upper crust, underlain by nonradioactive material.

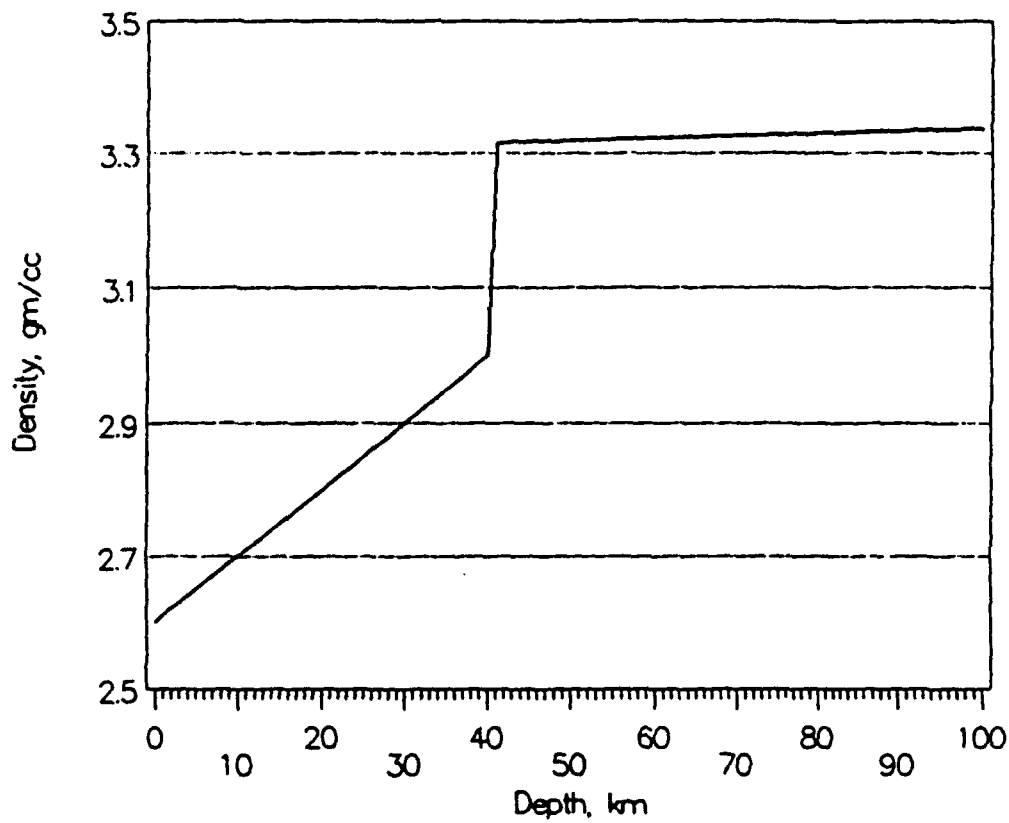


Figure 46. Initial density distribution for program HF2D. The upper 40 km consist of typical crustal density values, and the lower 60 km is that of mantle material.

distribution is for a crust of 40 km thickness, with a gradient resulting from overburden pressure.

The amplitude and width of the temperature pulse directly affects the resulting heat flow, uplift and gravity readings. Two curves of different width were used throughout this analysis: 1) using a power exponent of 0.0002, a curve with half width = 60 km was generated and is displayed with a zero offset amplitude of 100<sup>0</sup>C in Figure 47; and 2) using the same amplitude, Figure 48 shows a half-width of 37.5 km that reflects a power coefficient of 0.0005. By varying the amplitude, these perturbations are allowed to progress into the model with time, and their results are evaluated with respect to observed values.

A cross-section of the heat flow in the Rio Grande Rift is provided by Reiter and others (1978). They show an average peak value of 2.7 HFU over the axis of the anomaly, falling off to approximately 1.8 HFU about 90 km away (Figure 49). If the thermal anomaly lies at 100 km depth, the heat flow values generated by HF2D approach their curve at the axis only by a 1500<sup>0</sup>C amplitude with a power coefficient of 0.0002 (Figure 50). The "background" heat flow observed at distance is 1.5 HFU, which is less than Reiter and others (1978) background of 1.8 HFU. The difference is caused by dissimilar steady-state temperature

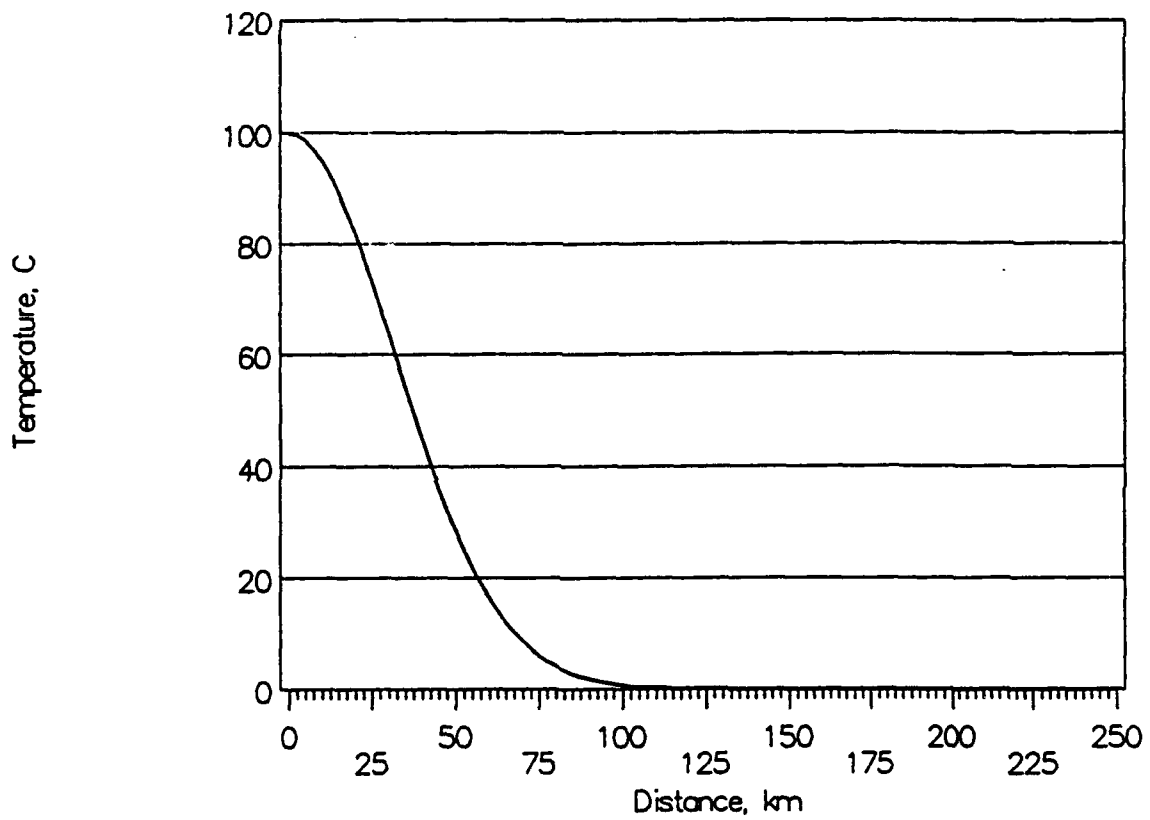


Figure 47. Gaussian curve with amplitude = 100, exponential coefficient term = 0.0005. Half-width of this pulse = 75 km due to symmetry about the origin.

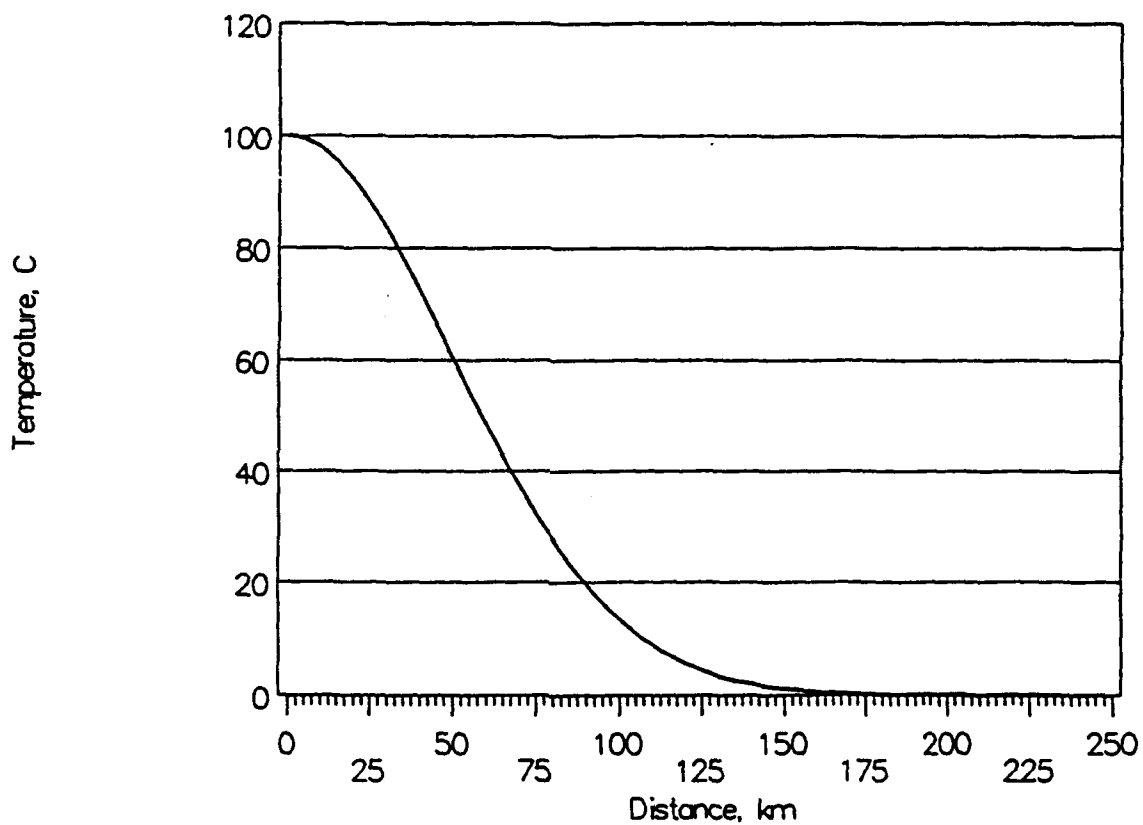


Figure 48. Gaussian curve with amplitude = 100, exponential coefficient term = 0.0002. Half-width of this pulse = 120 km due to symmetry about the origin.

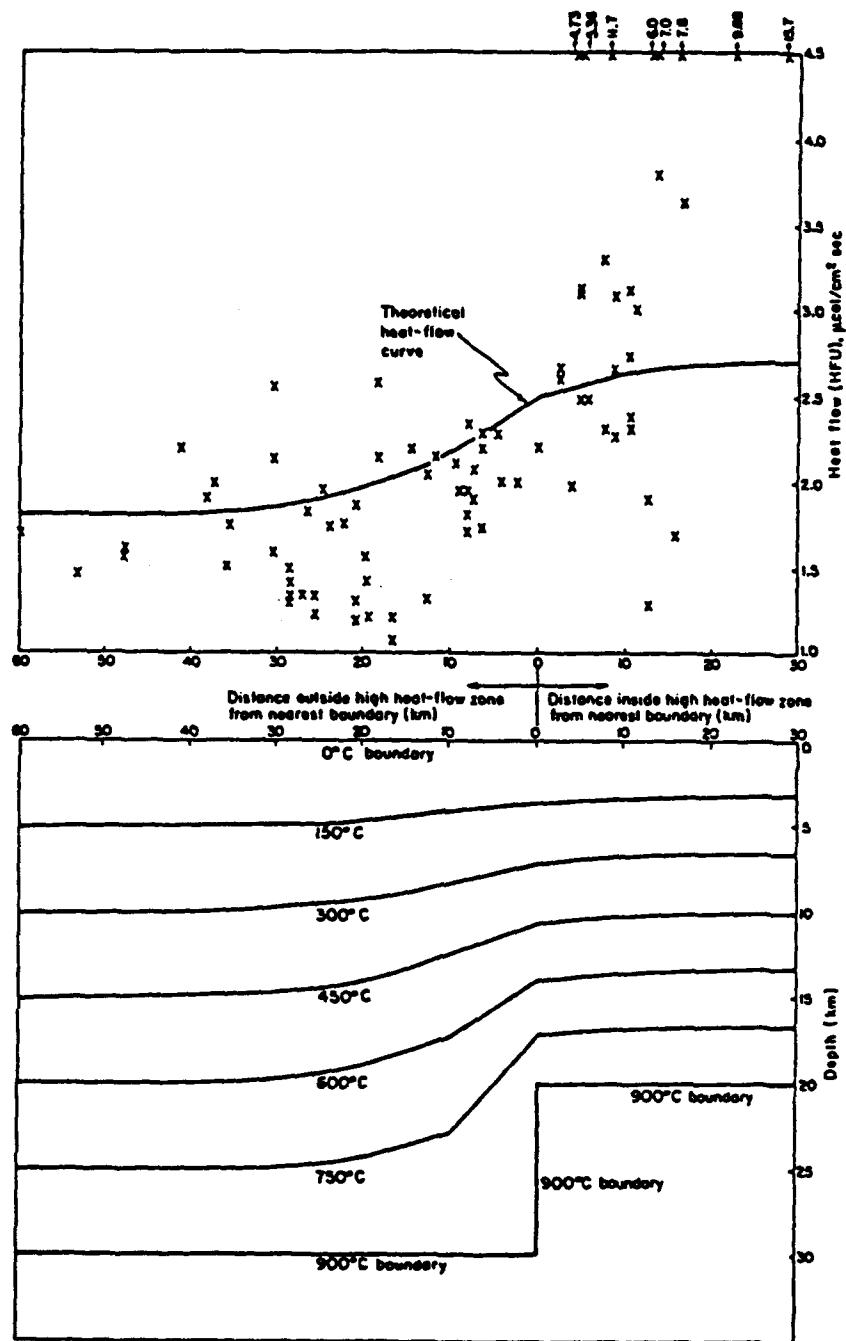


Figure 49. Thermal model of Reiter and others (1978) showing heat flow rise over the Rio Grande Rift.

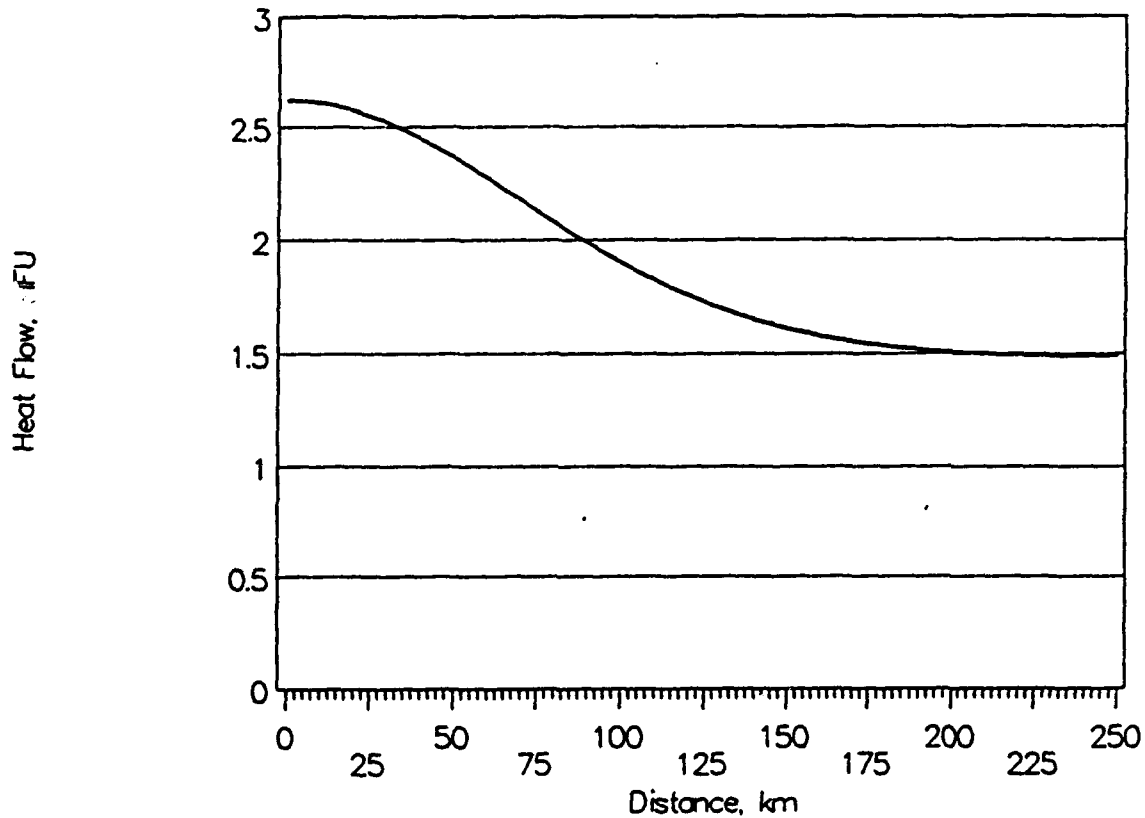


Figure 50. Calculated heat flow for a thermal pulse at 100 km depth after 40 Ma. The pulse is a gaussian curve centered on the origin, with a  $1500^{\circ}\text{C}$  amplitude and power coefficient of 0.0002. The heat flow generated by this model is similar to that found in Reiter and others (1978). As in all following figures, the origin is coincident with the axis of heat flow along the Rio Grande Rift.

gradients. It is observed that the heat flow anomaly is too broad for the rift. Furthermore, the calculated uplift of 5.5 km on the z-axis (Figure 51) shows this model to be unreasonable, since the regional uplift of the Colorado Plateau is observed to be about 2 km (Morgan and Swanberg, 1985). A perturbation of  $1500^{\circ}\text{C}$  at 100 km depth produces temperatures in excess of  $2700^{\circ}\text{C}$ , yielding a temperature gradient of  $27^{\circ}\text{C}/\text{km}$  through the entire lithosphere on the axis for the steady-state result. This value is unacceptably high for temperatures at 100 km depth. Furthermore, steady-state temperatures had not been achieved even after 40 Ma, equivalent to the time from the Laramide to the present. For these reasons, this model has been rejected as a solution to the present day tectonic state of the lithosphere.

Further analysis of Figure 51 determines that away from the axis, the values for isostatic uplift become negative and indicate a downwarp of about 350 m. This is attributable to the loss of the radioactive component to temperature values during the model evolution. Since the thermal effects of a temperature pulse at the axis should have little effect at distance, the effect of removing the radioactive component is that of a shift of the entire profile -350 m. The correct uplift is therefore estimated to be nearly 6 km at the axis for the model presented above.

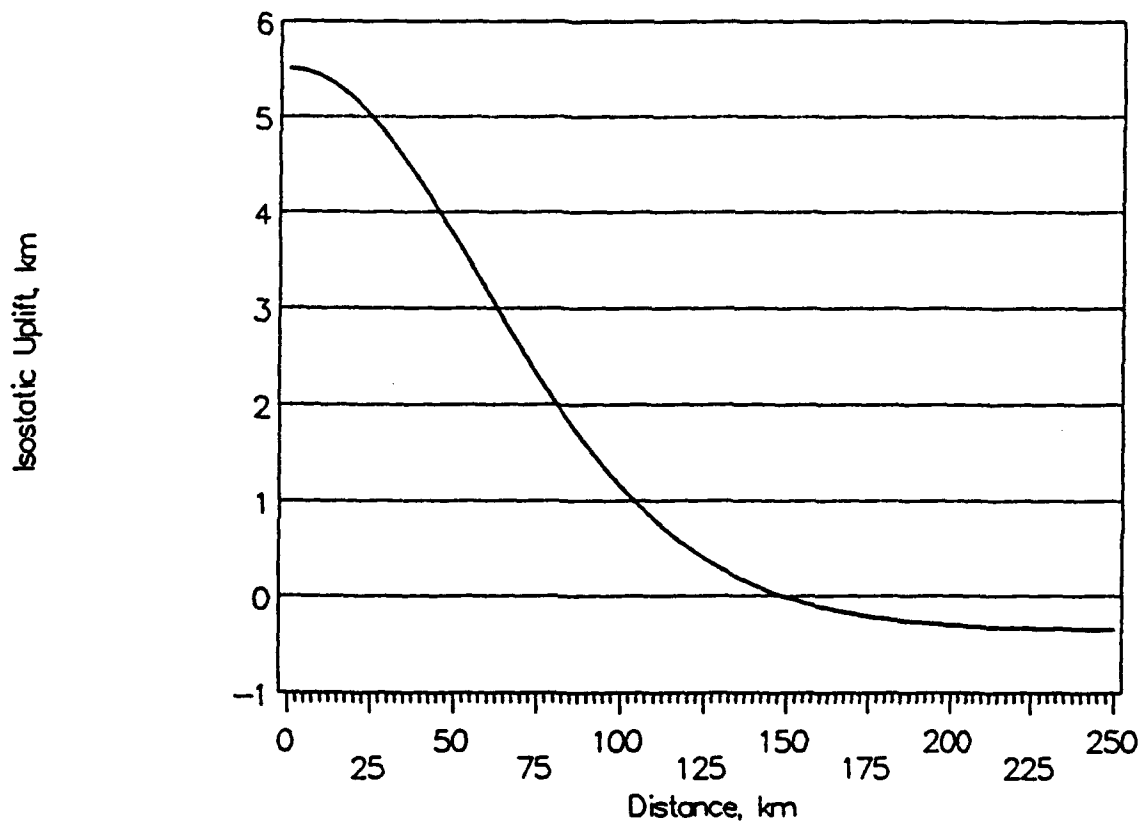


Figure 51. Calculated isostatic uplift for perturbation described in Figure 50. The negative values at large distances are caused by loss of the radioactive component during temperature evolution, which results in a DC shift of - 0.35 km to the data. The correct uplift is nearly 6 km.

The correct values for similar figures are hereafter referred to as uplift after "radioactive correction".

It is reasonable to expect the surface heat flow to decline from loss of the radioactive component as the model evolves. However, with an initial near-surface temperature gradient of  $24^{\circ}\text{C}$  and conductivity of  $2.5 \text{ W/m}^{\circ}\text{C}$ , the initial heat flow is 1.5 HFU. The lack of change of heat flow over time indicates that isostatic uplift is more sensitive to temperature changes throughout the lithosphere. The sole use of heat flow values can therefore be misleading when estimating tectonic change in the lithosphere.

Further evidence for this problem is presented in Figures 52 and 53, in which the thermal perturbation at 100 km depth has been reduced to  $400^{\circ}\text{C}$ . The heat flow (Figure 52) falls to 1.75 HFU on the axis representing a 33% drop in value. The total uplift after the radioactive correction has been reduced to approximately 1.5 km (Figure 53), a drop of 75%. In this case, both the heat flow and the uplift values are too low when compared to observations in central and southern New Mexico. For this example, the surface heat flow observed near the border of the Colorado Plateau cannot be created by a single thermal pulse at the base of the lithosphere.

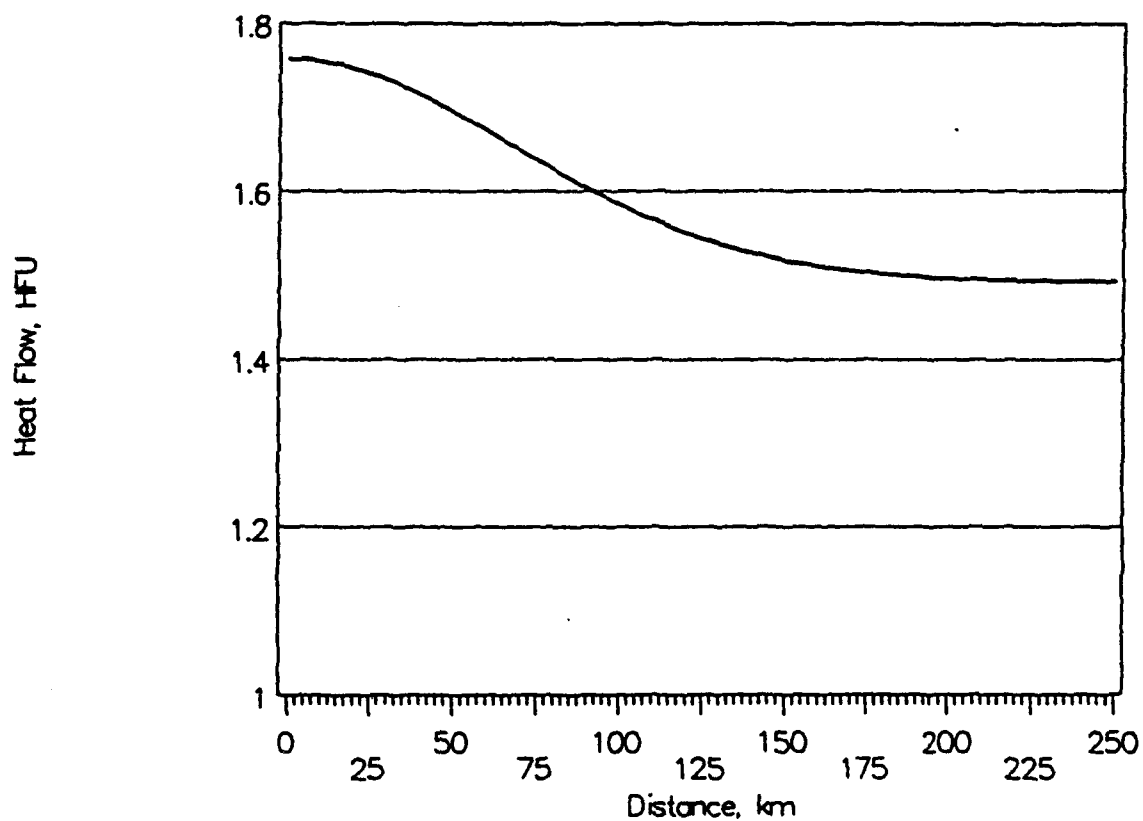


Figure 52. Calculated heat flow for a 400°C thermal pulse at 100 km depth. Power coefficient = 0.0002.

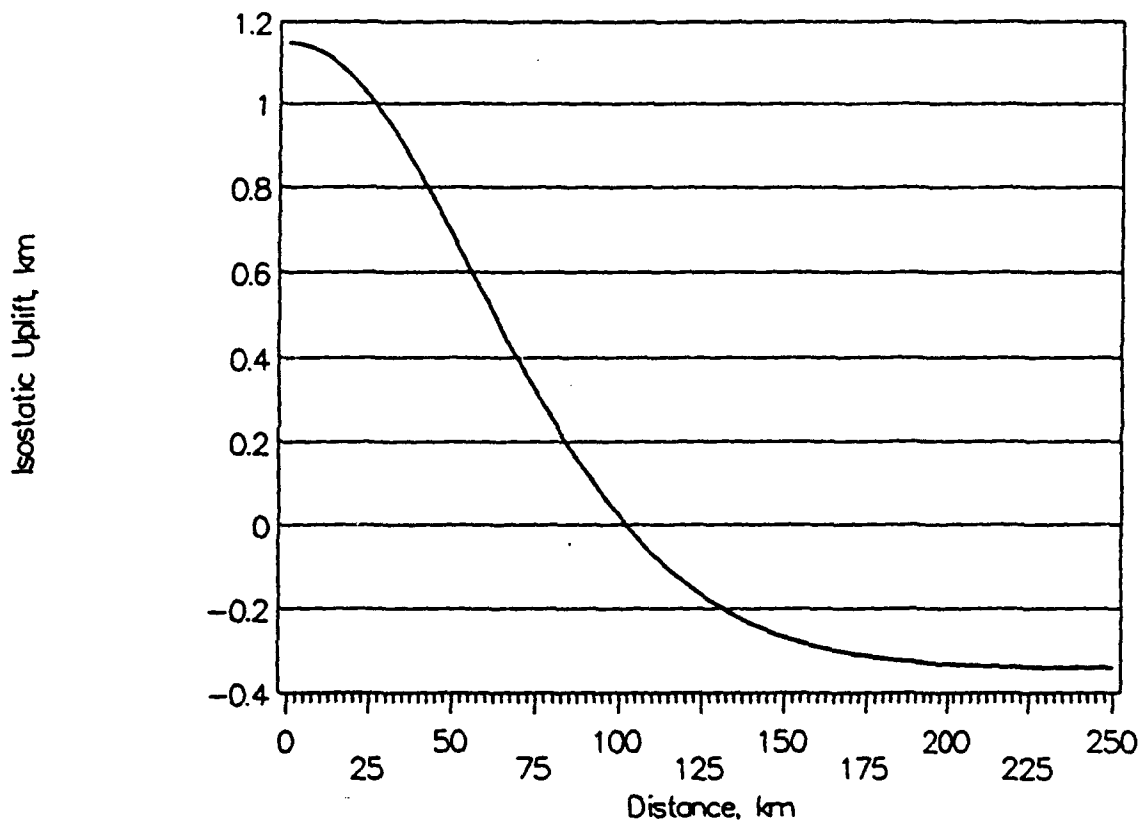


Figure 53. Calculated isostatic uplift for a 400°C thermal pulse at 100 km depth. Power coefficient = 0.0002. Total uplift after radioactive correction is 1.5 km (see Figure 51).

The effects of a thermal pulse at the base of the crust are therefore investigated. Because the highest heat flow readings are adjacent to the Colorado Plateau but within the Basin and Range and Rio Grande Rift provinces, the base of the crust is placed at 30 km. A  $350^{\circ}\text{C}$  pulse on the axis with a power coefficient = 0.0005 yields a heat flow of 2.8 HFU above the center of the anomaly (Figure 54), which is close to observed readings along the rift. The heat flow bulge also shows a half-width of about 40 km, which agrees reasonably well with the data of Reiter and others (1978). However, this thermal pulse yields an uplift after radioactive correction of only 0.39 km at the axis (Figure 55) indicating that this pulse is insufficient for the observed regional uplift.

At steady-state, this pulse would create a  $25^{\circ}\text{C}/\text{km}$  gradient to the anomaly at the base of the crust. From the arguments in the previous examples, this gradient cannot extend to the base of the lithosphere. The gradient must therefore flatten below the crust in order to prevent excessive uplift. Steady-state temperatures are reached for this perturbation in less than 5.5 Ma, which is close to the time of the most recent Basin and Range type extension and volcanism in the area, including the Jemez lineament (Luedke and Smith, 1978).

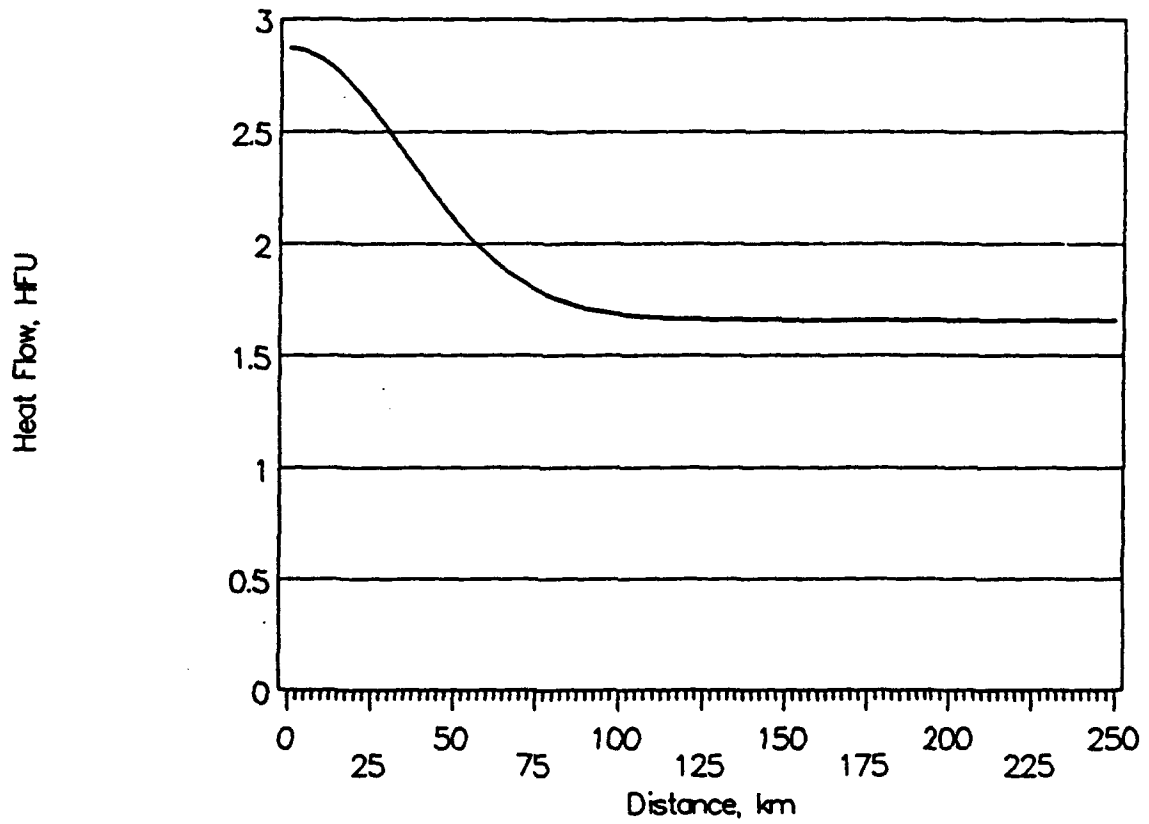


Figure 54. Calculated heat flow for a 350°C thermal pulse at 30 km depth.

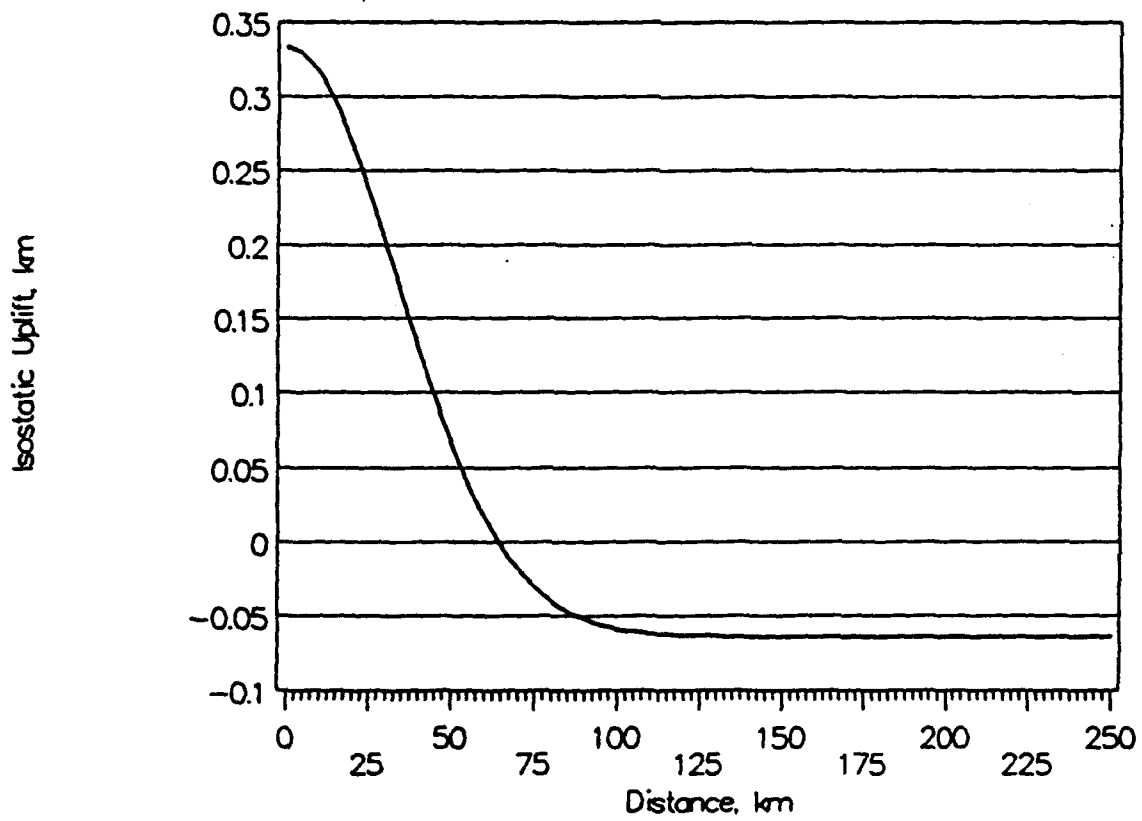


Figure 55. Calculated isostatic uplift for a 350°C thermal pulse at 30 km depth. Total amount of uplift after radioactive correction is 0.39 km (see Figure 51).

The cause of this temperature pulse may be the introduction of basaltic magma at the base of the crust, as proposed by Elston and others (1976a) and Davis and others (1989). From that position, the magma may have become the source for recent basaltic volcanism in the region (Luedke and Smith, 1978). Its presence may also have caused the recent thermal erosion of the crust described by Sinno and others (1981).

Because of the discrepancies between isostatic uplift and heat flow for models based on temperature pulses at 100 km and 30 km, they are insufficient to explain present-day values and therefore tectonic history. A better solution may be found by a combination of the above models. It is clear from these examples that temperature anomalies at 100 km depth have greater influence on uplift, and perturbations at 30 km have more impact on heat flow. By superimposing the 400°C temperature at 100 km and the 350°C pulse at 30 km, a solution that satisfies observed data may be obtained.

From arguments presented above, the temperature gradient must flatten below the crust if a 350°C pulse is located at 30 km depth. Since heat flow is dependent on temperature gradient, the deep anomaly has no effect for this condition. Therefore, no difficulties are encountered for heat flow data in this model.

Isostatic uplift must be some combination of the two models. In effect, raising the temperature by  $400^{\circ}\text{C}$  at 100 km depth raises the thermal gradient by  $4^{\circ}\text{C}/\text{km}$ . At 30 km, the temperature is raised  $120^{\circ}\text{C}$ . The uplift associated with this pulse after radioactive correction is about 1.5 km. Raising the temperature  $350^{\circ}\text{C}$  at 30 km depth with respect to initial conditions corresponds to an actual increase of only  $230^{\circ}\text{C}$  over the new "background" temperature. The additional uplift for the crustal component after radioactive correction is about 0.23 km on the z-axis (Figure 56), and the extra uplift for increased temperatures from 30 km to 100 km is about 0.64 km. The total uplift is about 2.37 km, which is slightly higher than the minimum amount of uplift required by Morgan and Swanberg (1985). With heat flow data, the combination of these temperatures at 30 km and 100 km depth appears to satisfy observed data. The steady-state temperature gradient is achieved for the deep pulse at 27.8 Ma implying that it was initiated during the mid-Tertiary.

The values for heat flow and isostatic uplift calculated from program HF2D are based on some assumptions that are violated by this explanation. For example, pooling of basalt fluids at the base of the crust implies a significant convective component to heat flow, while HF2D assumes heat transfer by conduction alone. Furthermore,

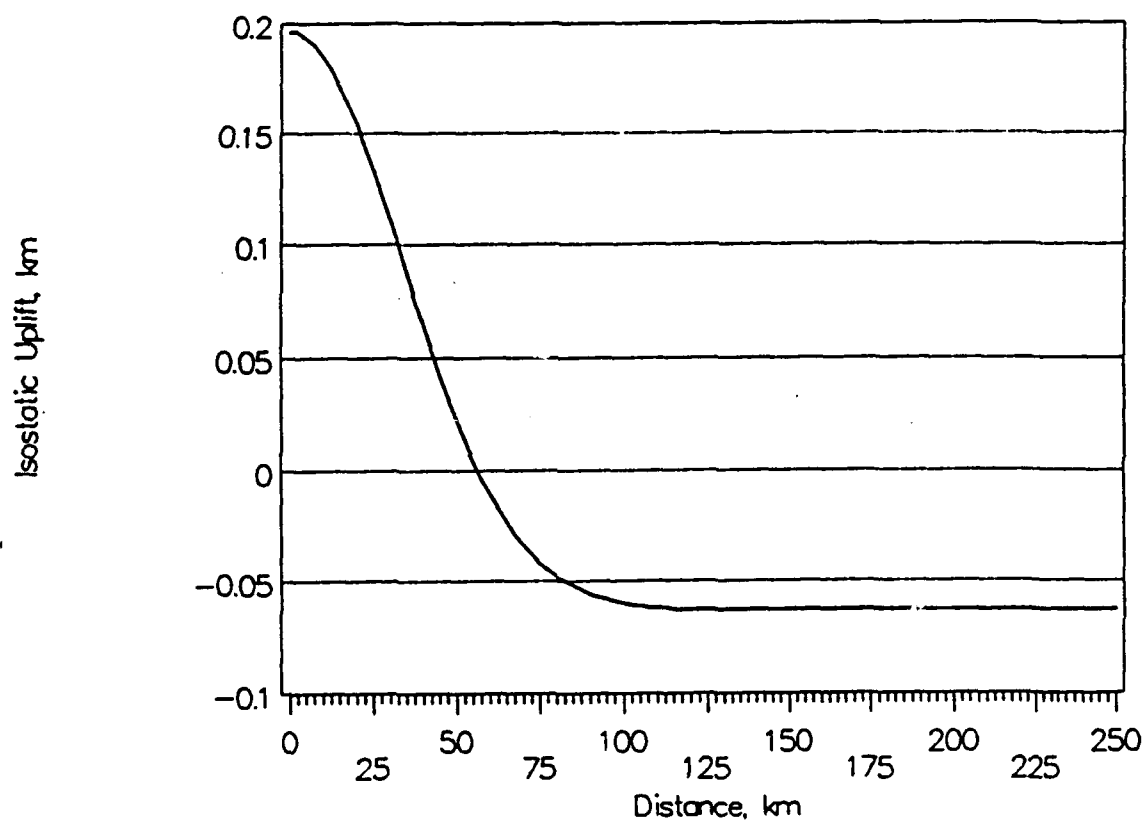


Figure 56. Calculated isostatic uplift for a  $230^{\circ}\text{C}$  thermal pulse at 30 km depth. Total uplift after radioactive correction (see Figure 51) is 0.25 km.

thinning of the crust introduces mantle material as a replacement for crustal material, which violates the program's assumption of change in density solely as a function of change in temperature. Since replacement of crustal material is suggested for the Rio Grande Rift and Basin and Range provinces, but not in the Colorado Plateau, lateral homogeneity as assumed by the program is also fallacious.

With these restrictions in mind, the program can still be used in a general way. The heat flow observed at the surface and calculated by the model does not rely on density changes from temperature change or convection. Because no assumptions were violated, the program is considered to be an accurate predictor of near-surface temperature gradients. Although assumptions behind uplift appear to be invalid in New Mexico and Arizona, regional uplift of the area is well documented and is reviewed in an earlier section of this report. The thinning of the crust and introduction of basalt at its base should result in relative downwarp with respect to neighboring regions, and is observed between the Colorado Plateau and the extensional provinces. Since this is spatially associated with high heat flow, the uplifts predicted by the paradigms in this study should be considered as maximum values.

It is therefore concluded from heat flow and uplift comparisons that southeastern Arizona and southwestern New Mexico is the site of two thermal anomalies: A long standing (about 28 Ma) thermal pulse at the base of the lithosphere along with a shorter term (5.4 Ma) anomaly at the base of the crust. These perturbations are likely to be related, and can explain the present state of volcanism, uplift, extension and rifting in southeastern Arizona and southwestern New Mexico. Because the uplift is regional, it is reasonable to expect that the deep anomaly is broader than the shallow pulse. Also, because of the narrow band of high heat flow and recent volcanic activity, the shallow anomaly is inferred to be spatially associated with the southeastern margin of the Colorado Plateau.

## CONCLUSIONS

This study addresses two fundamental problems in southeastern Arizona and southwestern New Mexico: the present day crustal geometry and the post-Laramide tectonic history of the southeastern margin of the Colorado Plateau. A solution to the former problem comes from the combined analysis of seismic refraction and gravity data, and the latter problem is investigated through the use of present day structure, surface geologic information and heat flow. To date, available data indicate a complex history that includes compression, uplift, tension, thermal disturbances and extensive volcanism throughout the region.

Keller and others (1975) determined that the physiographic and tectonic boundaries between the Colorado Plateau and Basin and Range provinces do not coincide in Utah. The boundary is therefore thought to be transitional instead of abrupt. This distinction is also supported in Arizona (Braumbaugh, 1987). The absence of a physiographic boundary east of the Mogollon Rim is therefore irrelevant to the determination of the tectonic transition zone in New Mexico. A complicating factor in the investigation of the transition zone in southeastern Arizona and southwestern New Mexico is the presence of the mid-Tertiary Mogollon-Datil

volcanic field (Elston and others, 1968, 1970, 1976a). The volcanics hide previous features and have influenced structural response to subsequent tectonic activity.

Because of the volcanic cover, it is possible to determine crustal structure only through the analysis of geophysical data constrained by geologic information. Previous geologic work has shown that a cluster of calderas that vented exclusively high-silica rhyolite is found on the Mogollon plateau (see e.g. Elston and others, 1976a). Although two calderas of the high-silica rhyolite suite occur outside this cluster, they are volumetrically minor with respect to the plateau. Rhodes (1976) has determined that rocks from each cauldron have certain unique chemical characteristics, but that the entire complex is intruded by dikes of consistent composition that have similarities to each cauldron fluid. Rhodes called the rocks contained in these dikes "framework lavas", and suggested a common source for all of the volcanics. Because no other volcanic suite was vented on the plateau during the development of these calderas, Elston and others (1976a) proposed that a near-surface magma chamber existed at that time. That chamber was thought to remain as a pluton (Coney, 1976a; Krohn, 1976), and was restricted to the area below the Mogollon plateau.

The integrated use of seismic refraction and gravity information resolves crustal structure to an extent not possible by either alone. Analysis of the data indicate the following:

1) Gravity and seismic refraction data provides evidence for a low-density, low-velocity body in the upper crust beneath southwestern New Mexico and southeastern Arizona. The proximity of mid-Tertiary volcanism with this body supports the interpretation of the presence of a pluton of similar age by Elston and others (1976a).

However, the geophysical data from both profiles examined in this study indicate that the pluton extends about 50 km north of the boundaries suggested by Elston and others (1976a), Krohn (1976), and McIntosh (1989).

2) The boundary of the pluton as predicted by gravity and seismic refraction analysis corresponds closely to the -20 mgal contour line of the 125 km low-pass gravity map over the study area. If this contour line follows the outline of the pluton, then the complex is larger than that predicted by the profiles used in this study. In

fact, it would be approximately 230 km by 155 km, extending northwest into Arizona (Figure 57).

3) The Moho markedly deepens approximately 90 km north of Silver City, from approximately 32 to 37 km over a distance of about 35 km. This region is located about midway between the north and south ends of the plutonic complex, and is north of the high-silica rhyolite cauldrons of the Mogollon plateau.

4) The Moho flattens at 38-40 km depth about 150 km north of Tyrone. This point is defined in this study as the southern edge of the Colorado Plateau. The final model describing current crustal structure (Figure 38) is similar to that described in central Arizona by Warren (1969). Therefore, the present day boundary of the Colorado Plateau trends west-southwest from central Arizona under the northern edge of the plutonic complex, then swings northward along the edge of the Rio Grande Rift (Figure 57).

5) Gravity data indicate that the Moho may become shallower by about 2 km near Grants. However, the data could also be explained by expansion of upper crustal layers at the expense of the lower crust

in that region, leaving the Moho flat. Seismic data was not obtained in that area, yielding lower resolution of major crustal boundaries.

6) If crustal thickness is used as a characteristic feature of the provinces in this region, then the plutonic complex overlaps the boundary between the Colorado Plateau and the extensional provinces to the south and east. The plutonic complex is spatially associated with the present day transition zone in Arizona and New Mexico.

The presence of a pluton with greater extent than the region under the Mogollon plateau points out some ambiguities in previous work. For example, Elston and others (1976a) suggest that the outer grabens which wrap around the Mogollon plateau are caused by Basin and Range type extension, and that the wrapping is caused by resistance of the pluton to through-going faulting. Since the pluton clearly extends to the north of the Plains of St. Augustine, this interpretation may be doubtful. Rhodes (1976) shows that the outer rim of the Mogollon plateau is associated with framework rhyolite, probably derived from faults tapping the magma body itself. The graben faults may

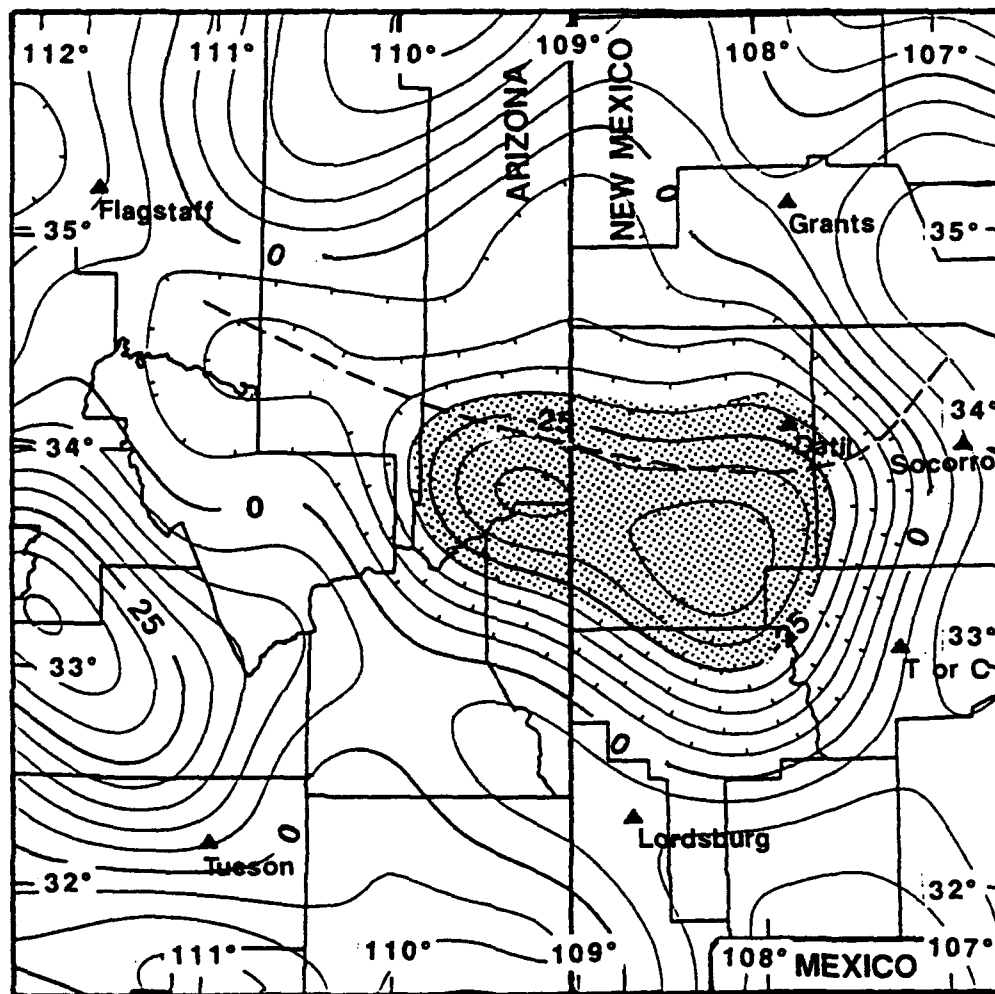


Figure 57. Extent of the proposed upper crustal pluton and its relationship to the 125 km low-pass gravity field. The southeastern margin of the Colorado Plateau is shown by the dashed line.

be associated with this plumbing system. Furthermore, the interior faults of these grabens show more movement than the exterior faults (Elston and others, 1976a). The spatial and chemical associations of these graben/fault systems may indicate that the volcanic complex itself is the causative factor, as explained below.

Coney (1976a) shows the Mogollon plateau to consist of a central, relatively undeformed region that has subsided with respect to its margin. Its boundaries, in turn, are uplifted and partly composed of framework rhyolite. The "Basin and Range" type faulting and associated grabens lie outside this rim. Thus, a possible explanation for faulting on the perimeter of the Mogollon plateau is the collapse of the entire high-silica rhyolite volcanic field above a huge vented magma chamber. The uplifted rims and associated faults are merely a giant ring-fracture, magma filled system. This would explain fracturing and faulting in terms of a high-silica rhyolite portion of a larger plutonic complex, as opposed to faulting associated with Basin and Range type extension.

The Plains of St. Augustine may be of different origin or have a different history than the other rim grabens. Chapin (1971) suggests that this may be a splay of the Rio Grande Rift. Chapin cites the presence of left-lateral

oblique slip faults at its northern and southern boundaries, that the down-faulted section almost completely includes the Datil group, and that structural relief is at least 1.1 km. Whether this is a branch of the rift is not determined in this study, but it is noteworthy that this offset is minor compared to 5000 m of movement at the edge of the rift in the nearby Lucero uplift area (Callender and Zilinski, 1976). Also, no crustal thinning associated with this feature is indicated from the present study.

The spatial relationship between the high-silica rhyolite pluton and the rest of the complex cannot be uniquely determined in this study. Furthermore, it remains undetermined whether the high-silica fluids come from a separate source area or are chemically related to the rest of the complex. Elston and others (1976a, 1976b) show tendencies for different volcanic suites to have different average chemical characteristics (such as  $^{87}\text{Sr}/^{86}\text{Sr}$  values and types of mineralization), but overlaps occur in these data sets. Separation of the high-silica rhyolite, calc-alkalic rhyolite and calc-alkalic andesite suites into unique source reservoirs is a step that remains to be proven.

An alternative interpretation to a unique high-silica magma chamber is one in which the high-silica fluids are

derived from a larger magma chamber. From sedimentary evidence, the crust under the Colorado Plateau in New Mexico was low relative to the south immediately prior to and during initial stages of mid-Tertiary volcanism (Cather and Johnson, 1986). The structural trend has subsequently reversed (Pierce and others, 1979; Morgan and Swanberg, 1985). It is possible that the most felsic components, including volatiles, worked their way to the top of the chamber as it developed. These pooled under the Mogollon plateau for the simple reason that it was the highest part of the pluton at the time. Subsequent cauldron-producing volcanic events were above the lightest, hottest material.

The two high-silica cauldron events outside the Mogollon plateau (Ratté and others, 1969; Rhodes and Smith, 1972) may reflect local maxima in the roof of the magma chamber. The density/chemistry stratification would satisfy the requirement that only high-silica rhyolites were vented within the Mogollon plateau during that time. This pooling effect may have caused a minor local uplift over the Mogollon plateau, creating the radial tension cracks reported by Elston and others (1976a). Subsequent collapse above a venting magma chamber caused normal faulting at the perimeter of the MP. Rocks of the calc-alkaline suite could

only be vented from the south end of the pluton after the overlying material was removed.

The cauldrons which did not vent high-silica rhyolite rocks yet are associated with the plutonic complex are not as clustered as those on the Mogollon plateau. Rhyolites are mapped in the Datil mountains and continue north to outcrops of Mesozoic sediments (New Mexico Geological Society Map, 1982). Intermediate volcanic rocks are also observed in east central Arizona, but much of that region is covered by more recent basalt flows (Wilson and others, 1969). However, these are not of the high-silica type found on the Mogollon plateau (Elston and others, 1976a). If these rocks were also vented from the pluton, a chemical differentiation may have existed and/or developed during the time of extrusion.

Other intermediate, calc-alkaline plutonic events in New Mexico and Arizona occur outside the boundary of the complex shown in Figure 57. This does not negate the argument that the magma chamber controlled volcanism where it was present. The entire region was affected by calc-alkaline volcanism as shown in Figure 10, so the presence of many cauldrons in the areas is expected during the mid-Tertiary. However, this interpretation concludes that the high-silica rhyolite suite developed as a result of the

ability to tap a magma chamber with a maximum volume of approximately  $180,000 \text{ km}^3$ .

The presence of a late Cenozoic episode of crustal thinning is supported in the Basin and Range province (Sinno and others, 1981). Also, low Pn velocities in the Rio Grande Rift (Sinno and others, 1986) and in this study indicate substantial present-day heating at the base of the crust. Recent regional uplift commenced around 5.5 Ma (Morgan and Swanberg, 1985), and includes the Colorado Plateau.

Despite this heating event, the crust under the Colorado Plateau appears to be resistant to thinning with respect to the Basin and Range province. This may imply a fundamental chemical difference in the lower crust between the Colorado Plateau, Rio Grande Rift and Basin-Range provinces. If present day crustal geology reflects that of mid-Tertiary time, then perhaps the high-silica rhyolite suite is a product of this difference in crustal chemistry.

A predictive model that calculates heat flow and isostatic uplift has been constructed to determine a temperature history of the region. Within the limitations placed on this model, a preliminary conclusion is that present day heat flow and elevation of the surface is best explained by two thermal anomalies: 1) a thermal pulse that

requires a maximum temperature increase of  $400^{\circ}\text{C}$  above stable continental values at 100 km depth has existed at least since mid-Tertiary time. This has resulted in regional isostatic uplift of about 1.5 km. 2) a temperature perturbation of about  $350^{\circ}\text{C}$  at the base of the crust was established approximately 5.4 Ma before present.

The deep anomaly yields a 1.5 km uplift at steady-state. Since 28 Ma is required for steady-state, this implies onset of the thermal pulse during the mid-Tertiary as a minimum estimate if temperatures have equilibrated. However, volcanism is present before this time in the region, which means this perturbation may be older than the minimum time needed. The earliest time for this pulse to be initiated is marked by the Cretaceous Mancos shale, required to be at or below sea level at the time of deposition (Morgan and Swanberg, 1985). The response to this anomaly may have been complicated by factors such as lithospheric strength, horizontal and vertical stress.

The younger event is likely related to the older, deeper anomaly and corresponds to the time of recent uplift (Morgan and Swanberg, 1985), rifting (Seager and Morgan, 1979) and volcanism (Luedke and Smith, 1978). It is spatially associated with the high heat flow zone at the southeastern boundary of the Colorado Plateau. It also

appears to be consistent with present day crustal structure determined by seismic refraction and gravity analysis in this study.

## REFERENCES

- Aiken, C. L. V., 1978, Gravity and aeromagnetic anomalies of southeastern Arizona: New Mexico Geological Society Guidebook, 29th Field Conference, p. 301-313.
- Aldrich, M. J., Jr., and Laughlin, A. W., 1984, A model for the tectonic development of the southeastern Colorado Plateau boundary: Journal of Geophysical Research, v. 89, p. 10,207-10,218.
- Ander, M. E., and Huestis, S. P., 1982, Mafic intrusion beneath the Zuni-Bandera volcanic field, New Mexico: Geological Society of America Bulletin, v. 93, p. 1142-1150.
- Anderson, D. A., Tannehill, J. C., and Fletcher, R. H., 1984, Computational Fluid Mechanics and Heat Transfers: Hemisphere Publishing Corporation, Washington, p. 115-119.
- Armstrong, R. L., 1968, Sevier orogenic belt in Nevada and Utah: Geological Society of America Bulletin, v. 79, p. 429-458.
- Baldrige, W. S., 1979, Petrology and petrogenesis of Plio-Pleistocene basaltic rocks from the central Rio Grande Rift, New Mexico, and their relation to rift structure: In Riecker, R. E. (ed.), Rio Grande Rift: Tectonics and Magmatism: American Geophysical Union, Washington, D.C., p. 323-354.
- Baldrige, W. S., Olsen, K. H., and Callender, J. F., 1984, Rio Grande Rift: Problems and perspectives: New Mexico Geological Society Guidebook, 35th Field Conference, p. 1-12.
- Baldrige, W. S., Perry, F. V., and Shafiqullah, M., 1987, Late Cenozoic volcanism of the southeastern Colorado Plateau: I. Volcanic geology of the Lucero area, New Mexico: Geological Society of America Bulletin, v. 99, p. 463-470.

- Baldrige, W. S., Perry, F. V., Vaniman, D. T., Nealy, L. D., Leavy, B. D., Laughlin, A. W., Kyle, P., Bartov, Y., Steinitz, G., and Gladney, E. S., 1989, Magmatism associated with lithospheric extension: Middle to late Cenozoic magmatism of the southeastern Colorado Plateau and central Rio Grande Rift, New Mexico and Arizona: New Mexico Bureau of Mines & Mineral Resources, Memoir 46, p. 187-202.
- Barker, D. S., 1979, Magmatic evolution in the Trans-Pecos province: University of Texas at Austin Bureau of Economic Geology, Guidebook 19, p. 4-9.
- Beghoul, N., and Barazangi, M., 1989, Mapping high Pn velocity beneath the Colorado Plateau constrains uplift models: Journal of Geophysical Research, v. 94, p. 7083-7104.
- Bennett, V. C., and DePaolo, D. J., 1987, Proterozoic crustal history of the western United States as determined by neodymium isotopic mapping: Geological Society of America Bulletin, v. 99, p. 674-685.
- Berg, R. R., 1962, Mountain flank thrusting in Rocky Mountain foreland, Wyoming and Colorado: American Association of Petroleum Geologists Bulletin, v. 46, p. 2019-2032.
- Bilodeau, W. L., 1984, Laramide sedimentation and tectonics in southeastern Arizona and southwestern New Mexico: Reactivation of pre-Laramide basement structures (abs.): Geological Society of America Abstracts with Programs, v. 16, p. 445.
- Blackwell, D. D., 1978, Heat flow and energy loss in the western United States: in Smith, R. B., and Eaton, G. P. (eds.), Cenozoic Tectonics and Regional Geophysics of the Western Cordillera: Geological Society of America, Memoir 152, p. 175-208.
- Bodell, J. M., and Chapman, D. S., 1982, Heat flow in the north-central Colorado Plateau: Journal of Geophysical Research, v. 87, p. 2869-2884.
- Bott, M. H. P., and Smithson, S. B., 1967, Gravity investigations of subsurface shape and mass distributions of granite batholiths: Geological Society of America Bulletin, v. 78, p. 859-878.

- Briggs, I. C., 1974, Machine contouring using minimum curvature: *Geophysics*, v. 39, p. 39-48.
- Brumbaugh, D. S., 1987, A tectonic boundary for the southern Colorado Plateau: *Tectonophysics*, v. 136, p. 125-136.
- Burchfiel, B. C., and Davis, G. A., 1972, Structural framework and evolution of the southern part of the Cordilleran orogen, western United States: *American Journal of Science*, v. 272, p. 97-118.
- Busby-Spera, C. J., 1988, Speculative tectonic model for the early Mesozoic arc of the southwest Cordilleran United States: *Geology*, v. 16, p. 1121-1125.
- Cady, J. W., 1980, Calculation of gravity and magnetic anomalies of finite-length right polygonal prisms: *Geophysics*, v. 45, p. 1507-1512.
- Callender, J. F., and Zilinski, R. E. Jr., 1976, Kinematics of Tertiary and Quaternary deformation along the eastern edge of the Lucero uplift, central New Mexico: *New Mexico Geological Society, Special Publication 6*, p. 53-61.
- Cather, S. M., and Chapin, C. E., 1989, Field guide to upper Eocene and lower Oligocene volcanoclastic rocks of the northern Mogollon-Datil volcanic field: *New Mexico Bureau of Mines & Mineral Resources, Memoir 46*, p. 60-68.
- Cather, S. M., and Johnson, B. D., 1986, Eocene depositional systems and tectonic framework of west-central New Mexico and eastern Arizona: *American Association of Petroleum Geologists, Memoir 41*, p. 623-652.
- Cervený, V., and Ravindra, R., 1971, *Theory of Seismic Head Waves*: University of Toronto Press, Toronto, Canada, p. 312.
- Chapin, C. E., 1971, The Rio Grande Rift, part 1: Modifications and additions: in James, H. L. (ed.), *San Luis Basin*: *New Mexico Geological Society, Guidebook 22*, p. 191-201.
- Christiansen, R. L., 1989, Volcanism associated with post-Laramide tectonic extension in the western U.S.: *New Mexico Bureau of Mines & Mineral Resources, Memoir 46*, p. 51.

- Christiansen, R. L., and Lipman, P. W., 1972, Cenozoic volcanism and plate tectonic evolution of the western United States, 2. Late Cenozoic: Philosophical Transactions of the Royal Society of London, Series A, v. 271, p. 249-284.
- Condie, K. C., 1982, Plate-tectonics model for Proterozoic continental accretion in the southwestern United States: *Geology*, v. 10, p. 37-42.
- Condie, K. C., 1986, Geochemistry and tectonic setting of early Proterozoic supracrustal rocks in the southwestern United States: *Journal of Geology*, v. 94, p. 845-864.
- Coney, P. J., 1976a, Structure, volcanic stratigraphy, and gravity across the Mogollon plateau, New Mexico: New Mexico Geological Society, Special Publication 5, p. 29-41.
- Coney, P. J., 1976b, Plate tectonics and the Laramide orogeny: New Mexico Geological Society, Special Publication 6, p. 5-10.
- Coney, P. J., 1978a, The plate tectonic setting of southeastern Arizona: New Mexico Geological Society Guidebook, 29th Field Conference, p. 285-290.
- Coney, P. J., 1978b, Mesozoic-Cenozoic Cordilleran plate tectonics: in Smith, R. B., and Eaton, G. B. (eds.), *Cenozoic Tectonics and Regional Geophysics of Western Cordillera*: Geological Society of America, Memoir 152, p. 33-50.
- Cook, F. A., Decker, E. R., and Smithson, S. B., 1978, Preliminary transient heat flow model of the Rio Grande Rift in southern New Mexico: *Earth and Planetary Science Letters*, v. 40, p. 316-326.
- Cook, F. A., McCullar, D. B., Decker, E. R., and Smithson, S. B., 1979, Crustal structure and evolution of the southern Rio Grande Rift: in Riecker, R. E. (ed.), *Rio Grande Rift: Tectonics and Magmatism*: American Geophysical Union, Washington, D.C., p. 195-208.
- Cox, K. G., Bell, J. D., and Pankhurst, R. J., 1979, *The Interpretation of Igneous Rocks*: George Allen & Unwin, London, p. 450.

- Daggett, P. H., Keller, G. R., Morgan, P., and Wen, C. L., 1986, Structure of the southern Rio Grande Rift from gravity interpretation: *Journal of Geophysical Research*, v. 91, p. 6157-6167.
- Dane, C. H., and Bachman, G. O., 1965, Geologic Map of New Mexico: U. S. Geological Survey, 2 sheets, scale 1:500,000.
- Davis, G. H., 1978, Monocline fold pattern of the Colorado Plateau: *Geological Society of America, Memoir 151*, p. 215-233.
- Davis, P. M., Slack, P., Dahlheim, H. A., Green, W. V., Meyer, R. P., Olsen, K. H., Achauer, U., and Glahn, A., 1989, Teleseismic tomographic deep sounding of the upper mantle beneath the world's major rift zones (abs.): *EOS*, v. 70, p. 1135.
- DeAngelo, M. V., and Keller, G. R., 1988, Geophysical anomalies in southwestern New Mexico: *New Mexico Geological Society Guidebook, 39th Field Conference*, p. 71-75.
- Decker, E. R., and Smithson, S. B., 1975, Heat flow and gravity interpretation across the Rio Grande Rift in southern New Mexico and west Texas: *Journal of Geophysical Research*, v. 80, p. 2542-2552.
- Drewes, H., 1981, Tectonics of southeastern Arizona: *United States Geological Survey, Professional Paper 1144*, p. 1-96.
- Edwards, C. L., Reiter, M., Shearer, C., and Young, W., 1978, Terrestrial heat flow and crustal radioactivity in northeastern New Mexico and southeastern Colorado: *Geological Society of America Bulletin*, v. 89, p. 1341-1350.
- Elston, W. E., 1976, Tectonic significance of mid-Tertiary volcanism in the Basin and Range province: A critical review with special reference to New Mexico: *New Mexico Geological Society, Special Publication 5*, p. 93-102.
- Elston, W. E., 1978, Mid-Tertiary cauldrons and their relationship to mineral resources, southwestern New Mexico: A brief review: *New Mexico Geological Society, Special Publication 7*, p. 107-113.

- Elston, W. E., 1989, Overview of the Mogollon-Datil volcanic field: New Mexico Bureau of Mines & Mineral Resources, Memoir 46, p. 43-44.
- Elston, W. E., and Abitz, R. J., 1989, Regional setting and temporal evolution of the Mogollon-Datil volcanic field, southwestern New Mexico: New Mexico Bureau of Mines & Mineral Resources, Memoir 46, p. 82.
- Elston, W. E., and Bornhorst, T. I., 1979, The Rio Grande Rift in context of regional post-40 m.y. volcanic and tectonic events: in Riecker, R. E. (ed.), Rio Grande Rift: Tectonics and Magmatism: American Geophysical Union, Washington, D.C., p. 416-438.
- Elston, W. E., Coney, P. J., and Rhodes, R. C., 1968, A progress report on the Mogollon plateau volcanic province, southwestern New Mexico: Colorado School Mines Quart., v. 63, p. 261-287.
- Elston, W. E., Coney, P. J., and Rhodes, R. C., 1970, Progress report on the Mogollon plateau volcanic province, southwestern New Mexico, No. 2: New Mexico Geological Society Guidebook, 21st Field Conference, Tyrone - Big Hatchet Mountains - Florida Mountains Region, p. 75-86.
- Elston, W. E., Rhodes, R. C., Coney, P. J., and Deal, E. G., 1976a, Progress report on the Mogollon plateau volcanic field, southwestern New Mexico, No. 3 - Surface expression of a pluton: New Mexico Geological Society, Special Publication 5, p. 3-28.
- Elston, W. E., Rhodes, R. C., and Erb, E. B., 1976b, Control of mineralization by mid-Tertiary volcanic centers, southwestern New Mexico: New Mexico Geological Society, Special Publication 5, p. 125-130.
- Epis, R. C., and Chapin, C. E., 1975, Geomorphic and tectonic implications of the post-Laramide, late Eocene erosion surface in the southern Rocky Mountains: Geological Society of America, Memoir 144, p. 1-40.
- Gish, D. M., Keller, G. R., and Sbar, M. L., 1981, A refraction study of deep crustal structure in the Basin and Range: Colorado Plateau of eastern Arizona: Journal of Geophysical Research, v. 86, p. 6029-6038.

- Grambling, J. A., Williams, M. L., and Mawer, C. K., 1988, Proterozoic tectonic assembly of New Mexico: *Geology*, v. 16, p. 724-727.
- Gries, J. C., 1979, Problems of delineation of the Rio Grande Rift into the Chihuahua tectonic belt of northern Mexico: In Riecker, R. E. (ed.), *Rio Grande Rift: Tectonics and Magmatism: American Geophysical Union, Washington, D.C.*, p. 107-114.
- Gries, J. C., 1983, North-south compression of Rocky Mountain foreland structures: in Lowell, J. D. (ed.), *Rocky Mountain Foreland Basins and Uplifts: Rocky Mountain Association of Geologists, Denver, Colorado*, p. 9-32.
- Hamilton, W., 1969, Mesozoic California and the underflow of Pacific mantle: *Geological Society of America Bulletin*, v. 80, p. 2409-2430.
- Harden, S., 1982, A seismic refraction study of west-central New Mexico: Unpublished M.S. thesis, University of Texas at El Paso, El Paso, Texas.
- Hauser, E. C., and Lundy, J., 1989, COCORP deep reflections: Moho at 50 km (16s) beneath the Colorado Plateau: *Journal of Geophysical Research*, v. 94, p. 7071-7081.
- Henry, C. D., and Price, J. G., 1986, Early Basin and Range development in Trans-Pecos Texas and adjacent Chihuahua: Magmatism and orientation, timing, and style of extension: *Journal of Geophysical Research*, v. 91, p. 6213-6224.
- Hill, D. P., Kissling, E., Luetgert, J. H., and Kradolfer, U., 1985, Constraints on the upper crustal structure of the Long Valley-Mono Craters volcanic complex, eastern California, from seismic refraction measurements: *Journal of Geophysical Research*, v. 90, p. 11135-11150.
- Hinojosa, J. H., 1989, Thermal model of the Colorado Plateau lithosphere (abs.): *EOS*, v. 70, p. 1361.
- Humphrey, J. R., and Wong, I. G., 1983, Recent seismicity near Capitol Reef National Park, Utah, and its tectonic implications: *Geology*, v. 11, p. 447-451.

- Hunt, C. B., 1956, Cenozoic history of the Colorado Plateau: United States Geological Survey, Professional Paper 279, p. 93.
- Jahns, R. H., McMillon, D. K., O'Brient, J. D., and Fisher, D. L., 1978, Geologic section in the Sierra Cuchillo and flanking areas, Sierra and Socorro counties, New Mexico: New Mexico Geological Society, Special Publication 7, p. 131-138.
- Jaksha, L. H., 1982, Reconnaissance seismic refraction-reflection surveys in southwestern New Mexico: Geological Society of America Bulletin, v. 93, p. 1030-1037.
- Jaksha, L. H., and Sanford, A. R., 1986, Earthquakes near Albuquerque, New Mexico, 1976-1981: Journal of Geophysical Research, v. 91, p. 6293-6304.
- Jenkins, R. D., and Keller, G. R., 1989, Interpretation of basement structures and geophysical anomalies in the southwestern Colorado Plateau: New Mexico Geological Society Guidebook, 40<sup>th</sup> field conference, p. 135-142.
- Karlstrom, K. E., and Bowring, S. A., 1988, Early Proterozoic assembly of tectonostratigraphic terranes in southwestern North America: Journal of Geology, v. 96, p. 561-576.
- Keller, G. R., 1986, Introduction to special section on the Rio Grande Rift: Journal of Geophysical Research, v. 91, p. 6142.
- Keller, G. R., Braile, L. W., and Morgan, P., 1979a, Crustal structures, geophysical models and contemporary tectonism of the Colorado Plateau: Tectonophysics, v. 61, p. 131-147.
- Keller, G. R., Braile, L. W., and Schlue, J. W., 1979b, Regional crustal structure of the Rio Grande Rift from surface wave dispersion measurements: in Riecker, R. E. (ed.), Rio Grande Rift: Tectonics and Magmatism: American Geophysical Union, Washington, D.C., p. 115-126.

- Keller, G. R., Callender, J. F., Hawley, J. W., Chamberlin, R. M., Kluth, C. F., Olsen, K. H., and Lozinsky, R. P., 1989, Rio Grande Rift: Field trip Guidebook, 28th International Geological Congress: American Geophysical Union, Washington, D.C., p. T318:1-37.
- Keller, G. R., Smith, R. B., and Braile, L. W., 1975, Crustal structure along the Great Basin-Colorado Plateau transition from seismic refraction studies: Journal of Geophysical Research, v. 80, p. 1093-1098.
- Kelley, S. A., and Duncan, I. J., 1986, Late Cretaceous to middle Tertiary tectonic history of the northern Rio Grande Rift, New Mexico: Journal of Geophysical Research, v. 91, p. 6246-6262.
- Kelley, V. C., 1955, Regional tectonics of the Colorado Plateau and relationship to the origin and distribution of uranium: University of New Mexico, Publications in Geology 5, p. 120.
- Kelley, V. C., 1979, Tectonics, middle Rio Grande Rift, New Mexico: In Riecker, R. E. (ed.), Rio Grande Rift: Tectonics and Magmatism: American Geophysical Union, Washington, D.C., p. 57-70.
- Kluth, C. F., 1986, Plate tectonics of the Ancestral Rocky Mountains: American Association of Petroleum Geologists, Memoir 41, p. 353-369.
- Krohn, D. H., 1976, Gravity survey of the Mogollon plateau volcanic province, southwestern New Mexico: New Mexico Geological Society, Special Publication 5, p. 113-116.
- Lachenbruch, A. H., and Sass, J. H., 1978, Models of an extending lithosphere and heat flow in the Basin and Range province: in Smith, R. B., and Eaton, G. P. (eds.), Cenozoic Tectonics and Regional Geophysics of the Western Cordillera: Geological Society of America, Memoir 152, p. 209-250.
- Larsen, S., Reilinger, R., and Brown, L., 1986, Evidence of ongoing crustal deformation related to magmatic activity near Socorro, New Mexico: Journal of Geophysical Research, v. 91, p. 6283-6292.

- Lipman, P. W., 1989, Oligocene-Miocene San Juan volcanic field, Colorado: New Mexico Bureau of Mines & Mineral Resources, Memoir 46, p. 303-305.
- Lipman, P. W., and Mehnert, H. H., 1979, The Taos volcanic field, northern Rio Grande Rift, New Mexico: In Riecker, R. E. (ed.), Rio Grande Rift: Tectonics and Magmatism: American Geophysical Union, Washington, D.C., p. 289-312.
- Lipman, P. W., Protska, H. J., and Christiansen, R. L., 1972, Cenozoic volcanism and plate tectonic evolution of the western United States, 1. Early and middle Cenozoic: Philosophical Transactions of the Royal Society of London, v. 271, p. 217-248.
- Luedke, R. G., and Smith, R. L., 1978, Map showing distribution, composition, and age of late Cenozoic volcanic centers in Arizona and New Mexico: United States Geological Survey Miscellaneous Investigations Series, Map I-1091-A, scale 1:1,000,000.
- Mayer, L., 1979, Evolution of the Mogollon Rim in central Arizona: Tectonophysics, v. 61, p. 49-62.
- McCullar, D. B., 1977, Seismic refraction analysis to the crust and upper mantle beneath the Rio Grande Rift in southern New Mexico: M. S. Thesis, University of Wyoming, Laramie, Wyoming, 127 p.
- McIntosh, W. C., 1989, Timing and distribution of ignimbrite volcanism in the Eocene-Miocene Mogollon-Datil volcanic field: New Mexico Bureau of Mines & Mineral Resources, Memoir 46, p. 58-59.
- Morgan, P., 1983, Constraints on rift thermal processes from heat flow and uplift: Tectonophysics, v. 94, p. 277-298.
- Morgan, P., and Golombek, M. P., 1984, Factors controlling the phases and styles of extension in the northern Rio Grande Rift: New Mexico Geological Society Guidebook, 35th Field Conference, p. 13-19.
- Morgan, P., Seager, W. R., and Golombek, M. P., 1986, Cenozoic thermal, mechanical and tectonic evolution of the Rio Grande Rift: Journal of Geophysical Research, v. 91, p. 6263-6276.

- Morgan, P., and Swanberg, C. A., 1985, On the Cenozoic uplift and tectonic stability of the Colorado Plateau: *Journal of Geodynamics*, v. 3, p. 39-63.
- New Mexico Geological Society Map, 1982, New Mexico Highway Geologic Map: Scale 1:1,000,000.
- Olsen, K. H., Baldrige, W. S., and Callender, J. F., 1987, Rio Grande Rift: An overview: *Tectonophysics*, v. 143, p. 119-139.
- Olsen, K. H., Keller, G. R., and Stewart, T. N., 1979, Crustal structure along the Rio Grande Rift from seismic refraction profiles: in Riecker, R. E. (ed.), *Rio Grande Rift: Tectonics and Magmatism*: American Geophysical Union, Washington, D.C., p. 127-143.
- Pedersen, J., and Hermance, J. F., 1981, Deep electrical structure of the Colorado Plateau as determined from magnetotelluric measurements: *Journal of Geophysical Research*, v. 86, p. 1849-1857.
- Peeples, W. J., Coultrip, R. L., and Keller, G. R., 1986, Quasi-ideal spatial filters for large maps: *Annales Geophysicae*, v. 4, p. 547-554.
- Perry, F. V., Baldrige, W. S., and DePaolo, D. J., 1987, Role of asthenosphere and lithosphere in the genesis of late Cenozoic basaltic rocks from the Rio Grande Rift and adjacent regions of the southwestern United States: *Journal of Geophysical Research*, v. 92, p. 9193-9213.
- Perry, F. V., Baldrige, W. S., and DePaolo, D. J., 1988, Chemical and isotopic evidence for lithospheric thinning beneath the Rio Grande Rift: *Nature*, v. 332, p. 432-434.
- Pierce, H. W., Damon, P. E., and Shafiqullah, M., 1979, An Oligocene (?) Colorado Plateau edge in Arizona: *Tectonophysics*, v. 61, p. 1-24.
- Press, W. H., Flannery, B. P., Teukolsky, S. A., and Vetterling, W. T., 1986, *Numerical Recipes: The Art of Scientific Computing*: Cambridge University Press, Cambridge, New York, 818 p.
- Price, J. G., and Henry, C. D., 1984, Stress orientations during Oligocene volcanism in Trans-Pecos Texas:

- Timing the transition from Laramide compression to Basin and Range tension: *Geology*, v. 12, p. 238-241.
- Ratté, J. C., 1989, Selected volcanic features of the western Mogollon-Datil volcanic field: New Mexico Bureau of Mines & Mineral Resources, Memoir 46, p. 68-69.
- Ratté, J. C., Landis, E. R., Gaskill, D. L., and Raabe, R. G., 1969, Mineral resources of the Blue Range Primitive Area, Greenlee county, Arizona, and Catron county, New Mexico, with a section on aeromagnetic interpretation by G. P. Eaton: United States Geological Survey Bulletin 1261-E, p. 91.
- Rehrig, W. A., and Heidrick, T. L., 1976, Regional tectonic stress during the Laramide and late Tertiary intrusive periods, Basin and Range province: *Arizona Geological Society Digest*, v. 10, p. 205-228.
- Reilinger, R. E., Brown, L. D., and Oliver, J. E., 1979, Recent vertical crustal movements from leveling observations in the vicinity of the Rio Grande Rift: In Riecker, R. E. (ed.), *Rio Grande Rift: Tectonics and Magmatism*: American Geophysical Union, Washington, D.C., p. 223-236.
- Reiter, M., and Clarkson, G., 1983, A note on terrestrial heat flow in the Colorado Plateau: *Geophysical Research Letters*, v. 10, p. 929-932.
- Reiter, M., Edwards, C. L., Hartman, H., and Weidman, C., 1975, Terrestrial heat flow along the Rio Grande Rift, New Mexico and southern Colorado: *Geological Society of America Bulletin*, v. 86, p. 811-818.
- Reiter, M., Eggleston, R. E., Broadwell, B. R., and Minier, J., 1986, Estimates of terrestrial heat flow from deep petroleum tests along the Rio Grande Rift in central and southern New Mexico: *Journal of Geophysical Research*, v. 91, p. 6225-6245.
- Reiter, M., Mansure, A. J., and Shearer, C., 1979, Geothermal characteristics of the Colorado Plateau: *Tectonophysics*, v. 61, p. 183-195.
- Reiter, M., Shearer, C., and Edwards, C. L., 1978, Geothermal anomalies along the Rio Grande Rift in New Mexico: *Geology*, v. 6, p. 85-88.

- Rhodes, R. C., 1976, Petrologic framework of the Mogollon plateau volcanic ring complex, New Mexico - Surface expression of a major batholith: New Mexico Geological Society, Special Publication 5, p. 103-112.
- Rhodes, R. C., and Smith, E. I., 1972, Geology and tectonic setting of the Mule Creek caldera, New Mexico, U.S.A.: Bulletin of Volcanology, v. 36, p. 401-411.
- Rinehart, E. J., Sanford, A. R., and Ward, R. M., 1979, Geographic extent and shape of an extensive magma body at midcrustal depths in the Rio Grande Rift near Socorro, New Mexico: In Riecker, R. E. (ed.), Rio Grande Rift: Tectonics and Magmatism: American Geophysical Union, Washington, D.C., p. 237-252.
- Roller, J. C., 1965, Crustal structure in the eastern Colorado Plateaus province from seismic refraction measurements: Seismological Society of America Bulletin, v. 55, p. 107-119.
- Ross, C. A., and Ross, J. R. P., 1986, Paleozoic paleotectonics and sedimentation in Arizona and New Mexico: American Association of Petroleum Geologists, Memoir 41, p. 653-668.
- Sanford, A. R., Mott, R. P., Jr., Shuleski, P. J., Rinehart, E. J., Caravella, F. J., Ward, R. M., and Wallace, T. C., 1977, Geophysical evidence for a magma body in the crust in the vicinity of Socorro, New Mexico: in Heacock, J. G. (ed.), The Earth's Crust: American Geophysical Union, Monograph 20, p. 385-403.
- Sass, J. H., Stone, C., and Bills, D. J., 1982, Shallow subsurface temperatures and some estimates of heat flow from the Colorado Plateau of northeastern Arizona: United States Geological Survey, Open-File Report 82-994, 112 p.
- Schlue, J. W., Singer, P. J., and Edwards, C. L., 1986, Shear wave structure of the upper crust of the Albuquerque-Belen basin from Rayleigh wave phase velocities: Journal of Geophysical Research, v. 91, p. 6277-6282.
- Seager, W. R., and Mack, G. H., 1986, Laramide paleotectonics of southern New Mexico: American

- Association of Petroleum Geologists, Memoir 41, p. 669-685.
- Seager, W. R., and Morgan, P., 1979, Rio Grande Rift in southern New Mexico, west Texas, and northern Chihuahua: In Riecker, R. E. (ed.), Rio Grande Rift: Tectonics and Magmatism: American Geophysical Union, Washington, D.C., p. 87-106.
- Seager, W. R., Shafiqullah, M., Hawley, J. W., and Marvin, R. F., 1984, New K-Ar dates from basalts and the evolution of the southern Rio Grande Rift: Geological Society of America Bulletin, v. 95, p. 87-99.
- Shannon, W. M., 1989, Middle Proterozoic alkaline granites: Franklin mountains, El Paso, Texas (abs.): New Mexico Bureau of Mines & Mineral Resources, Memoir 46, p. 239.
- Shearer, C., and Reiter, M., 1981, Terrestrial heat flow in Arizona: Journal of Geophysical Research, v. 86, p. 6249-6260.
- Silver, L. T., and Anderson, T. H., 1974, Possible left-lateral early to middle Mesozoic disruption of the southwestern North American craton margin (abs.): Geological Society of America, Abstracts with Programs, v. 6, p. 955-956.
- Sinno, Y. A., Daggett, P. H., Keller, G. R., Morgan, P., and Harder, S. H., 1986, Crustal structure of the southern Rio Grande Rift determined from seismic refraction profiling: Journal of Geophysical Research, v. 91, p. 6143-6156.
- Sinno, Y. A., and Keller, G. R., 1986, A Rayleigh wave dispersion study between El Paso, Texas, and Albuquerque, New Mexico: Journal of Geophysical Research, v. 91, p. 6168-6174.
- Sinno, Y. A., Keller, G. R., and Sbar, M. L., 1981, A crustal seismic refraction study in west-central Arizona: Journal of Geophysical Research, v. 86, p. 5023-5038.
- Smith, D. L., and Jones, R. L., 1979, Thermal anomaly in northern Mexico: An extension of the Rio Grande Rift?: In Riecker, R. E. (ed.), Rio Grande Rift: Tectonics and Magmatism: American Geophysical Union, Washington, D.C., p. 269-278.

- Stewart, S. W., and Pakiser, L. C., 1962, Crustal structure in eastern New Mexico interpreted from the Growe explosion: Bulletin of the Seismological Society of America, v. 55, p. 877-886.
- Sumner, J. S., 1985, Crustal geology of Arizona as interpreted from magnetic, gravity and geologic data: In Hinze, W. J. (ed.), The Utility of Regional Gravity and Magnetic Anomaly Maps: Society of Exploration Geophysicists, Tulsa, Oklahoma, p. 164-180.
- Swain, C. J., 1976, A FORTRAN IV program for interpolating irregularly spaced data using the difference equations for minimum curvature: Computer Geoscience, v. 1, p. 231-240.
- Swanberg, C. A., 1979, Chemistry of thermal and nonthermal groundwaters in the Rio Grande Rift and adjacent tectonic provinces: In Riecker, R. E. (ed.), Rio Grande Rift: Tectonics and Magmatism: American Geophysical Union, Washington, D.C., p. 279-288.
- Swanberg, C. A., and Morgan, P., 1985, Silica heat flow estimates and heat flow in the Colorado Plateau and adjacent areas: Journal of Geodynamics, v. 3, p. 65-85.
- Talwani, M., Worzel, J. L., and Landisman, M., 1959, Rapid gravity computations for two-dimensional bodies with applications to the Mendocino Submarine Fracture zone: Journal of Geophysical Research, v. 64, p. 49-59.
- Thompson, G. A., and Zoback, M. L., 1979, Regional geophysics of the Colorado Plateau: Tectonophysics, v. 61, p. 149-181.
- Thompson, S. III, and Bieberman, R. A., 1975, Oil and gas exploration wells in Dona Ana County, New Mexico: New Mexico Geological Society, 26th Annual Fieldtrip Guidebook, p. 171-174.
- Topozada, T. R., and Sanford, A. R., 1976, Crustal structure in central New Mexico interpreted from the Gasbuggy explosion: Seismological Society of America Bulletin, v. 66, p. 877-886.

- Tweto, O., 1975, Laramide (Late Cretaceous - early Tertiary) orogeny in the southern Rocky Mountains: Geological Society of America, Memoir 144, p. 1-44.
- Warren, D. H., 1969, A seismic-refraction survey of crustal structure in central Arizona: Geological Society of America Bulletin, v. 80, p. 257-282.
- Warren, R. G., Kudo, A. M., and Keil, K., 1979, Geochemistry of lithic and single-crystal inclusions in basalt and a characterization of the upper mantle-lower crust in the Engle basin, Rio Grande Rift, New Mexico: In Riecker, R. E. (ed.), Rio Grande Rift: Tectonics and Magmatism: American Geophysical Union, Washington, D.C., p. 393-415.
- Wilson, E. D., Moore, E. T., and Cooper, J. R., 1969, Geologic map of Arizona: Arizona Bureau of Mines and United States Geological Survey, scale 1:500,000.
- Zimmerman, C., and Kudo, A. M., 1979, Geochemistry of andesites and related rocks, Rio Grande Rift, New Mexico: In Riecker, R. E. (ed.), Rio Grande Rift: Tectonics and Magmatism: American Geophysical Union, Washington, D.C., p. 355-381.

## ABBREVIATIONS

- BRP = Basin and Range province
- CP = Colorado Plateau
- Ga = Giga-annum
- GPP = Great Plains province
- HFU = Heat flow unit =  $41.87 \text{ mWm}^{-2}$
- Ma = Mega-annum
- MDVF = Mogollon-Datil volcanic field
- MP = Mogollon plateau
- PcR = P-wave reflection from the top of the lower crustal layer
- Pg = P-wave refracted through the upper crust
- PgR = P-wave reflection from the top of the intermediate crustal layer
- PmP = P-wave reflection from the top of the Moho
- Pn = P-wave refracted through the upper mantle
- RGR = Rio Grande Rift
- Sn = S-wave refracted through the upper mantle

APPENDIX I

LIST OF SOURCE PARAMETERS

<u>DATE</u>	<u>TIME</u>	<u>UTM COORDINATES (meters)</u>	
8-13-87	13:34:58.76	-3,279.349	3,612,255.476
8-14-87	11:11:44.05	-3,553.669	3,611,615.396
8-14-87	11:12:02.88	-3,797.509	3,611,874.476
8-29-87	11:04:20.27	-3,462.229	3,612,255.476
3-28-88	11:08:32.98	-3,218.389	3,612,072.596
3-28-88	11:29:59.82	-3,157.429	3,612,316.436
3-29-88	11:18:10.44	-3,462.229	3,611,523.956
6-1-89	13:40:00.62	-3,462.229	3,612,316.436
6-3-89	11:08*	-3,492.709	3,611,981.156
6-3-89	11:08:43.59	-3,492.709	3,611,981.156
6-4-89	11:25*	-3,584.149	3,612,255.476
6-23-89	11:29*	-3,218.389	3,612,255.476
6-26-89	11:07*	-3,888.949	3,612,133.556
6-27-89	11:15*	-3,523.189	3,612,133.556
6-29-89	11:08*	-4,010.869	3,612,011.636
8-27-89	11:09:23.89		

## Notes:

Base station coordinates =       -3,439.369       3,611,737.316

UTM coordinates referenced to -108.5° longitude

\* Origin times to the nearest minute: at least one record from these dates occupied the same site as a record with a positively identified origin time.

APPENDIX II

LIST OF RECORDING STATIONS, LOCATIONS, AND ELEVATIONS

<u>STATION</u>	<u>LATITUDE</u>	<u>LONGITUDE</u>	<u>QUADRANGLE</u>	<u>ELEVATION (FT)</u>
base	32.659523	108.341568	Tyrone	6425
ts-1	32.697453	108.338661	Tyrone	5989
ts-2	32.712688	108.296310	Tyrone	5700
ts-3	32.740116	108.274460	Tyrone	5948
tg-2	32.841309	108.223999	Ft. Bayard	6730
tg-3	32.872486	108.215538	Ft. Bayard	6925
tg-4	32.894783	108.234818	Twin Sister	6570
tg-5	32.909691	108.228325	Twin Sister	6760
tg-7	32.945950	108.196449	Twin Sister	7475
tg-9	32.975708	108.207985	Twin Sister	7250
tg-10	33.015926	108.229034	Copperas Peak	6920
tg-11	33.039646	108.219048	Copperas Peak	5840
tg-12	33.061916	108.209946	Copperas Peak	6120
tg-13	33.098026	108.194870	Copperas Peak	6640
tg-14	33.120518	108.189758	Copperas Peak	7400
tg-15	33.159019	108.197685	Gila Hot Spr.	6440
tg-16	33.202793	108.214050	Gila Hot Spr.	5600
tg-17	33.185028	108.028549	Middle Mesa	6780
tg-18	33.214706	108.028084	Middle Mesa	7520
tg-19	33.241726	108.061966	Middle Mesa	7080
tg-20	33.275455	108.060669	Wall Lake	6510
tg-21	33.307198	108.070786	Wall Lake	6910
tg-22	33.340206	108.063293	Wall Lake	6510
tg-23	33.373352	108.080505	Wall Lake	7090
tg-27a	33.450386	108.054703	Spring Canyon	7000
tg-28a	33.478180	108.017639	Taylor Peak	7118
tg-29a	33.506470	107.980049	Indian Peaks E.	7204
tg-30a	33.534870	107.935738	Indian Peaks E.	7222
tg-30	33.547806	107.919258	Indian Peaks E.	7300
tg-31	33.566269	107.905579	Indian Peaks E.	7325
tg-32	33.595684	107.883057	Indian Peaks E.	7398
tg-33	33.631451	107.872169	Paddy's Hole	7460
tg-34	33.659649	107.858421	Paddy's Hole	7515
tg-36	33.722771	107.820694	Paddy's Hole	7600
tg-38	33.760544	107.790253	Luera Mts. E.	7460
tg-42a	33.896481	107.832504	C-N Lake	7105
tg-43a	33.911167	107.844986	C-N Lake	7045
tg-44a	33.930710	107.848915	C-N Lake	7060
tg-45a	33.947365	107.840919	C-N Lake	6965
tg-46a	33.966145	107.835365	C-N Lake	7090
tg-47a	33.991222	107.823097	C-N Lake	7132
tg-48a	34.031307	107.808899	Anderson Pk.	7079
tg-49a	34.056866	107.805618	Anderson Pk.	7156
tg-50a	34.069225	107.773674	Anderson Pk.	7063
tg-51a	34.091316	107.774948	Anderson Pk.	7119

<u>STATION</u>	<u>LATITUDE</u>	<u>LONGITUDE</u>	<u>QUADRANGLE</u>	<u>ELEVATION</u> <u>(FT)</u>
tg-43	33.908760	107.781120	C-N Lake	6910
tg-45	33.986760	107.800285	C-N Lake	6897
tg-46	34.010395	107.774895	Anderson Pk.	6968
tg-47	34.039173	107.768524	Anderson Pk.	6999
tg-48	34.067383	107.768425	Anderson Pk.	7050
tg-49	34.093628	107.768356	Anderson Pk.	7096
tg-50	34.169605	107.808144	Datil	7519
tg-52	34.207268	107.862831	Datil	7590
tg-54	34.239124	107.831161	Datil	7800
tg-55	34.264240	107.810883	Cal Ship Mesa	7940
tg-56	34.274857	107.789024	Cal Ship Mesa	8120
tg-58	34.307701	107.759628	Cal Ship Mesa	8100
tg-59	34.330269	107.767693	Cal Ship Mesa	7780
tg-58a	34.305569	107.688385	Dog Springs	7361
tg-59a	34.327656	107.713844	Dog Springs	7590
tg-60	34.344658	107.743675	Dog Springs	7520
tg-61	34.359093	107.725433	Dog Springs	7490
tg-62a	34.383461	107.683365	D Cross Mtn.	7365
tg-63a	34.413815	107.667313	D Cross Mtn.	7180
tg-64	34.442356	107.653877	D Cross Mtn.	6760
tg-65	34.468246	107.637146	D Cross Mtn.	6482
tg-66	34.493443	107.577156	Table Mountain	6320
tg-67	34.515568	107.578476	Pueblo Viejo M.	6430
tg-68	34.536659	107.579109	Pueblo Viejo M.	6470
tg-69	34.554462	107.596077	Pueblo Viejo M.	6540
tg-70	34.583324	107.571724	Pueblo Viejo M.	6630
tg-74	34.689655	107.596329	Broom Mountain	7260

APPENDIX III

LIST OF RECORDING STATIONS AND DISTANCE TO EACH SITE

<u>STATION</u>	<u>DISTANCE (KM)</u>	<u>STATION</u>	<u>DISTANCE (KM)</u>
ts-1	4.40	tg-37	129.99
ts-2	7.30	tg-38	132.46
ts-3	11.22	tg-39	137.27
tg-1	20.40	tg-42a	145.13
tg-2	22.97	tg-42	145.5
tg-3	26.40	tg-43a	146.31
tg-4	27.91	tg-43	148.06
tg-5	29.76	tg-44a	148.24
tg-6	31.88	tg-45a	150.21
tg-7	34.50	tg-46a	152.37
tg-8	35.54	tg-44	152.50
tg-9	37.20	tg-44.5	153.42
tg-10	40.92	tg-47	155.36
tg-11	43.72	tg-45	155.58
tg-12	46.30	tg-45.5	156.94
tg-13	50.59	tg-46	158.84
tg-14	53.07	tg-48a	159.99
tg-15	57.02	tg-46.5	160.63
tg-15.5	59.07	tg-47	162.01
tg-16	61.44	tg-49a	162.78
tg-17	65.18	tg-48	164.98
tg-18	68.16	tg-50a	165.03
tg-19	69.63	tg-51a	167.33
tg-20	73.16	tg-49	167.79
tg-21	76.14	tg-49.75	172.96
tg-22	79.86	tg-50	174.63
tg-23	82.83	tg-50.5	175.86
tg-24	85.71	tg-52	177.32
tg-25	89.90	tg-53	179.44
tg-27a	91.71	tg-54	181.48
tg-26	94.00	tg-55	184.68
tg-28a	95.68	tg-56	186.35
tg-27	97.49	tg-57	188.82
tg-28	99.75	tg-57a	190.48
tg-29a	99.79	tg-58	190.62
tg-29	102.47	tg-58a	192.37
tg-30a	104.21	tg-59	192.80
tg-30	106.09	tg-59a	193.98
tg-31	108.48	tg-60	194.95
tg-32	112.30	tg-61	197.00
tg-33	116.34	tg-62a	200.71
tg-34	119.71	tg-63a	204.38
tg-35	122.71	tg-64	207.77
tg-36	127.52	tg-65	210.97

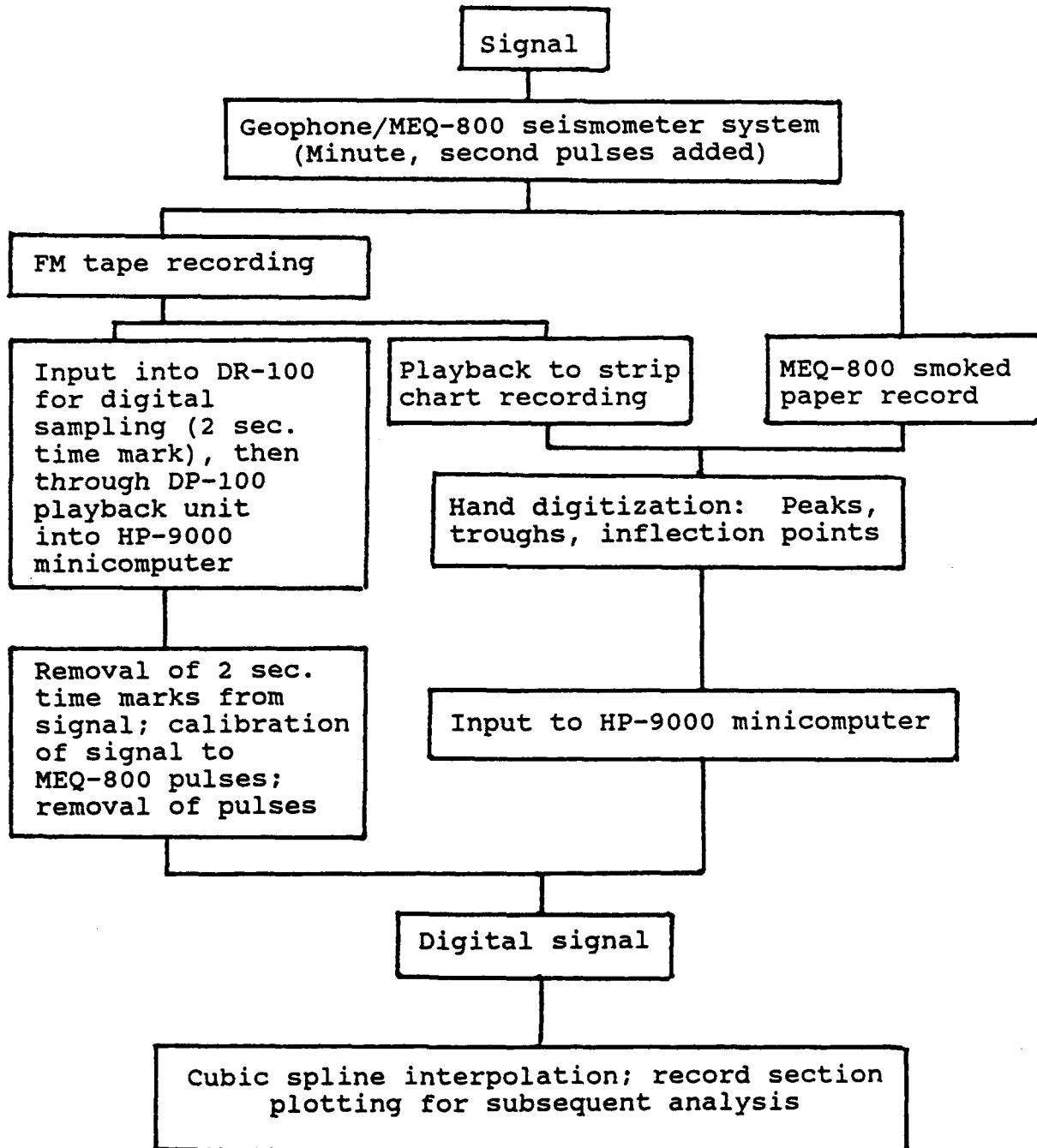
<u>STATION</u>	<u>DISTANCE (KM)</u>
tg-66	215.40
tg-67	217.68
tg-68	219.87
tg-69	221.25
tg-70	224.98

<u>STATION</u>	<u>DISTANCE (KM)</u>
tg-71	227.38
tg-72	229.48
tg-73	233.41
tg-74	235.51

APPENDIX IV

PROCEDURES FOR SEISMIC DATA RETRIEVAL

## Flow Chart of Seismic Processing



APPENDIX V

PROGRAM HF2D

```

C*****
C
C      Program HF2D by R. V. Schneider
C
C      Program to determine the flow of heat in a
C      two-dimensional region using the Alternating
C      Direction Implicit (ADI) method
C
C      This model assumes that the number of nodes in
C      the x- and z-directions are equal. Also, the
C      side boundary conditions are that lateral heat
C      flow is set equal to zero, i.e. all heat flow
C      is in the vertical direction.
C
C*****
C
C      This program requires the following data for
C      setup:
C
C      Card 1:  Format(i5,2f5.1)
C      Isize   Number of nodes on each side (square
C              region, max 101) (NOTE: Isize
C              must be an ODD NUMBER)
C      Delx    Distance (km) between nodes in the
C              x-direction
C      Delz    Distance (km) between nodes in the
C              z-direction
C
C      Card 2:  Format(3i5)
C      Idt     Time increment (thousands of years)
C              between time steps
C      Numt    Maximum number of time steps in model
C              evolution
C      Itstep  Values for all parameters will be
C              written to file at increments of Itstep.
C              E.G. for Idt of 10 and Itstep of 50,
C              parameter values will be written every
C              500,000 years
C
C      Card 3:  Format(2f6.5)
C      Diff    Diffusivity of material (cm squared per
C              second)
C      Cond    Conductivity , (W /cm C)
C
C      Card 4:  Format(2f5.1,f6.4)
C      Tt     Top temperature of model
C      Coef   Leading coefficient for a gaussian
C              temperature distribution at the bottom
C              boundary of the model
C

```

```

C          Pc          Coefficient of the power term in the      *
C          gaussian equation                                     *
C                                                                 *
C*****
C
C          Program hf2d(infile)
C
C          Integer      Isize, Idt, Numt, Itstep, Num, maxdim
C          Parameter    (maxdim=101)
C          Real         T(maxdim), Temp(maxdim,maxdim),
C          &            Last(maxdim,maxdim),
C          &            Temp2(maxdim,maxdim), ba(maxdim),
C          &            a(maxdim), b(maxdim), c(maxdim),
C          &            r(maxdim), u(maxdim), Q(maxdim), Rho(maxdim),
C          &            Temp1(maxdim,maxdim) iu(maxdim)
C          Real         Alpha, Beta, Amp, Lamp, Coef, Pc, Cond,
C          &            Delx, Delz, Delt, Tt
C          Character*20 infile
C          Common /parameters/ Isize, Texp, Cond, Delx, Delz
C
C          Open(10, file=infile, status='old')
C             Read(10,6) Isize, Delx, Delz
C             Read(10,3) Idt, Numt, Itstep
C             Read(10,4) Diff, Cond
C             Read(10,5) Tt, Coef, Pc
C          Close(10)
C          3 Format(3i5)
C          4 Format(2f6.5)
C          5 Format(2f5.1, f6.4)
C          6 Format(i5, 2f5.1)
C
C          Delt = Float(Idt) * 1000.
C          Isize = (Isize/2) * 2 + 1
C          D = Diff * .003156
C          Cond = Cond * 1.e5
C          Alpha = (D * Delt) / ( 2. * (Delx)**2 )
C          Beta = (D * Delt) / ( 2. * (Delz)**2 )
C          Texp = .00003
C          Num = 0
C
C*****
C          Set up the initial model
C*****
C          Initial temperature distribution
C
C          Call tempinit(Isize, delz, tt, T, maxdim)

```

```

c
  Do 8 i=1, Isize
    Q(i) = 0.0
    ba(i) = 0.0
    iu(i) = 0.0
    Do 7 j=1, Isize
      Temp(i,j) = T(j)
      Temp2(i,j) = T(j)
7    Continue
8  Continue

c
c*****  Temperature boundary condition, bottom
c
  Do 15 i=1, Isize
    Temp(i,1)=T(1)+Coef*exp(-(Pc*(Float(i-1)*Delx)**2))
    Temp2(i,1)=T(1)+Coef*exp(-(Pc*(Float(i-1)*Delx)**2))
    Temp(i,Isize) = Tt
    Temp2(i,Isize) = Tt
15  Continue

c
c*****  Initial density distribution
c
  Call density(Isize,delz,Rho,T,maxdim)

c
c*****  Write initial values to file
c
  Open(11,file='rho0',status='new')
  Open(13,file='ba0',status='new')
  Open(14,file='iu0',status='new')
  Open(15,file='T0',status='new')
  Do 11 j=1,Isize
    Write(11,13) j,rho(j)
    Write(13,13) j,ba(j)
    Write(14,13) j,iu(j)
    Write(15,13) j,T(Isize-j+1)
11  Continue
13  Format(i3,2x,f8.3)
14  Format(2i3,2x,f7.2)
20  Format(11(1x,f6.1))
    Close(11)
    Close(13)
    Close(14)
    Close(15)
  Open(12,file='tm0',status='new')
  Do 22 j=1,Isize
    Do 21 i=1,Isize
      Write(12,14) i,j,Temp(i,j)
21  Continue
22  Continue

```

```

      Close(12)
C
C*****
C
C      Begin the calls to the subroutine 'tridag' for
C      heat flow evolution.  All of this will be inside
C      of a large loop that will increment time over
C      values set by the user
C
C*****
C
C      Do 999 k = 1, Numt
C
C      b(1) = 1. + (2. * Alpha)
C      c(1) = -2. * Alpha
C      b(Isize) = b(1)
C      a(Isize) = c(1)
C
C      Do 70 n=2, Isize-1
C      a(n) = -Alpha
C      b(n) = 1. + (2. * Alpha)
C      c(n) = -Alpha
C      70 Continue
C
C*****  The first call to tridag involves holding j
C*****  constant while incrementing i.  That is, each row
C*****  will be calculated for the first call, the '1/2
C*****  Time step'.
C
C      Do 200 j = 2, Isize-1
C
C*****  Determine RHS values before calling tridag
C
C      Do 100 i=1, Isize
C      r(i) = Beta * (Temp(i, j-1) + Temp(i, j+1)) +
C      &      (1. - (2. * Beta)) * Temp(i, j)
C      100  Continue
C
C*****  First call to tridag
C
C      Call tridag(a, b, c, r, u, Isize, maxdim)
C
C*****  Now place the u vector in its correct spot in
C*****  the new model:
C
C      Do 150 i=1, Isize
C      Temp2(i, j) = u(i)
C      150  Continue
C      200  Continue

```

```

c
204   Format(11(1x,f6.1))
c
c*****   Set up a,b,c's for the second call
c
      b(1) = 1.
      c(1) = 0.
      a(Isize) = 0.
      b(Isize) = 1.
      r(Isize) = Tt
      Do 250 m=2,Isize-1
          a(m) = -Beta
          b(m) = 1. + (2. * Beta)
          c(m) = -Beta
250   Continue
c
c*****   Now set up the second call by holding i constant
c*****   and incrementing j.  Thus the columns will now
c*****   be calculated.
c
      Do 400 i=1,Isize
          r(1) = Temp2(i,1)
          If(i.eq.1) Then
              Do 270 j=2,Isize-1
                  r(j) = (1. -(2.*Alpha))*Temp2(1,j) +
&                      (2.*Alpha)*Temp2(2,j)
270   &          Continue
              Else If(i.eq.Isize) Then
                  Do 290 j=2,Isize-1
                      r(j) = (1. -(2.*Alpha))*Temp2(Isize,j)
&                      + (2.*Alpha)*Temp2(Isize-1,j)
290   &          Continue
              Else
                  Do 310 j=2,Isize-1
                      r(j) = Alpha*(Temp2(i+1,j)+Temp2(i-1,j)) +
&                      (1.- 2.*Alpha)*Temp2(i,j)
310   &          Continue
              Endif
          Call tridag(a,b,c,r,u,Isize,maxdim)
c
          Do 350 j=2,Isize-1
              Temp(i,j) = u(j)
350   &          Continue
400   &          Continue
c
c*****   Check evolution of model after this time step
c
      Lamp = 0.0
      Do 600 i=1,Isize

```

```

        Do 550 j=1,Isize
            Amp = Abs(Temp(i,j) - Last(i,j))
            If(Amp.gt.Lamp) Lamp = Amp
550    Continue
600    Continue
        If(Lamp.le.0.1) go to 1000
        Do 800 i=1,Isize
            Do 750 j=1,Isize
                Last(i,j) = Temp(i,j)
750    Continue
800    Continue
C
C*****    Determine if output file should be written
C
            If (mod(k,Itstep).eq.0) Call
            &     evolve(T,Temp,Rho,Num,maxdim)
C
999    Continue
1000   Call evolve(T,Temp,Rho,Num,maxdim)
        l=k-1
        Open(15,file='tstep')
        Write(15,*) 'Number of time steps = ',l
        Close(15)
        Stop
        End
C
        Subroutine tempinit(Isize,delz,tt,T,maxdim)
C
C*****
C
C        Subroutine to set up a typical temperature
C        distribution within the lithosphere
C
C*****
C
        Real qs,qm,tt,hg,tcon,depth,delz,Ten
        Dimension T(maxdim)
        Integer Isize
C
C*****    Set up initial parameters
C
        qs = 15000.
        qm = 7000.
        hg = 800.
        tcon = 600.
C
        Do 10 j=1,Isize
            depth = float(j-1) * delz
            If (depth.le.10.0) Then

```

```

      T(Isize-j+1) = tt + (qs * dcpth)/tcon-(hg *
&      depth**2)/(2.*tcon)
      Ten = T(Isize-j+1)
      Else
      T(Isize-j+1) = Ten + qm * (depth - 10.) / tcon
      Endif
10  Continue
      Return
      End

C
      Subroutine density(Isize,delz,Rho,T,maxdim)
C
C*****
C
C      Subroutine to initialize density values      *
C      in the lithosphere                          *
C
C*****
C
      Real Texp,delz
      Dimension Rho(maxdim),T(maxdim)
      Integer Isize
      Texp = 3.E-5
C
      Do 25 j=1,Isize
      Depth = Float(j-1)*delz
      If(Depth.le.40.0) Then
      Rho(j) = 2.6 + (0.01*depth)
      Else
      Rho(j) = 2.3 + (1. - Texp * (T(j) - T(1)))
      Endif
25  Continue
      Return
      End

C
      Subroutine tridag(a,b,c,r,u,n,maxdim)
C
C*****
C
C      Solves for a vector u of length n, the tridagonal *
C      linear set given by equation (2.6.1), in          *
C      "Numerical Recipes in Fortran".                  *
C
C      a, b, c, r are input vectors and are not modified. *
C
C*****
C
      Dimension gam(maxdim),a(maxdim),b(maxdim),c(maxdim),
&      r(maxdim),u(maxdim)

```

```

      Real bet
C
      If (b(1).eq.0.) Pause
      bet = b(1)
      u(1) = r(1)/bet
      Do 50 j=2,n
          gam(j) = c(j-1)/bet
          bet = b(j) - a(j) * gam(j)
          If(bet.eq.0.) Pause
          u(j) = (r(j) - a(j) * u(j-1))/bet
50 Continue
      Do 60 j=n-1,1,-1
          u(j) = u(j) - gam(j+1) * u(j+1)
60 Continue
      Return
      End

C
      Subroutine evolve(T,Temp,Rho,Num,maxdim)
C
C*****
C
C          Subroutine to calculate output values
C
C*****
C
      Integer maxdim
      Dimension T(maxdim),Temp(maxdim,maxdim),
&              Rho(maxdim),F(maxdim)
      Real      hf(maxdim),ba(maxdim),Drho(maxdim,maxdim),
&              iu(maxdim) Sumout,out,
&              DDrho(maxdim*2,maxdim),TD(maxdim,maxdim)
      Integer   Isize,Num
      Character str*4,Name*6
      Common /parameters/ Isize,Temp,Cond,Delx,Delz

C
      Num = Num + 1
      Write(str,'(i4)') Num
      Call STRIP(str)

C
C*****  Surface heat flow:
C
      Name = 'hf'//str
      Open(11,file=Name,status='new')
      Do 10 i=1,Isize
          hf(i) = -Cond * (Temp(i,Isize) -
&                      Temp(i,Isize-1)) / Delz
          hf(i) = hf(i) / 4.187e4
          Write(11,111) hf(i)
C
          write(11,113) i,hf(i)

```

```

10 Continue
Close(11)
C
C***** Establish delta rho
C
Do 15 i=1,Isize
Do 14 j=1,Isize
TD(i,j) = Temp(i,j) - T(j)
If(j.eq.Isize) Then
Drho(i,j) = 0.0
Else
Drho(i,j) = -Rho(j)*Texp*TD(i,j)
Endif
14 Continue
15 Continue
C
C***** Isostatic uplift:
C
Name = 'iu'//str
Open(12,file=Name,status='new')
Do 19 i = 1,Isize
Do 18 j = 1,Isize
F(j) = Drho(i,j)
18 Continue
Call Simpson(F,out,maxdim)
iu(i) = -out
Write(12,111) iu(i)
19 Continue
Close(12)
C
C***** Write temperature distribution to file
C
Name = 'tm'//str
Open(14,file=Name,status='new')
Do 65 j=1,Isize
Do 55 i=1,Isize
Write(14,114) i,j,Temp(i,j)
55 Continue
65 Continue
Close(14)
C
111 Format(f15.10)
112 Format(i3,2x,f15.10)
114 Format(2(2x,f4.0),2x,f7.2)
115 Format(11(1x,f6.1))
116 Format(6(f10.5,2x))
C
Return
End

```

## Subroutine Simpson(F,Sum,maxdim)

```
C
C*****
C
C      Subroutine to apply the extended Simpson's rule
C      procedure
C
C*****
C
C      Real Sum,Sum1,Sum2,delz
C      Dimension F(maxdim)
C      Integer Isize
C      Common /parameters/ Isize,Text,Cond,Delx,Delz
C
C      Sum1 = (17. * (f(1) + f(Isize))
&          + 59. * (f(2) + f(Isize-1))
&          + 43. * (f(3) + f(Isize-2))
&          + 49. * (f(4) + f(Isize-3)))/48.
C      Sum2 = 0.0
C      Do 40 j=5,Isize-4
C          Sum2 = Sum2 + f(j)
40 Continue
C      Sum = (Sum1 + Sum2)*delz
C      Return
C      End
```

## CURRICULUM VITAE

Robert Vincent Schneider, the son of Joseph R. and Avelina T. Schneider, was born on September 15, 1958 in Saint Paul, Minnesota. He graduated from Saint Thomas Academy (Saint Paul) in 1976. He received the Bachelor of Science degree in geology from the University of Minnesota, Duluth in May 1981. He received the Master of Science in Geophysics from the University of Texas at El Paso in 1985. His M.S. thesis was entitled "The vertical distribution of Uranium, Thorium and Potassium in the Canadian Shield, Sudbury, Ontario, Canada". In 1985, he married Susan Elizabeth Jore. In 1987, he published the article "Investigations and interpretations of the vertical distribution of U, Th, and K: South Africa and Canada" in Geophysical Research Letters. He has been an author and co-author on several papers presented at regional and national professional conventions. He entered the doctoral program at the University of Texas at El Paso in the fall of 1985. In January 1990, he began work as a Petroleum Geophysicist at Amoco Production Company, Houston, Texas.

Permanent Address: 14800 Memorial Drive #92  
Houston, Texas 77079

This dissertation was typed by Susan Elizabeth Schneider.